Counter electrode materials based on carbon nanotubes for dye-sensitized solar cells

Shahzad, N.[a,], Lutfullah[b,c], Perveen, T.[d], Pugliese, D.[e], Haq, S.[f], Fatima, N.[g], Salman, S. M.[c], Tagliaferro, A.[e], Shahzad, M. I.[b,*]**

[a] US-Pakistan Centre for Advanced Studies in Energy (USPCAS-E), National University of Science and Technology (NUST), 44000-Islamabad, Pakistan.

[b] Nanosciences and Technology Department (NS&TD), National Centre for Physics (NCP), 44000-Islamabad, Pakistan.

[c] Department of Chemistry, Islamia College Peshawar (ICP), University Campus, 25120-Peshawar, Pakistan.

[d] Department of Chemistry, Quaid-i-Azam University (QAU), 44000-Islamabad, Pakistan.

[e] Department of Applied Science and Technology (DISAT) and RU INSTM, Politecnico di Torino, 10129-Turin, Italy.

[f] Chemistry Department, Azad Jammu & Kashmir University (AJKU), 13100-Muzaffarabad, Azad Kashmir, Pakistan.

[g] Department of Chemistry, Bacha Khan University (BKUC), 24420-Charsadda, Pakistan.

Corresponding Author:

***Muhammad Imran Shahzad, PhD (**imran.shahzad@ncp.edu.pk**)**

Nanosciences and Technology Department (NS&TD), National Centre for Physics (NCP), Quaid-i-Azam University (QAU) Campus, Shahdra Valley Road, 44000-Islamabad, Pakistan

Phone: +92 313 6961143

****Nadia Shahzad, PhD (**nadia-shahzad@live.com**)**

US-Pakistan Centre for Advanced Studies in Energy (USPCAS-E), National University of Science and Technology (NUST), 44000-Islamabad, Pakistan

Abstract

Efficiency, stability, and cost-effectiveness are the prime challenges in research of materials for solar cells. Technologically as well as scientifically, attention gained by dye sensitized solar cells (DSSCs) stems from their low material and fabrication costs as well as high efficiency projections. The aim of this study is to explore the carbon nanotubes (CNTs) based counter electrode (CE) materials for DSSCs and to reconnoiter the suitable alternative materials in place of noble metals such as Platinum (Pt), and Gold (Au) etc. Various classes of CE materials based on CNTs including pure single walled, double walled, and multiwalled CNTs, doped CNTs and their hybrid composites with various polymers, and transition metal compounds are discussed comprehensively in light of the research work started since the inspection of DSSCs and CNTs. The properties, associated with such materials including surface morphology, structural determination, thermal stability, and electrochemical activity, are also thoroughly analyzed and compared. This work provides a thorough insight into the possibility of CNTs as alternative CE materials.

Keywords

Carbon nanotubes; dye-sensitized solar cell; counter electrode; photovoltaics; cyclic voltammetry; electrochemistry.

Highlights

- The working principle of dye sensitized solar cells and new materials for their components are discussed.
- The effect of counter electrode materials on DSSCs performance is comprehensively discussed.
- The role of carbon nanomaterials, mainly CNTs as effective counter electrodes for DSSCs is discussed.
- Counter electrodes based on pure, doped, and modified CNTs are comprehensively reviewed.
- Counter electrodes based on different CNTs composites are also extensively reported.

Abbreviations

AC	Activated charcoal
ACNTs	Aligned carbon nanotubes
ALD	Atomic layer deposition
APPJ	Atmospheric pressure plasma jet
CB	Conduction band
cBSA	Serum bovine albumin
C_{dl}	Double-layer capacitance
CE	Counter electrode
CFF	Carbon fibre fabric
CMC	Carboxy methylcellulose
CNTf	Carbon Nanotubes fibers
CNTY	CNTs yarns
CPC	Cetylpyridinium chloride
CVD	Chemical vapor deposition
DBSA	Dodecyl benzene sulfonic acid
DBSNa	Sodium dodecylbenzenesulfonate
DSSCs	Dye sensitized solar cells
DWCNTs	Double walled carbon nanotubes
EIS	Electrochemical impedance spectroscopy
fCNTs	Functionalized CNTs
FF	Fill factor
FTO	Fluorine Doped Tin Oxide
GO	Graphene oxide
HFP	Hexafluoropropylene
HOMO	Highest occupied molecular orbital
HSPM	Poly(maleic acid-co-phydroxystyrene)-block-poly(p-hydroxystyrene)
LUMO	Lowest unoccupied molecular orbital
MOF	Metal Organic Framework
MWCNTs	Multi walled carbon nanotubes
NBIP	N-annulated benzoindenopentaphene
NCs	Nanocomposites
NF	Nanofilament

NPs	Nanoparticles
P3HT	Poly(3-hexylthiophene)
PANI	Polyaniline
PCE	Power/Photo conversion efficiency
PDA	Polydopamine
PDDA	Poly diallyldimethylammonium chloride
PEDOT	Poly(3,4-ethylenedioxythiophene)
PEO	Polyethylene
PMMA	Polymethyl methacrylate
PPy	Polypyrole
PSCs	Perovskite solar cells
PSS	Polystyrene sulfonate
PTh	Polythiophene
PVA	Polyvinyl acetate
PVDF	Polyvinylidene fluoride
PVP	Polyvinylpyrrolidone
QDs	Quantum dots
R_{ct}	Charge transfer resistance
RF	Radiofrequency
rGO	Reduced Graphene Oxide
R_s	sheet resistance
SDBS	Sodium Dodecyl Benzene Sulphonate
SWCNTs	Single walled carbon nanotubes
TAOB	Tetraoctylammonium bromide
Z_N	Electrolyte diffusion impedance

Graphical abstracts

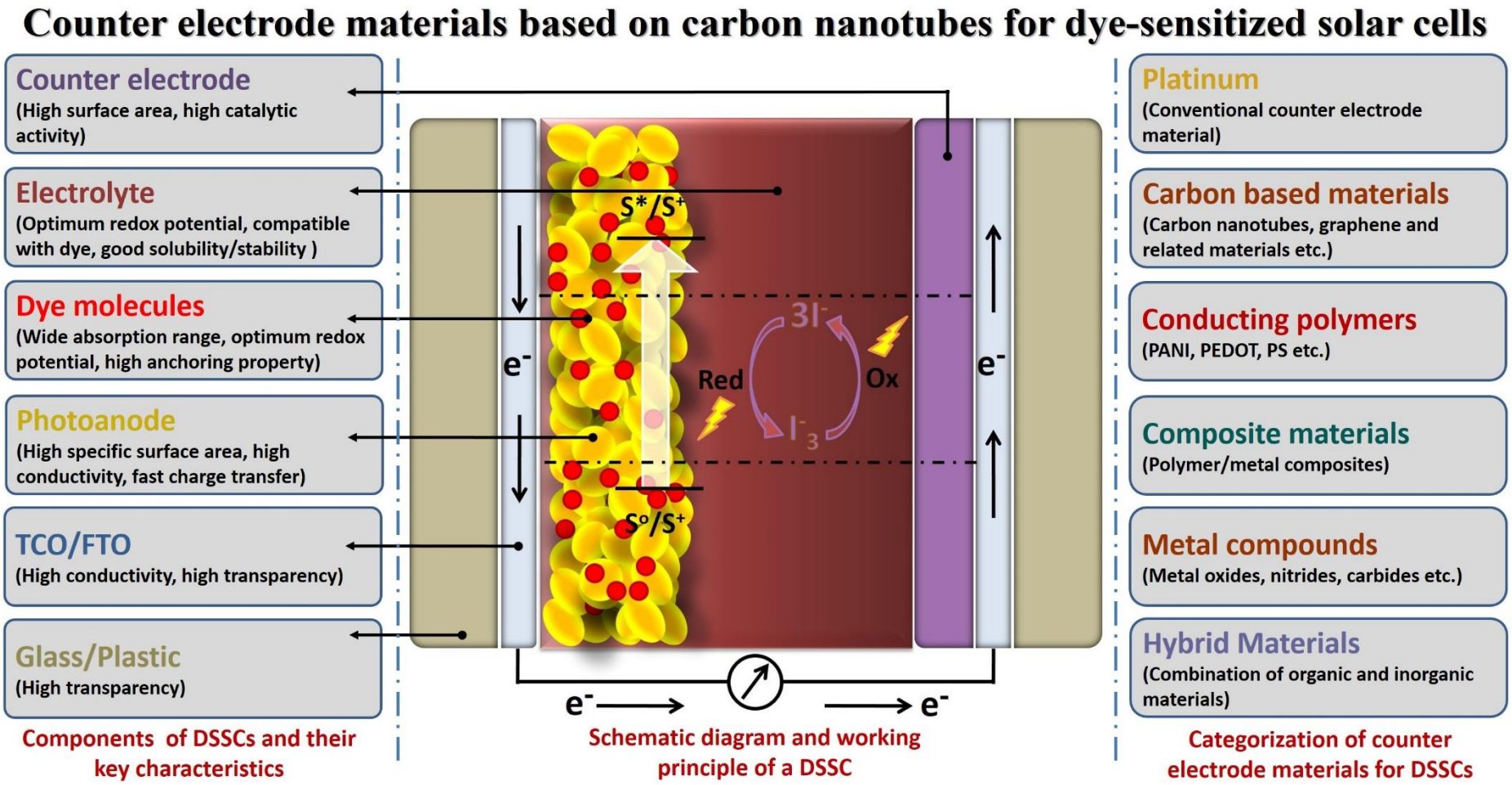

1 Introduction

The main challenge for humanity in the current scenario is the development of reliable, clean, and low-cost energy sources, since the world is going through a phase of energy crisis due to the rapid increase in population and industrialization. Fossil fuels, which are the primary energy source, contribute to almost 80% of the world total energy, however they are non-renewable and destined to run out over time. Furthermore, they also cause carbon dioxide (CO_2) emission that is a greenhouse gas, responsible for global warming. The remaining ~20% of the energy is provided by utilizing renewable and nuclear energy sources [1, 2]. The renewable resources such as wind, hydro and solar power etc. are clean energy resources, therefore, it is need of hour to increase their share in world energy market in order to address the problems associated with non-renewable energy sources. Solar energy is the most appropriate source among all as it exploits the abundant energy reserve (~174,000 TW per year) [3]. Therefore, development of solar power will lessen the problem of energy crisis, limited reserves, and global warming.

Nanomaterials have great potential in developing solar power and increasing its shares because of their peculiar properties which can provide breakthrough solutions to the problems hindering the progress of solar technology [4]. They also have enormous prospects in various other fields including biotechnology [5], energy storage [6], information technology [7], and medicine [8]. Furthermore, the nanomaterials in the form of tubes, rods, particles, and sheets possess unique physical, structural, chemical, electrical, and mechanical properties, which can bring benefit in diverse applications. Therefore, using nanomaterials as light harvester, catalyst, electron accumulator and electron transporter in solar cells will increase the overall efficiency of cells and ultimately rise world energy share [4].

Solar cells are devices that are used for conversion of sunlight into electricity through the photovoltaic effect. The share of solar energy in producing electricity was 1.9% toward the end

of 2017 [2], which is 26% higher than that of 2016 [9]. It was further raised to 2.4% by the end of 2018 [10], thus showing that the adoption of solar energy technologies has experienced a constant growth in recent times as it is an economical and environmental friendly source of energy having wide reserves. In recent years, various types of photovoltaics (PV) devices have been studied which include; i). Silicon based first generation solar cells [11] showing power conversion efficiency (PCE) of 25% [3], ii). Second generation solar cells focused on thin films of different materials [12] exhibiting PCEs ranging between 20-28% [3], and iii). emerging photovoltaic technologies commonly known as third generation solar cells [13] (see **Fig. 1**).

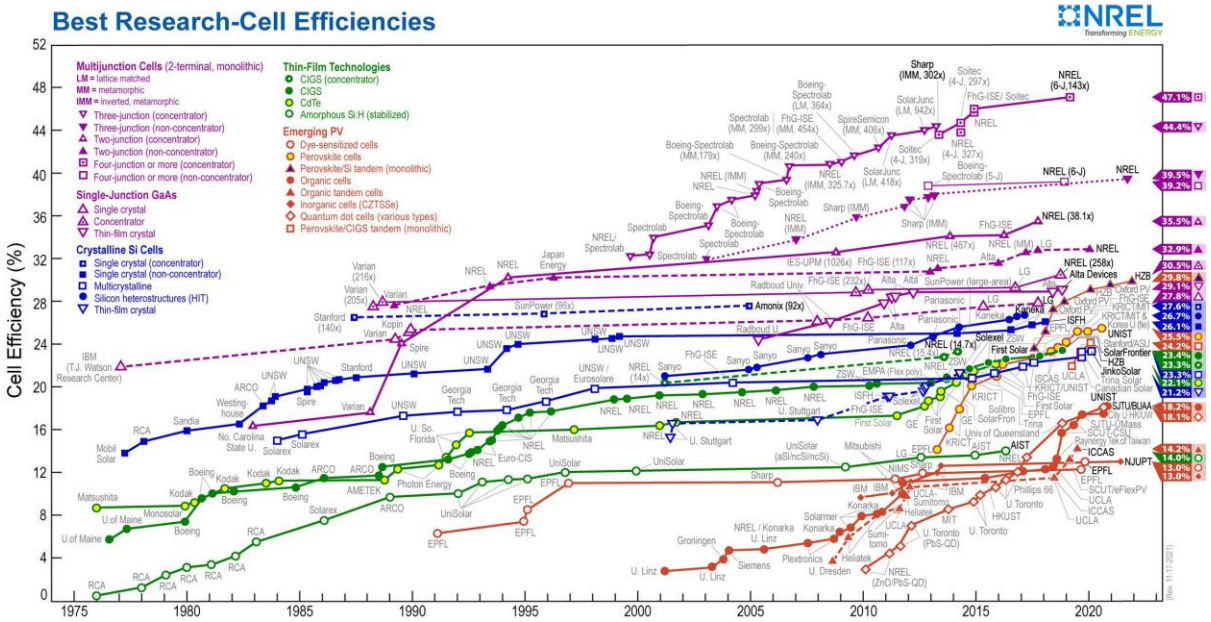

Fig. 1. Best Research Cell Efficiencies [13] (The plot is courtesy of the National Renewable Energy Laboratory, Golden, CO.)

First and second generation solar cells are able to provide the highest PCE at present, however, at the same time they are highly expensive due to their complicated fabrication process and high material cost. Within this framework, in order to get low cost energy harvesting devices with reasonable efficiency and stability, emerging PV technologies have been introduced. These emerging devices include DSSCs [14] (PCE~14.3% [15], theoretically predicted 32% [16]), perovskite solar cells (PSCs) [17] (PCE~25.2% [13], theoretically predicted 30.5% [18]),

organic/polymer solar cells [19] (PCE ~11.5%) and quantum dot solar cells [20] (PCE~13.43% [21], theoretically predicted more than 65% [4]). One of the key elements in such devices is the electrocatalyst layer which is of paramount significance, as it supports electrons accumulation from the external circuit and catalyzes the process of electrolyte reduction [22].

DSSCs were firstly introduced by Grätzel in 1991 [23]. Their CE is typically constituted of a conductive glass, which enhances the rate of electron transfer and decreases the recombination, coated with an electrocatalyst layer, usually platinum (Pt). It is considered as one of the best CE material because of its good catalytic activity, electrical conductivity, stability and efficiency [24], however, the abundance of Pt in the Earth's crust is very low, which inevitably leads to high cost and makes its large scale production difficult [25]. Furthermore, Pt has low corrosion resistance against most frequently used redox couple (I^-/I_3^-) in DSSCs. Therefore, alternative classes of materials are being investigated and carbon nanomaterials are the most common among them. Carbon nanomaterials display several nanoforms, i.e. fullerenes [26], carbon nanotubes (CNTs) [27], and graphene [28] etc. Due to their exceptional chemical and physical features, these materials are applied in various fields, particularly in energy harvesting [29] (solar cells [30] and fuel cells [31]) and energy storage [32] (supercapacitors [33] and batteries [34]). Owing to unique properties, such as elevated aspect ratio, enhanced specific surface area, and remarkable electrical conductivity, CNTs have become good alternative electrocatalyst [30] and have been widely studied as CE material for DSSCs [35].

In this review, the advantages exhibited by CNTs based CEs are comprehensively discussed. These electrodes have been employed several times in DSSCs, but they might have applications also in other sensitized solar cells and energy storage devices. Before broadly stating the progress towards replacing the precious Pt with low cost and easy to fabricate CNTs electrodes, we will briefly discuss the components and the working principle of DSSCs, focusing on the role of the CE in achieving a smooth and efficient functioning of these devices.

2 Working principle and components of DSSCs

DSSCs have great potential in replacing silicon-based solar cells because of their low cost, flexibility, semi-transparency, durability, and simple assembling process. A typical DSSC contains a dye-loaded TiO_2 electrode deposited on a conductive glass, I^-/I_3^- based electrolyte solution and a Pt CE **(see Fig. 2).** The dye molecules introduce electrons into conduction band of the TiO_2 layer upon illumination. The electrons are then diffused through the nanostructured film of TiO_2 and are accumulated at the front contact of FTO. A closed regenerative circuit is obtained by the redox couple ions present in the electrolyte, which drain the electrons from the external circuit at the CE and reduce the oxidized dye molecules **[36]**.

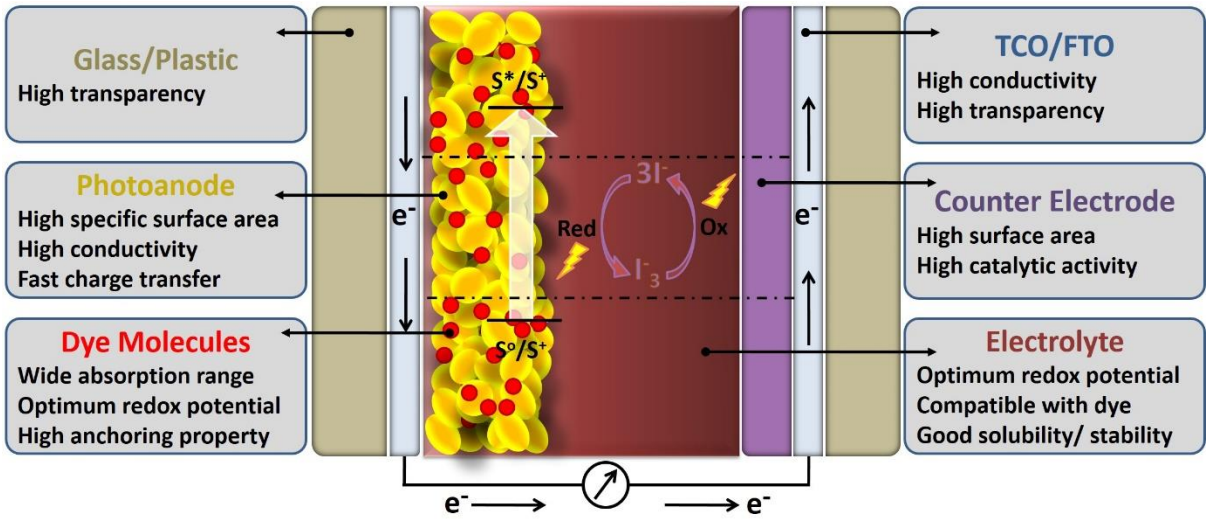

Fig. 2. Working mechanism of a dye-sensitized solar cells (DSSCs)

2.1 Sensitizer

The sensitizer, commonly known as dye, is the key component of a DSSC. The main function accomplished by the sensitizer is to absorb photons and to produce electrons, which are successively transferred into the conduction band (CB) of the semiconducting oxide. For its efficient performance, the sensitizer needs to reveal suitable lowest unoccupied molecular orbital (LUMO) and highest occupied molecular orbital (HOMO) in order to promote a higher

charge injection in the CB of the semiconductor oxide, dye regeneration from the redox electrolyte, enhanced molar extinction coefficient in the visible and near-infrared regions and improved solubility and photostability [37, 38]. It should also possess groups in its structure which help its chemisorption on the semiconductor oxide and should be able to sustain redox turnovers, which correspond to an operation lifetime of 20 years [39, 40].

Numerous sensitizers are employed in DSSCs, like metal complex [41], metal-free organic [42], hemisquaraine dye [43] and natural dyes [44]. The most common sensitizer for DSSC is Ruthenium (II) polypyridyl [45], because of its various beneficial characteristics such as high absorption, extended excited-state lifetime and enhanced metal-to-ligand charge transport properties. With light absorbing capability extended up to 350 nm [46], the highest PCE achieved by the Ru (II) dye based DSSCs were 11.2% in 2005 [47] and 11.7-12.1% in 2010 [48]. The relatively low molar extinction coefficient and the high cost are the main drawbacks showed by Ru (II) dyes [49]. Metal free organic dyes are an alternative class of materials that are being intensively investigated since 2004, and their employment has led to a noticeable PCE of around 10% [50]. Co-sensitization of such dyes can further enhance the PCE of DSSCs, and Yella et al. in 2011 achieved a maximum PCE of 12.3% (which exceeds 13% under a different light intensity) by co-sensitizing zinc porphyrin dye with another organic dye [51]. The same 13% efficiency was also achieved by Mathew et al. in 2014 using a single dye without co-sensitization [52]. The efficiency was further enhanced up to15% by using co-sensitization of organosilicon based dyes [53]. A study on metal free dyes has reported an efficiency of 12% using a phenothiazine based metal free organic dye [54]. In the category of metal free sensitizers, the maximum efficiency of 12.6% has been achieved by employing a noncyclic aromatic hydrocarbon, N-annulated benzoindenopentaphene (NBIP) based metal free D-A dye C293 without using any co-adsorbent [55]. Natural dyes are reliable alternatives to expensive organic dyes thanks to their low cost, easy extraction and non-toxicity. The maximum

efficiency achieved using these dyes are 2.06% and 2.00% for purple wild Sicilian prickly pear dye and pomegranate dye, respectively [56].

Other classes of sensitizers include inorganic semiconductor quantum dots (QDs) [57] and perovskite material based dyes. QDs based dyes exhibit certain significant characteristics such as variable band gap energy, which strongly depends on the size and shape of QDs, light absorption coefficients, dipole moments and several extraction and generation features. All these properties make them suitable sensitizers for DSSCs with efficiency reaching 13% [58]. The maximum efficiency (13.43%) was achieved by using cesium based colloidal QDs [21]. Perovskite materials, displaying a band gap lower than 1.5 eV, were first investigated in 2009 as sensitizer in DSSCs showing a PCE of approximately 4% [59]. Further research on these materials showed promising results, i.e. an efficiency near 22.1% was achieved by using mixed halide based perovskite materials [60]. This efficiency was further increased to 23.3% and another study reported a maximum efficiency of 25.5% in 2019 [13]. Despite their noticeable photovoltaic performance in DSSCs, nevertheless perovskite materials suffer some important disadvantages, as they are not environmental friendly because of hazardous heavy metals, show phase transition at the solar cell operation temperature range, instability with variation in ambient conditions and sensitivity to the moisture present in the environment [60].

2.2 Photoanode

A semiconductor film, usually termed as photoanode, plays a vital role in the operation of DSSCs. The key functions played by the photoanode are to support the sensitizer, accept the electrons from the sensitizer and to transport those photoexcited electrons to the external circuit. Therefore, ideally, a photoanode should possess vast surface area for dye loading and suitable band gap, which will enable it to effectively accept and transfer electrons to the external circuit. Usually the criteria demand the CB of semiconductor to be 0.2 or 0.3 eV lower than that of the sensitizer [61]. Apart from that, the band gap should be large enough to

effectively transfer all the illuminating light to the sensitizer with minimum losses and the structure should possess least number of crystal boundaries and defects in order to lessen the recombination process of electrons [62]. However, the nanostructured photoanode should exhibit a scattering effect to capture and transfer more and more light to the sensitizer. Additionally, photoanode should also have a bandgap wider than the sensitizer should, so that the absorption range of sensitizer and photoanode should not overlap with each other. In case of overlap of absorption band, more light from solar spectrum will be absorbed by the nanostructured photoanode which may lead to poor charge carrier transport. This effect will also reduce the light absorption by the sensitizer (**see Fig. 3**).

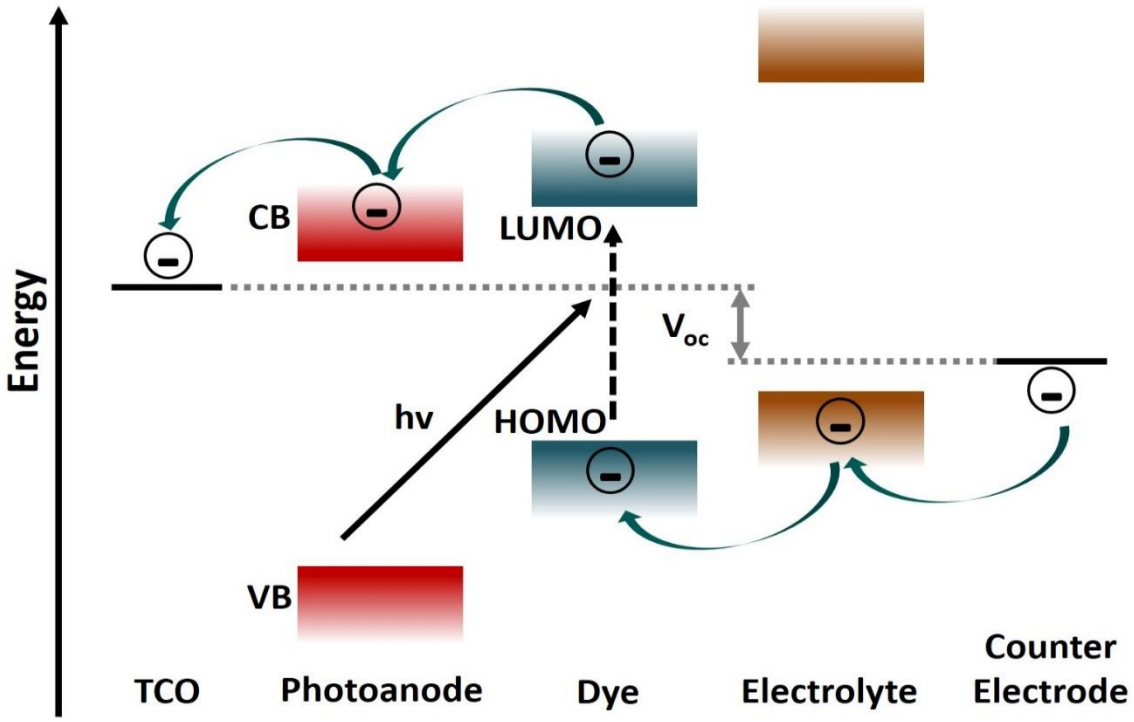

Fig. 3. Energy levels in typical dye sensitized solar cells

DSSCs photoanodes are commonly constituted by a thick film (10 μm) of TiO_2 [63, 64], as it displays the advantages of being cheap, abundant, nontoxic, biocompatible, and it also possesses an appropriate band structure [40]. TiO_2 in various morphologies such as one-dimensional (1D) nanoparticles, nanotubes, nanowires, nanorods and 3D hierarchal structures

such as spheres or beads has been employed as photoanode in DSSCs. By utilizing this morphology engineering strategy, an efficiency as high as 10% was reported by several researchers [62]. Other semiconductors have also been applied as photoanode in DSSCs because they possess similar band structure to that of TiO_2 and bring their own unique characteristics to the cell. These semiconductors include ZnO [65, 66] (extensively studied after TiO_2), SnO_2 [67], Nb_2O_5 [68], WO_3 [69], Ta_2O_5 [70], CdSe [71], CdTe [72], CdS [71] and PbS [73] nanostructures. To improve the performance of the photoanode, these nanostructures can be doped with various ions such as Zn^{2+}, La^{3+}, Nd^{3+}, Er^{3+} and Ho^{3+} and can also be decorated with different noble metals such as silver, chromium, copper, and gold [74-79].

The recombination of electrons within the photoanode is a key problem in DSSCs as it lowers their PCE. To overcome such limitation, a compact layer, usually named as blocking layer [80], is sometimes introduced between the substrate and the photoanode. Several materials have been used for the preparation of blocking layers, which include ZnO [81], SnO_2 [82], TiO_2 [83-85], g-C_3N_4 [86], Nb_2O_5 [87], Nb-TiO_2 [88], and Al_2O_3-TiO_2 [89]. Such blocking layers play a key role in maintaining the efficient charge generation and reduced recombination under light.

2.3 Electrolyte

The electrolyte in DSSCs performs the task of dye regeneration after the electron injection in the photoanode CB and is responsible for the inner charge carrier transport between the two electrodes. Therefore, the most relevant electrolyte characteristics include large electrical conductivity, rapid distribution of the electrons due to little viscosity, high interfacial interaction with the nanostructured photoanode and the CE, low affinity for sensitizer desorption from the oxidized surface, and reduced light absorption in the visible range [40]. The role of the electrolyte is vital as it affects both the stability and the efficiency of DSSCs. The electrolyte contains redox ions, which act as mediators between the photoanode and the CE. The most commonly employed electrolyte is based on the iodide/triiodide redox couple

dissolved into an organic matrix, which allowed achieving an efficiency of 11.7-12.1% [48]. Despite their promising photovoltaic performance, nevertheless the I^-/I_3^- based electrolytes display some important drawbacks, such as leakage and contamination of the environment with organic components and volatilization of the redox couple, which lowers their concentration and leads to the increase of the cell's internal resistance [90]. Other redox couples have also been investigated, and recently Kakiage et al. achieved a maximum efficiency of 14.3% by employing a cobalt-based redox shuttle in combination with a Pt-free CE [53].

To overcome the problems related to the liquid electrolytes such as electrolyte sealing, volatility of solvents and long term stability [91], several strategies have been proposed such as replacing liquid electrolytes with quasi-solid [90, 92] and solid [93] ones. Quasi solid-state electrolytes show the stability of solids and the mobility of liquids as they are prepared by solidifying liquid electrolytes with the help of organic or inorganic gelators. The maximum efficiency reported for these electrolytes is higher than 10%, however, they still highlight the disadvantage of leakage because of liquid component [94]. To overcome the leakage issue, in recent years, solid state electrolytes based on polyvinylidinefluoride (PVDF), polyethylene oxide (PEO), and polyvinyl acetate (PVA) etc. have been thoroughly investigated [95]. The maximum PCE achieved with such electrolytes is 8% except for all solid QDs and perovskite solar cells, in which PCEs of 13.34% [21] and 20% [60] have been reported, respectively.

2.4 Counter electrode

An electrode is an electronic conductor, which assists the smooth flow of electrons through an electrolyte or any other medium. Commonly, two electrodes known as cathode and anode constitute a cell. In the DSSCs system, TiO_2 coated over FTO glass substrate constitutes the photoanode, while Pt coated FTO acts as cathode, also known as CE. It serves three important functions, i.e. it accumulates electrons provided by the outer circuit, it catalyzes the process of electrolyte reduction [22], and it acts as a mirror for the unabsorbed light in order to enhance

the overall efficiency of the cell [96]. A qualified CE for DSSCs therefore must possess sufficient exchange current density in comparison to photoanode that is manifested by its ability for fast reduction of I^-/ I_3^- redox couple and the easy and quick diffusion of triiodide ions. The reduction reaction of the redox couple at CE is not a spontaneous process. It is controlled by the intrinsic electrocatalytic ability of the material used as CE.

The electrocatalytic ability in turn depends upon the active surface area of the electrode. Greater the active surface area, higher number of sites will be available for reduction and faster will be the reaction rate. Therefore, the measurement of charge transfer resistance (R_{ct}) and electrolyte diffusion impedance (Z_N) are important parameters for the evaluation of a CE material. These parameters are typically measured using electrochemical impedance spectroscopy (EIS) of a symmetric DSSC in order to avoid disturbance from its other components. A typical Nyquist plot obtained using EIS is reported in **Fig. 4**, where the semicircle at high frequencies shows the R_{ct} present between the electrolyte and the CE, while the low frequencies represents the Z_N of triiodide ions. Low R_{ct} and Z_N values imply high electrocatalytic activity of the CE material and fast diffusion rate of triiodide ions. These parameters are effected greatly by morphology, electrode preparation route and material microstructure [97]. Additionally, the material must possess high conductivity, good chemical and thermal stability, appropriate energy levels with respect to the redox couple, high corrosion resistance against the electrolyte, good adhesion to the substrate, and optimum thickness.

Different catalysts have been explored as CEs for DSSC, but the most commonly used is Pt. Enhanced exchange current density, high electrocatalytic activity, high transparency and noticeable PCE make Pt electrode a standard choice as CE in DSSCs [40]. Despite these promising features, it also possesses some disadvantages, such as high cost, limited availability, corrosive behavior towards the electrolyte and ineffective against other electrolytes such as $Co^{3+/}Co^{2+}$, T^2/T^-, and polysulfide electrolytes. Thus, noticeable research efforts have been

devoted to develop highly stable and more efficient electrodes featured by a low cost and an easy fabrication process. For this purpose, various materials such as metals [98], alloys [99], inorganic metal compounds [100-106], conductive polymers [107], carbon-based materials [108] and composites [109] have been proposed as CE in DSSCs. Among the various available materials, carbon nanomaterials and their composites with polymers and transition metal oxides are potentially suitable to replace the Pt electrode because of their huge abundance, large-scale production, high conductivity, high catalytic activity, large surface area, high thermal stability, excellent corrosion resistance towards iodine, and high reactivity towards iodine redox couple [110-112]. Moreover, the current density obtained in presence of carbon-based CEs is higher with respect to that of Pt because of the larger availability of catalytic sites. In the coming Sections, we will highlight the properties of CNTs based CEs for DSSCs and their progress in the replacement of conventional CE materials (Pt).

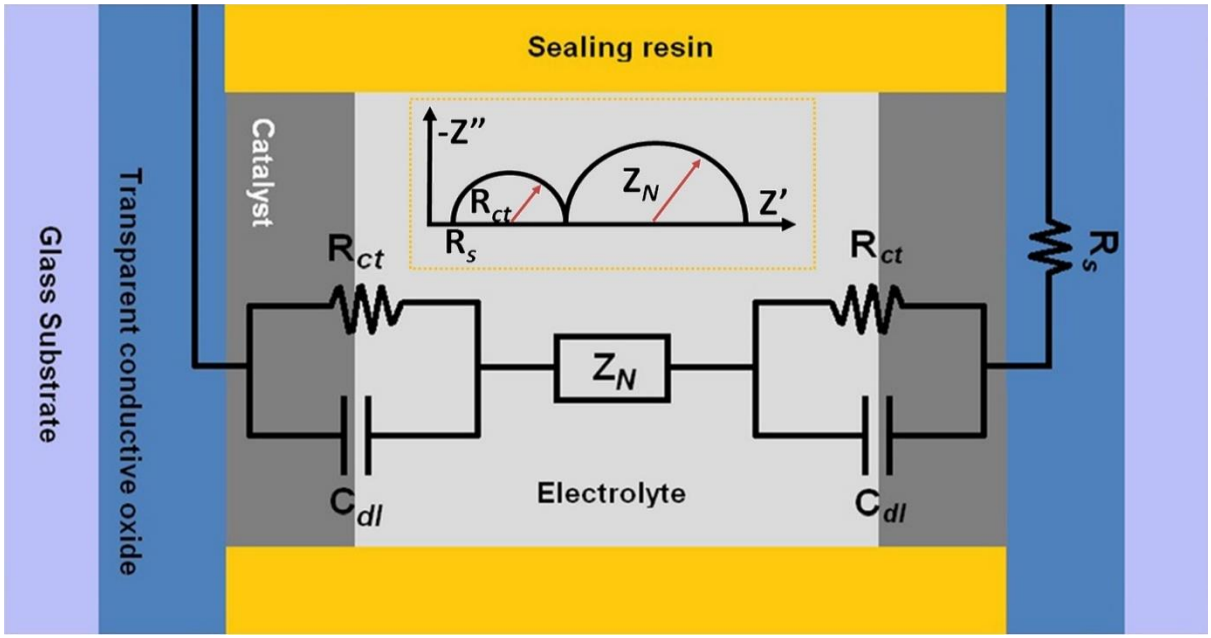

Fig. 4. Symmetric DSSC, equivalent circuit, and typical Nyquist plot. R_s, R_{ct}, Z_N and C_{dl} are the sheet resistance, the charge-transfer resistance, the electrolyte diffusion impedance, and the double-layer capacitance, respectively. (Reproduced with the permission from Ref. [113], Copyright 2015 Wiley-VCH Verlag).

3 Carbon nanotubes based CEs for DSSCs

Carbon based materials can generate, store and transport energy. That's why they can be employed as promising electrode materials in various electronic devices [114], such as fuel cells [115], solar cells [116], batteries [117], super capacitors [118], water electrolysis systems [119], transistors [120], photo catalysis [121, 122] and hydrogen storage devices [123, 124]. It has already been mentioned that scientifically and technologically, interest gained by DSSCs is due to their low fabrication and materials costs and high efficiency forecast. CE plays a vital role in achieving high conversion efficiencies in DSSCs. Carbon nanomaterials are highly striking to be used in place of Pt CEs in DSSCs, as they possess promising properties. Graphitic constituents like graphite, graphene [125], CNTs [126], activated carbon [127], carbon black [128], carbon powder [129], carbon nanofibers [130] and their composites, metal oxide carbon compounds and poly aromatic hydrocarbon have also been used in DSSC as they are able to provide sufficient electrical conductivity to the thin film carbon electrodes. The efficiency achieved with carbon-based materials is quite good, thus encouraging the researchers to work on them to replace Pt and other rare metals based electrodes. In 1996 Kay and Grätzel used for the first time a carbonaceous material for the CE fabrication achieving a device efficiency of 6.7% [1], which is lower than that obtained with a conventional DSSC (up to 10%) but still encouraging. The CE was fabricated starting from an aqueous dispersion of graphite powder, nanocrystalline TiO_2 and carbon black through doctor blading technique. Since then, the efficiency and stability of various CEs based on carbon materials for DSSCs have been tested.

In recent decades, CNTs have been deeply studied as a sound alternative to the conventional Pt in view of obtaining a cheaper CE for DSSCs because of their promising properties such as high electrical and thermal conductivities along with good mechanical strength. They are defined as 1D allotropes of carbon because they grow only in one dimension (length), the other 2D are in nanoscale and are formed by rolling graphene sheets. CNTs are broadly classified

into three categories depending upon the number of graphene layers that are rolled i.e. single-walled CNTs (SWCNTs), double-walled CNTs (DWCNTs) and multi-walled CNTs (MWCNTs). As the name indicates SWCNTs are made by rolling one graphene sheet with outer and inner diameters from 0.4 to 2–3 nm and length in the micrometer range [131]. DWCNTs are made up of two graphene sheets with outer and inner diameters from 0.5 to 2–5 nm and length in the micrometer range [132-135]. MWCNTs are made by rolling a number of graphene sheets with diameters in nm range and length in the μm range [131]. The different properties of CNTs depend upon the angle of rolling, number of walls and length [131, 136].

DWCNTs structure consists of two homocentric SWCNTs that interact with each other through weak Van der Walls inter layer interactions [134]. MWCNTs structure can be explained by two models, i.e. Parchment's and Russian Doll's. In Parchment's model the single sheet of graphene is rolled like rolling a paper, where in the latter case the diameters of the inner and outer tubes do not match. They are stronger and more inert in comparison to SWCNTs because the outer walls shield and protect the inner walls [131]. The electronic properties of SWCNTs depend upon the chirality, that is determined by the rolling angle between the axis of its hexagonal pattern and the tube axis [136]. DWCNTs can exist in four different forms, i.e. both outer and inner tubes are metallic or semiconducting, outer is metallic and inner is semiconducting, and *vice versa*. In one case the material becomes semiconducting, while in the other three the material will show conductivity [134]. MWCNTs are composed of several SWCNTs with at least one of them showing metallic character, therefore they are metallic in nature and not affected by chirality [137]. In this case, the conductivity is inhomogeneous due to the presence of semi-conductive nanotubes as well. The conductivity of CNTs is due to the delocalized π-electrons present in its structure.

CNTs possess high specific surface area. Theoretically, calculated surface area for SWCNTs is 1315 m^2/g, which decreases as the number of shells increases. For DWCNTs it is in the range

680-850 m^2/g; for five-walled CNTs, it ranges between 295 and 430 m^2/g; for MWCNTs with 40 walls and 35 nm in diameter it has been measured to be 50 m^2/g. Diameter also affects the surface area but its effect is minimal. Another factor that influences the CNTs specific surface area is the formation of bundles, either because they are grown in such configuration from a single catalytic particle, or because Van der Walls forces bring them together after each has grown from an individual catalytic particle. It was found that a small bundle of seven SWCNTs exhibits a specific surface area of 751 m^2/g, which decreases to 151 m^2/g for a very large bundle of 217 SWCNTs. The catalyst used for the growth of CNTs also affects the surface area and better results were obtained with Cobalt [138]. Due to the presence of strong covalent bonds between carbon atoms, CNTs possess extremely high mechanical properties with good flexibility that helps them to maintain their structure under different stresses applied. The reported Young's modulus for SWCNTs is 1.25 TPa whereas for MWCNTs is 1.8 TPa, which is 9 times higher than alloy steel [137, 139].

CNTs electrical conductivity as explained above leads to low R_{ct} and favors fast electron transport. The tube-like structure usually interconnects to form network-like structures, which are required for fast ion transport thus leading to low Z_N values. CNTs also possess large surface area that provides various electrocatalytic active sites for the reduction of the electrolyte ions. Surface area has a direct correlation with electrocatalytic activity, more in detail higher the surface area higher will be the PCE. They also show excellent corrosion resistance towards iodine, good thermal and chemical stability, high mechanical strength, and remarkable flexibility, which make them able to preserve their structure even after prolonged use of the device where they are used. In light of all these promising features, CNTs are employed in various forms as CE in DSSCs. They are used in pure state, in the form of random or aligned tubes or as composites by mixing with polymers, metal oxides, sulfides etc., as represented in **Fig. 5**. The unique geometric structure and nanometer scale of CNTs make the electron transfer

in a CNTs based film faster than in Pt based CE and thus their performance comparable. Efficiencies up to 13% were obtained with devices employing CNTs based electrodes [52].

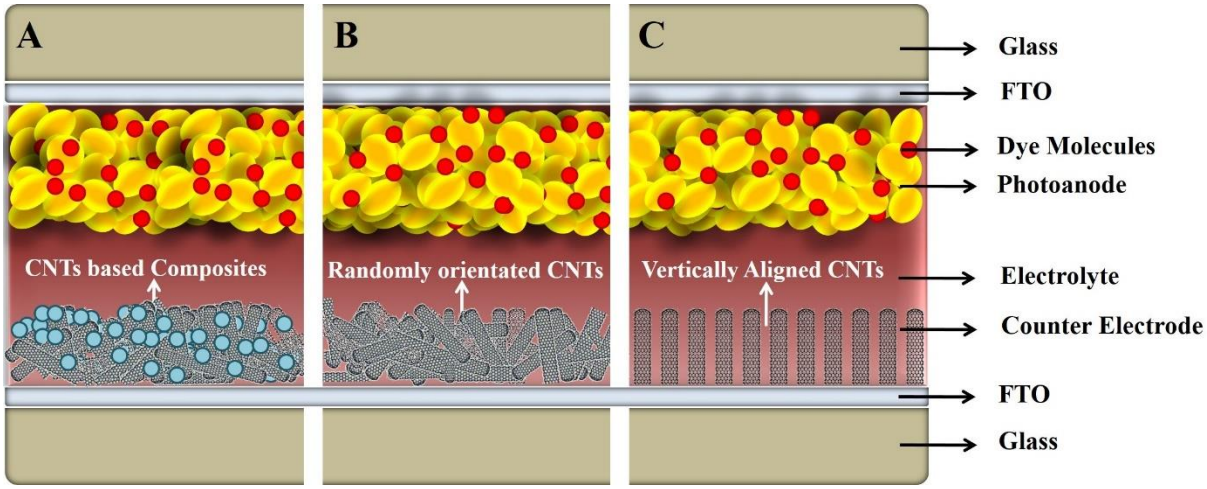

Fig. 5. Different forms of CNTs used as CE materials of DSSCs.

3.1 Pure and modified CNTs based CEs

Pure CNTs of various types (SWCNTs, DWCNTs, and MWCNTs), in different configurations (bundles, forest, vertically or horizontally aligned etc.), and with different modifications and functionalization have been studied as CE in DSSCs with promising performance. Owing to their high surface area and reduced sheet resistance, SWCNTs were successfully employed for the first time as CE material in DSSCs by Suzuki et al. [140] and consequently their performance was analyzed and compared with that of other electrodes. SWCNTs based CE films were prepared by ultrasonically mixing CNTs in water then dropwise placing the obtained suspension on FTO glass or filtering it through a Teflon membrane. The efficiencies achieved with such CEs were 3.5 and 4.5%, respectively. The higher efficiency in the latter case was attributed to the high conductivity and low charge transfer resistance of the membrane.

DWCNTs were also employed as CE material for DSSCs because recently great improvements have been achieved in their manufacturing and refinement processes; however, a facile manufacturing process is still under research. They exhibit a double walled structure, which is

intermediate between SWCNTs and MWCNTs; therefore, they are expected to possess a greater thermal and chemical stability than those shown by the SWCNTs [113]. Zhang et al. fabricated a DWCNTs based CE by blending terpineol and ethyl cellulose and depositing the blend on a conducting FTO substrate via screen printing technique, followed by annealing at 300 °C [141]. The attained efficiency (~6.05%), catalytic activity and performance results were comparable with those of Pt based CEs (PCE~6.80%). The efficiency of DWCNTs based CEs was also investigated by Siuzdak et al. using a ruthenium-based dye. They achieved a maximum PCE of 4.56%, which revealed to be greater than the 3.96% obtained with Pt. They made use of a cost effective spray coating technique for the preparation of the CE followed by annealing at different temperatures, out of which 300 °C annealed film produced the best results [142]. The better performance was attributed to the 3D network formed by several tangled DWCNTs that facilitate triiodide ions reduction due to greater surface area.

To boost the efficiency of DSSCs, MWCNTs were also employed for the fabrication of CEs. Chen et al. [143] also studied the fabrication of MWCNTs based CEs by screen printing technique followed by calcination utilizing an ultrafast approach which made use of a nitrogen atmospheric-pressure plasma jet (APPJ) instead of a conventional calcination. This method proved ecofriendly and cost saving as the energy consumption per unit processing area was estimated to be 500 J/cm^2, which is approximately 1/5 than that spent for the synthesis of CEs via the traditional furnace technique. A maximum PCE of 5.65% was achieved at APPJ treatment time interval of 5 seconds, while an additional increase in the APPJ treatment time resulted in a decrease of the photovoltaic performance. Lee et al. [126] fabricated MWCNTs based CE on FTO glass using tape casting technique and achieved an efficiency of 7.67% (Pt = 7.83%), which increased up to 7.96% (Pt = 8.03%) when light intensity was decreased down to 54 mW/cm^2 (see **Fig. 6**). The electrode was prepared from a paste containing MWCNTs, carboxymethyl cellulose, sodium salt and distilled water. Beside the good efficiency, these

MWCNTs based CEs are very stable and show a lower charge transport resistance than Pt due to the presence of a large number of defect-rich edge planes.

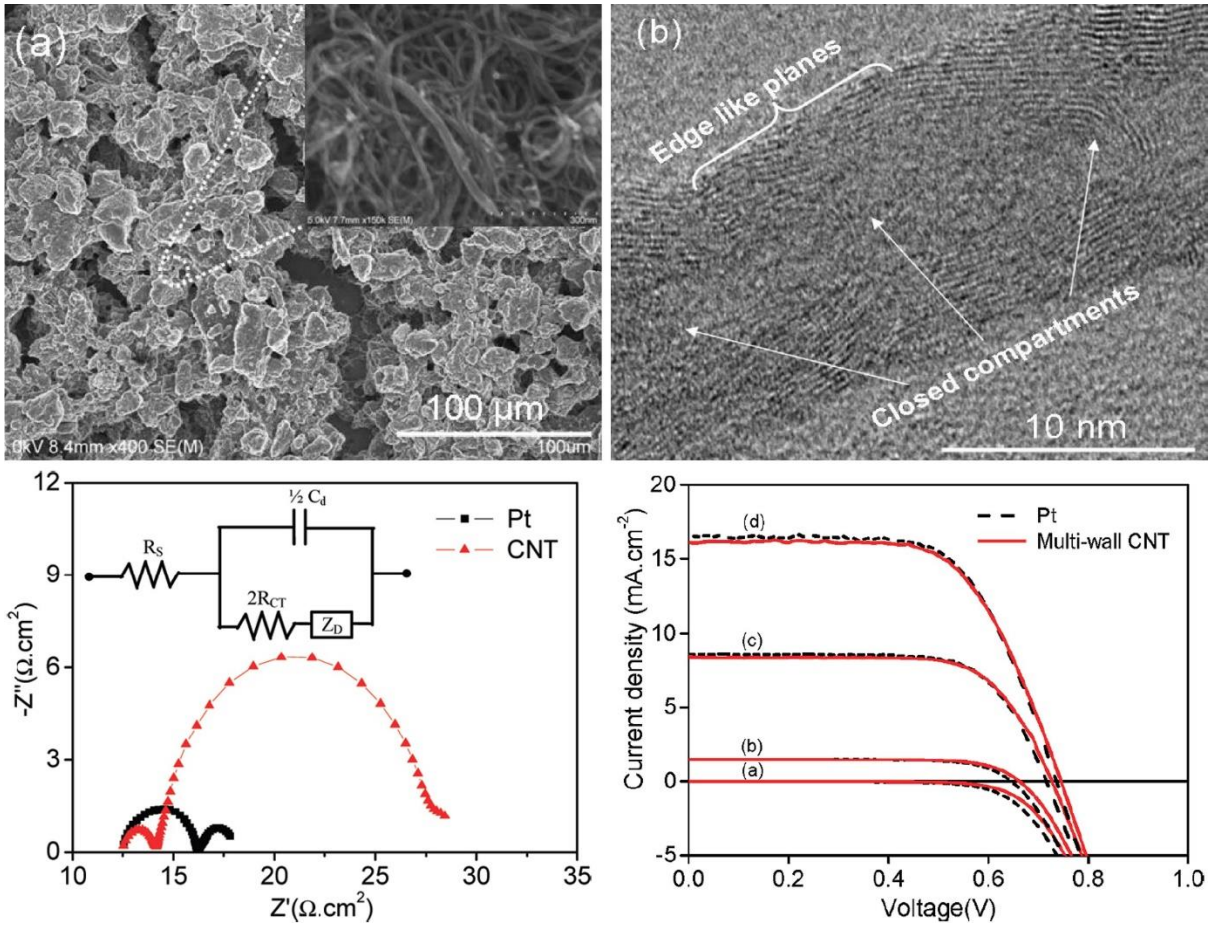

Fig. 6. a). FE-SEM image of a MWCNTs composite film, b). TEM image of the bamboo-like structure in MWCNTs, c). Nyquist plot of a thin-layered symmetric cell and its corresponding equivalent circuit, and d). J-V characteristics of DSSCs, whereas curve (a) shows the DSSC performance in the dark while the curves (b), (c), and (d) were acquired under 0.1, 0.5, and 1 sun illumination respectively. (Reproduced with the permission from Ref. [126], Copyright 2009 ACS Publications).

CNTs are able to assume various structures like bundle, forest, vertical and horizontal alignments and random network [144-147]. These structures display a noticeable effect on the performance of the final device. In 2010 Nam et al. [148] used vertically aligned and randomly oriented MWCNTs, synthesized by the chemical vapor deposition (CVD) and screen printing

techniques, respectively, as CE materials for DSSCs. A maximum PCE of 10.04% was obtained by using the aligned CNTs based CE, while the devices employing the reference Pt and the randomly oriented MWCNTs based CEs showed lower efficiency values equal to 8.80 and 8.03%, respectively. Alignment in the CNTs structure facilitates electron and ion transport that significantly improve the fill factor (FF) and thus efficiency. Seo et al. synthesized highly disordered MWCNTs using a low temperature thermal CVD process and successfully employed them as a CE material for DSSCs [149]. The CNT catalysts were effective in improving the FF value in DSSCs when used in combination with electrolytes with large molecules. In particular, the efficiency increased from 6.51 up to 7.13% by interchanging the traditional Pt catalyst with MWCNTs catalyst and Li^+ electrolyte with 1-butyl-3-methylimidazolium cations based electrolyte. Recently Kim et al. [150] also employed CNTs yarn (CNTY) as a CE for SS fiber-shaped DSSCs. The device structure consisted of Ti wire, N719 dye impregnated TiO_2, SS electrolyte and Pt wire or CNTY CE. They obtained a PCE of 4.00%, which was consistently higher than that shown by the Pt based CE device (2.64%). After 600 bending cycles and 10 washing cycles the fabricated device maintained more than 90% of the efficiency. This paves the way toward the application of this type of devices in wearable fiber electronics and energy textiles.

Several kinds of CNTs including SWCNTs, DWCNTs and MWCNTs have been employed by Zhang et al. as CEs for DSSCs for comparison purpose [151]. The electrodes were fabricated by screen printing technique using pastes constituted by the different CNTs and an organic binder. The PCEs obtained were 8.0, 7.61 and 7.06 for DWCNTs, SWCNTs, and MWCNTs, respectively (see **Fig. 7**). Owing to their high specific area (>450 m^2g^{-1}), and chemical strength, the DWCNTs facilitate the electron transport rate between the CE and the electrolyte. Surface area of SWCNTs is >400 m^2g^{-1} which is comparable to DWCNTs but due to their smaller diameter they agglomerate easily. MWCNTs possess a very small surface area compared to the

other two leading to a lower PCE of DSSCs. However, the more complicated growth process of DWCNTs with respect to the ones of SWCNTs and MWCNTs represents a significant drawback of such CE [35].

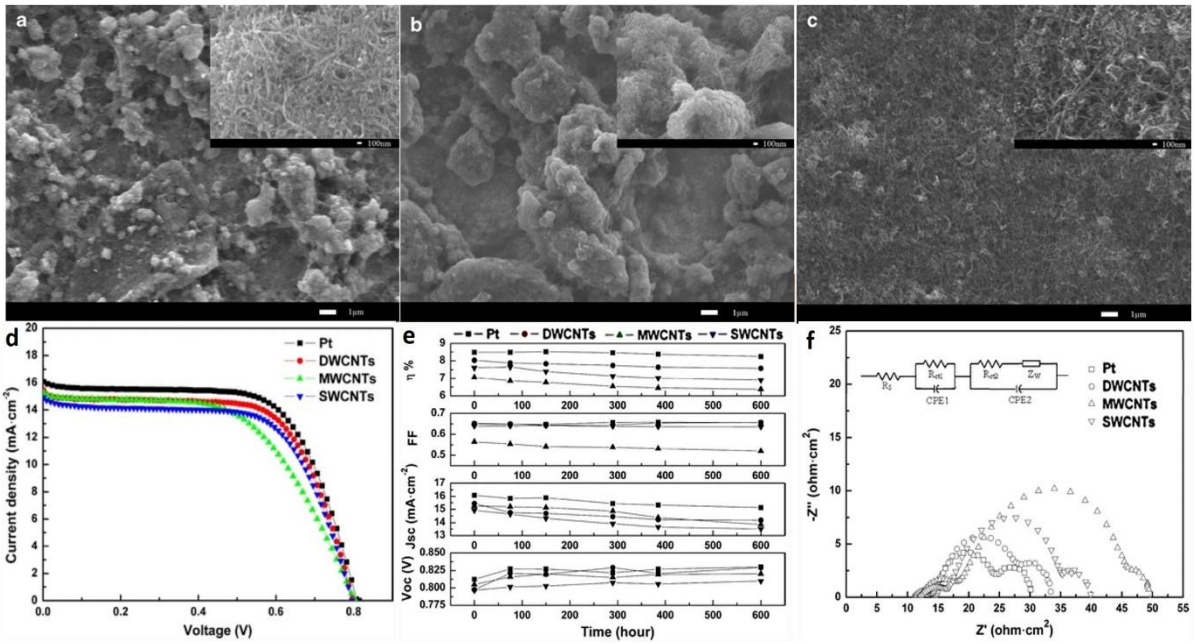

Fig. 7. FESEM images of DWCNTs (a), SWCNTs (b), and MWCNTs (c) CE layers deposited on FTO substrates. Corresponding DSSCs photocurrent density-voltage (J-V) characteristics (d), short term evaluation of photovoltaic parameters (e) and Nyquist plots (f). (Reproduced wth the permission from Ref. [151], Copyright 2011 Springer).

Functionalization of CNTs is commonly adopted to improve their dispersibility, adhesion to the substrate and to achieve a smooth and uniform film, which ultimately lead to the improvement of the performance for the targeted application. CNTs can be functionalized both covalently and non-covalently [152]. Different functional groups have been attached to CNTs, such as acetonitrile, carboxylic acid and acetyl acetone [153]. Chou et al. [154] prepared a CE film from SWCNTs functionalized with Tetraoctylammonium bromide (TAOB) dispersed in 2 different solvents, namely acetyl acetone and N,N-dimethylacetamide. The as-prepared dispersions were coated onto FTO-covered glasses by drop casting technique and subsequently

sintered at different temperatures. A maximum efficiency of around 1.2266% (Pt = 1.25%), ascribable to the better dispersibility of the SWCNTs, was achieved by employing the acetyl acetone dispersed SWCNTs based CE. To further enhance the performance of the CE, a silver (Ag) film was also placed between the FTO glass and the SWCNTs based electrode, thus leading to a drastic increase of the cell efficiency up to 1.3037%. Kim et al. [155] also functionalized MWCNTs with an acid as well as a base and used them as CEs in DSSCs employing nanocellulose as dispersant. They observed a higher efficiency for base functionalized MWCNTs in comparison to pristine and acid functionalized. This was attributed to the better dispersion of base functionalized MWCNTs and nanocellulose mixture, in line with the electrical conductivity trend.

Arbab et al. fabricated CEs for DSSCs composed of MWCNTs functionalized with different enzymes (laccase, glucose oxidase and lipase) [156]. The paste of the enzymatic solution of lipase was prepared in ethanol, followed by the addition of MWCNTs and carboxy methylcellulose (CMC) in the solution and aging overnight. The CE film was synthesized on FTO glass through tape casting method. The laccase and glucose oxidase enzymes produced MWCNTs with amalgamated structures showing no cracks but less uniformity, while the lipase enzyme produced a uniform and well-ordered structure with interconnectivity between the tubes and showed increased adhesion to substrate. This led to the availability of a large number of active sites for the electrocatalysts of triiodide ions. In addition, TEM analysis revealed high-density defect-rich edge planes, which allowed increased contact between the CE and the electrolyte and enhanced the electron transportation, thus leading to a noticeable PCE of 7.52% comparable to Pt (8.00%). Muino et al. [157] prepared CNTs fibers (CNTf) from direct spinning floating catalyst CVD method and used them as CE in DSSCs with Co^{2+}/Co^{3+} redox couple electrolytes. The optimum CNTf sample i.e. highly functionalized and with 9 wt% Fe impurities, allowed obtaining a DSSC PCE of 2%, which was higher than that achieved using

a Pt CE (1.5%). Their results showed that the surface chemistry of CNTf has a significant effect on the adsorption process of the redox active cobalt species near the metallic impurities, which act as catalytic centers. The charge transfer process is facilitated by the presence of metallic impurities, while functionalization of CNTs helps in electrolyte regeneration. An in-depth study of the electrochemical stability of the cobalt-based electrolytes towards CNTf CEs is required to enhance the DSSCs photovoltaic performance.

Siwach et al. [158] prepared acid functionalized MWCNTs and MWCNTs/Pt based CEs by utilizing doctor blade technique and compared them with a pure Pt-based CE prepared through drop casting technique. The DSSCs were assembled by using ZnO photoanode, iodide based electrolyte and the prepared ITO coated CEs. A maximum PCE of 3.78% was obtained using the composite electrode followed by Pt (2.69%) and MWCNTs (2.26%) based electrode. Mithari et al. utilized a cost effective dip and dry coating technique to produce acid functionalized MWCNTs based CEs with different thickness [159]. The latter varied from 0.5 to 3 μm when the dip and dry coating cycles were carried out for 10, 15, 18 and 20 times. They fabricated the DSSCs using a ZnO based anode and Eosin-Y dye instead of ruthenium based dye to reduce the overall cost of the cell. The films made with 18 cycles showed the nearest performance (0.295%) to that of the Pt based CE (0.797%) as compared to all other CEs. The best performance exhibited by the 18-cycle film was ascribed to the availability of a greater number of MWCNTs on the surface of the electrode with lower agglomeration in comparison to the others. This led to a greater number of active sites available for the triiodide ions reduction, with consequent DSSC lower charge transfer resistance and greater current density.

Electrode thickness is an important parameter to be considered, since it affects the charge transfer resistance and conductivity of the film obtained. Ahn et al. [160] prepared transparent conductive MWCNTs based CEs on FTO glass by aerosol deposition process, achieving a maximum PCE of 5.18% when the deposition was carried out for 60 h and the thickness of the

film obtained was equal to 42.5 μm. The efficiency was slightly higher than the one shown by the Pt based electrode (4.96%). By increasing the deposition time and consequently the thickness of the film, the overall conversion efficiency and current density of the CEs enhanced because of the low charge transfer resistance as well as improved catalytic activity. Ramasamy et al. [161] prepared a MWCNTs based CE on FTO conductive glass through spray coating technique, and a maximum efficiency of 7.59% was attained when the spraying time was increased to 200 second (see **Fig. 8**). This was attributed to the decrease in MWCNTs charge transfer resistance while increasing the spraying time.

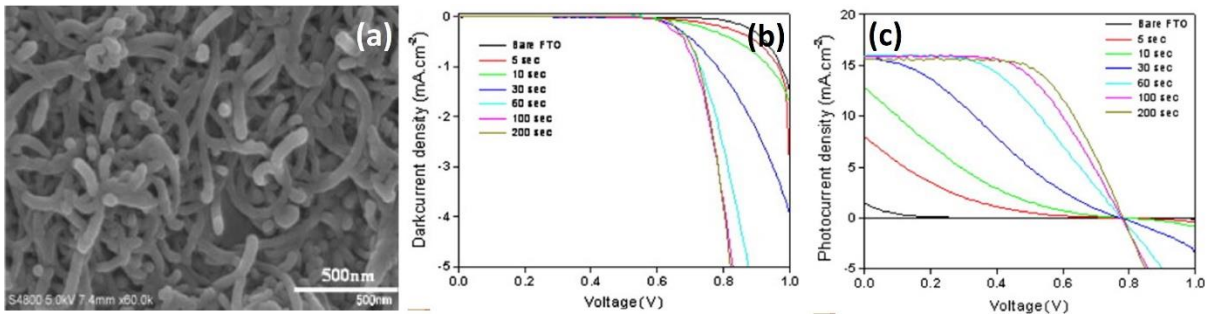

Fig. 8. FESEM image of spray coated MWCNTs film on FTO substrate (a), dark current density voltage (b) and photocurrent density voltage (c) of the DSSCs. (Reproduced wth the permission from Ref. [161], Copyright 2008 Elsevier).

Noticeable research effort has been devoted nowadays to substitute the liquid electrolyte with solid or quasi-solid electrolytes. Sun et al. [162] evaluated the compatibility of a CE based on lipase functionalized MWCNTs coated over FTO with liquid filled, gel filled and pristine electro-spun PVDF-co-hexafluoropropylene (PVDF-HFP) membranes. As discussed above, Lipase functionalization promoted the formation of a uniform highly interconnected defect-rich edges structure. DSSCs PCE values of 6.66% (liquid), 5.77% (gel) and 6.04% (membrane), analogous to the one exhibited by the Pt based CE, were achieved. Similarly, Arbab et al. [163] fabricated a quasi-SS DSSC in which the electrolyte was made up of a 5 wt% PEO gel infused PVDF-HPF membrane. An iodine based redox couple and a TiO_2 based photoanode were used.

The CE was constituted of an ink made by functionalizing MWCNTs with cationic lipase enzyme followed by mixing with CMC and aging overnight. The uniform black ink was then spin coated over a chopped carbon fiber (CFF). The fabricated cell delivered an efficiency of 8.90%, which was slightly lower than that showed by a Pt/CFF based DSSC (9.78%).

Despite nanocrystalline, TiO_2 revealed to be the most efficient photoelectrode material in DSSCs; nevertheless, it suffers low inherent electron mobility. Consequently, materials with better conductivity have been commonly incorporated into TiO_2 or the latter has been replaced with other semiconducting materials displaying a greater mobility, such as ZnO and SnO_2. Recently, MWCNTs have also been investigated as CE material for DSSCs based on such alternative photoanodes. Younas et al. successfully employed MWCNTs as CE for nWO_3-TiO_2 photoanode based DSSCs [164]. A maximum PCE of 6.12%, better than Pt CE (5.18%), was achieved when keeping the concentration of nWO_3 1% in the TiO_2 matrix. Similarly, Siwach et al. used MWCNTs for ZnO-graphene based DSSCs, and an efficiency of 2.04%, which is slightly lower than 3.17% of Pt CE based DSSCs, was obtained [165].

The CNTs based CEs for DSSCs are commonly fabricated either by CVD method or by coating on FTO starting from a dispersion. Both these methods highlight some drawbacks, such as high cost, low scalability for the former while the latter suffers from pre-functionalization, which is essential to prepare a proper dispersion. To address these issues, Bernal et al. have recently employed few layer highly porous and well crystalline interconnected CNT fibers (CNTf), also known as CNTs yarns (CNTY), both as CE and current collector in DSSCs [166] (see **Fig. 9c**). A remarkable PCE of 8.8% was obtained, which was higher than the 8.7% achieved with Pt based CE. Previously, Chen et al. applied aligned carbon nanotubes (ACNTs) fibers as both photo-electrode and CE of DSSCs achieving an efficiency of 2.94%, which was comparable to that of Pt (3.3%) [167] (see **Fig. 9a**). Similarly, Pan et al. [168] has used ACNTs fibers both as photoanode and counter electrode of a DSSC and achieved efficiencies of around 7.33 and

5.97% employing organic thiolate/disulfide and iodine redox couples, respectively (see **Fig. 9b**). The efficiencies were remarkably higher than that obtained with a Pt based CE (2.06%).

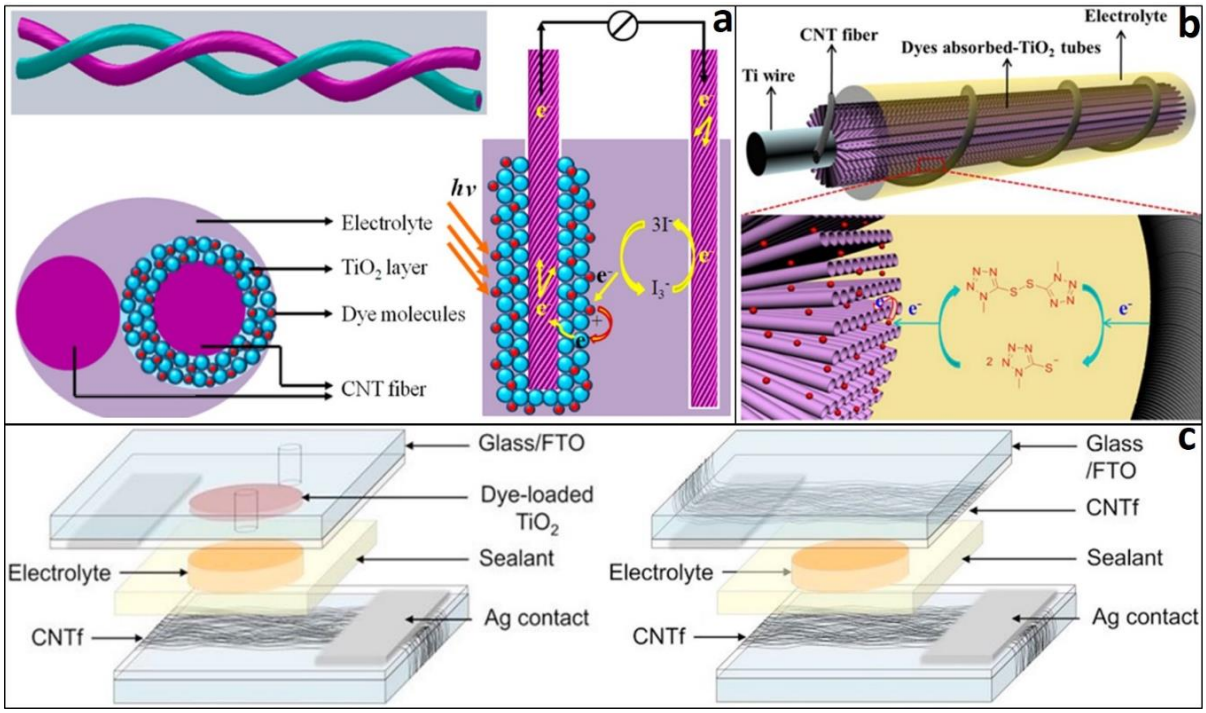

Fig. 9. Schematic illustration of various configurations; a). Wire-shaped DSSC fabricated from two CNT fibers (Reproduced with the permission from Ref. [167], Copyright 2012 ACS Publication), b). Photovoltaic wire with a CNT fiber as the CE. (Reproduced with permission from Ref. [168], Copyright 2013 ACS Publication), and c) Typical and symmetric cells with CNTf based CE (Reproduced with the permission from Ref. [166], Copyright 2019 Elsevier).

To summarize, all the three types of CNTs are thoroughly investigated as CE for DSSCs, but most research is conducted on MWCNTs. The different types of CNTs as well as the same type of CNTs have shown different efficiencies when employed in the solar device. This variation in the photovoltaic performance can be attributed to the different strategies used for their manufacturing, that lead to the presence of different types of impurities and surface areas for catalytic activity and different types of networks for ion diffusion. Comparative study performed by Zhang et al. [151] indicated better results for DWCNTs due to their larger surface area as compared to the other two types of CNTs. However, they show the disadvantage of

high cost in comparison to MWCNTs and do not have a well-commercialized preparation process. SWCNTs represent a good choice but they also possess the disadvantage of having high cost as well as a weak structure stability due to their single wall and small diameter. MWCNTs exhibit small specific surface area and inhomogeneous conductivity, but they can be easily manufactured, are cheap, and are always conductive. Their structure can be easily modified as the outer wall usually interacts only with the attacking reagents, while the integrity of inner walls remains preserved. Various reagents are commonly adopted to modify MWCNTs, such as enzymes, acids, and bases. A comparative study between acid and base functionalized CNTs showed better performance for base functionalized CNTs. Enzyme functionalization is also a good strategy to produce defects-rich highly interconnected and uniform CNTs films with good adhesion to the substrate. The more effective enzyme was found to be lipase, which allowed achieving even better efficiencies than Pt CEs. Aligned, porous, and highly interconnected CNTs morphologies revealed better or comparable results with respect to Pt as they facilitate electron and ion transport, thus leading to lower R_{ct} and higher efficiency. The aligned CNTs are usually manufactured directly over FTO through CVD process. Self-standing CNT yarns having highly interconnected and well crystalline structure also showed better performance than Pt based CEs. The electrocatalytic behavior of MWCNTs is still controversial: some researchers associate it with the defects present in the structure, others with the metallic impurities generated during the manufacturing process. MWCNTs are also employed as CE in SS or quasi-SS DSSCs, in combination with different photoanodes than conventional TiO_2 and cobalt and thiolate based redox shuttles. In all the cases, comparable and even better performance with respect to Pt was obtained.

The main characteristics and the photovoltaic performance of DSSCs assembled with pure and modified CNTs based CEs are reported in **Tab. 1**.

Tab. 1. Main features and photovoltaic performance of DSSCs fabricated with pure and modified CNTs based CEs

No.	**CE material**	**Deposition method**	**Photoanode**	**Sensitizer**	**Redox couple**	**PCE (%)**	**PCE vs Pt (%)**	**Ref.**
1	MWCNTs	Doctor blading	TiO_2	N719	I_3^-/I^-	7.67	7.83	[126]
2	SWCNTs	Drop wise placement on FTO Filtration through membrane	TiO_2	N719	I_3^-/I^-	3.5 4.5	5.4	[140]
3	DWCNTs	Screen printing	TiO_2	D102	I_3^-/I^-	6.05	6.80	[141]
4	DWCNTs	Spray coating	TiO_2	N3	I_3^-/I^-	4.59	3.96	[142]
5	MWCNTs	Screen printing + AJJP calcination	TiO_2	N719	I_3^-/I^-	5.65	n.a.	[143]
6	VA-MWCNTs RO-MWCNTs	CVD Screen printing	TiO_2	N719	I_3^-/I^-	10.04 8.03	8.80	[148]
7	Disordered MWCNTs	Low temperature CVD	TiO_2	N719	I_3^-/I^-	7.13	6.52	[149]
8	CNTY	n.a.	TiO2	N719	I_3^-/I^-	4.00	2.64	[150]
9	SWCNTs DWCNTs MWCNTs	Screen printing	TiO_2	N719	I_3^-/I^-	7.61 8.03 7.06	8.49	[151]
10	f-SWCNTs Ag Paste+f-SWCNTs	Drop casting	TiO_2	N719	I_3^-/I^-	1.2266 1.3037	1.25	[154]
11	MWCNTs Laccase-f-MWCNTs Glucose oxidase-f-MWCNTs Lipase-f-MWCNTs	Doctor blading	TiO_2	D719	I_3^-/I^-	2.89 4.79 5.87 7.52	8.00	[156]
12	MWCNTs MWCNTs-Pt	Doctor blading	ZnO	N749	I_3^-/I^-	2.26 3.78	2.69	[158]

13	MWCNTs (18 cycle film)	Dip and dry coating	ZnO	Eosin-Y	I_3^-/I^-	0.293	0.797	[159]
14	MWCNTs	Aerosol deposition	TiO_2	N719	I_3^-/I^-	5.18	4.96	[160]
15	MWCNTs	Spray coating	TiO_2	N719	I_3^-/I^-	7.59	n.a.	[161]
16	Lipase f-MWCNTs	Doctor blading	TiO_2	D719	Liquid Gel (I_3^-/I^-) Membrane	6.66 5.77 6.04	7.32 6.83 6.53	[162]
17	Cationic lipase f-MWCNTs	Spin coating	TiO_2	N719	I_3^-/I^-	8.90	9.78	[163]
18	MWCNTs	Doctor blading	nWO_3-TiO_2	N719	I_3^-/I^-	6.12	5.18	[164]
19	MWCNTs	Doctor blading	ZnO-GO	D749	I_3^-/I^-	2.04	3.17	[165]
20	Mesoporous CNTs fibers	n.a.	TiO_2	N719	I_3^-/I^-	8.8	8.7	[166]
21	ACNTs fiber	n.a.	CNT-TiO_2	N719	I_3^-/I^-	2.94	3.3	[167]
22	ACNTs fiber	n.a.	TiO_2	N719	I_3^-/I^- thiolate	5.97 7.33	2.06	[168]

3.2 CNTs-polymer composites based CEs

Certain polymers possess electrical conductivity in the range of few to 500 S/cm in the doped state due to the presence of conjugated double bonds [97]. They also exhibit electrocatalytic ability to reduce triiodide ions. Therefore, polymers are commonly combined with CNTs due to their collective benefits including high specific surface area, brilliant electrical conductivity, noticeable electrocatalytic properties, and high durability typical of CNTs, and good flexibility, rich supply, strong adhesion, and easy manufacturing typical of polymers. For this purpose, several conducting polymers, such as Poly(3,4-ethylenedioxxythiophene) (PEDOT) [169] and Polyaniline (PANI) [170] have been used. Due to the different structural features and degree of polymerization of polymers, inconsistent results are observed when the composites are utilized as CE in DSSCs. Several processes have been tested for the CNTs-polymer composites synthesis. Certain non-conducting polymers such as PVP [171] and PVDF [172] are also used as carbon coating source in the preparation of CEs. Polymers can serve various functions in preparing composite CEs. They can be used as conductive agent, dispersant and both carbon source plus dispersant to intensify the properties of CNTs, which can act as either matrix or filler. Electrodes conductivity is strictly affected by the CNTs amount and the thickness of the polymer layer. With decreasing thickness of the polymer layer, the porosity of the film increases, which leads to a better penetration of the electrolyte and reduced diffusion resistance.

Park et al. [171] used PVP as dispersant for synthesizing SWCNTs based CEs (see **Fig. 10**) using a simple casting technique followed by calcination in order to remove binder and convert PVP, which was wrapped smoothly around SWCNTs into carbon. The PVP presence resulted in a smooth and uniform film without aggregation of CNTs. The film was subsequently employed as CE of a DSSC and showed a PCE of 4.5%, which was higher than that exhibited by the bare SWCNTs film (2.34%). The improved PCE can be attributed to the lower charge transfer resistance induced by the presence of PVP.

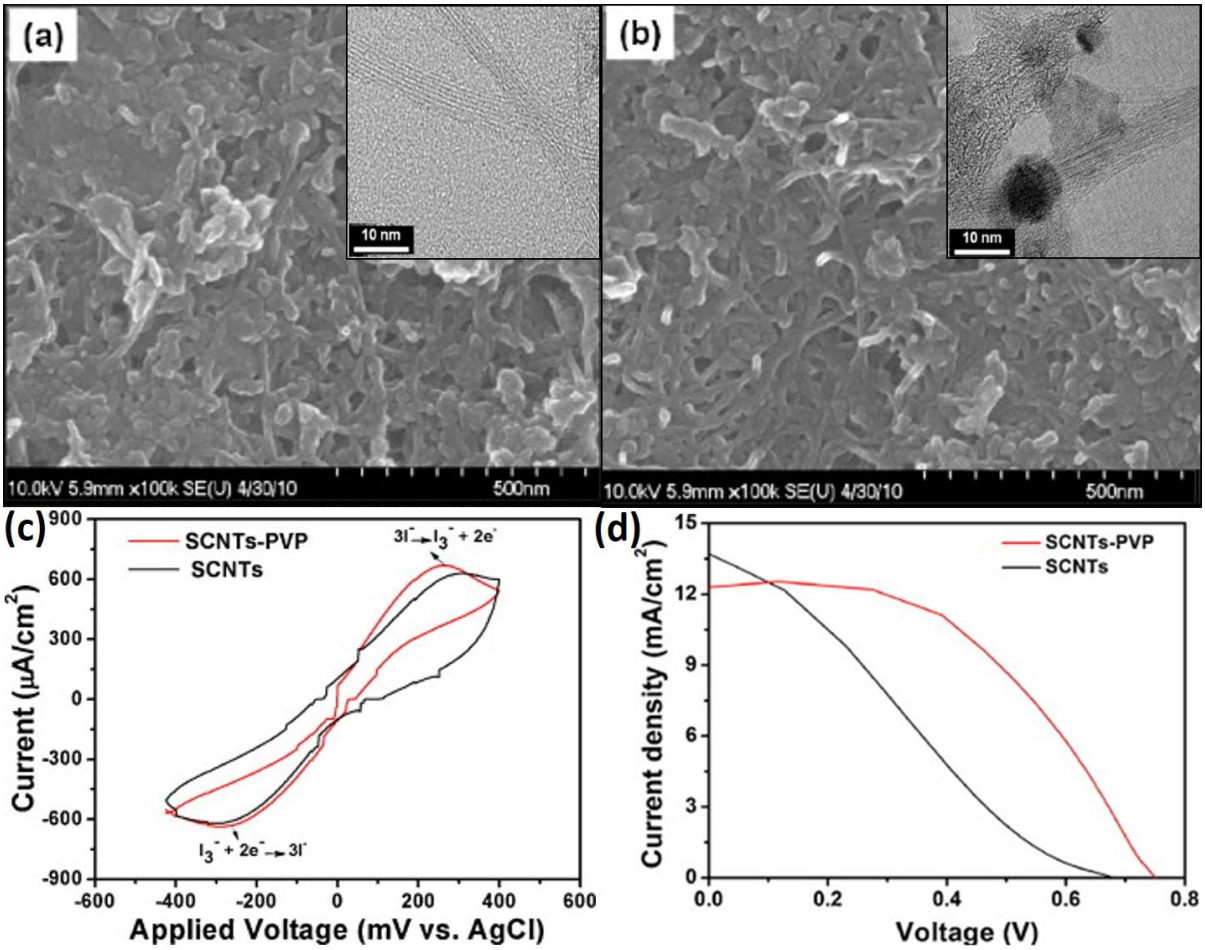

Fig. 10. SEM and TEM (inset) images of SWCNTs based electrodes without (a) and with (b) PVP, cyclic voltammetry in acetonitrile (c), and J-V curve of DSSCs under light intensity of 100 mW/cm^2 (d). (Reproduced with the permission from Ref. [171], Copyright 2012 Elsevier)

Hi et al. [173] prepared covalently bonded SWCNTs/PPy composites by mixing pyrrole with SWCNTs through refluxing followed by in-situ polymerization. Different concentrations of SWCNTs were added and a maximum PCE of 8.30% was obtained with a concentration as high as 2.0 wt %. The better performance with respect to the one showed by bare PPy (PCE~6.31%) was attributed to the lower charge transfer resistance. With SWCNTs, PPy and PANI are found to be the main conductive polymers for CE fabrication through in-situ electrochemical polymerization. Better results were obtained for PPy polymer. Li et al. synthesized honeycomb PPy using sacrificial template method. PMMA was deposited by spin coating technique over an acid functionalized MWCNTs-FTO substrate followed by

dissolution in chloroform solvent after electrodeposition of PPy [174]. The obtained CE was applied in bifacial DSSCs. The efficiencies for front and rare illuminations were 7.07 and 4.11%, respectively, which were higher than that obtained with flat PPy.

Recently, Lee et al. synthesized a PPy/MWCNT/SDS based CE using electrochemical polymerization and applied it in DSSCs and SS-DSSCs obtaining PCEs of 6.15 and 1.79%, respectively. These values are comparable to those exhibited by Pt CE, i.e. 6.36% in DSSCs and 2.5% in SS-DSSCs. The EIS data revealed low charge transfer resistance at the interface between the electrolyte and CE and enhanced electrocatalytic activity for the electrolyte [175]. MWCNTs-PPy composites were fabricated and employed as DSSCs CE by Hou et al. (see **Fig. 11**). The MWCNTs were spin-coated on FTO substrate, while the PPy was electrodeposited on MWCNT layer by means of a CVD technique. An excellent PCE of 7.15% was obtained, that can be attributed to the enhanced catalytic activity due to the presence of PPy [176].

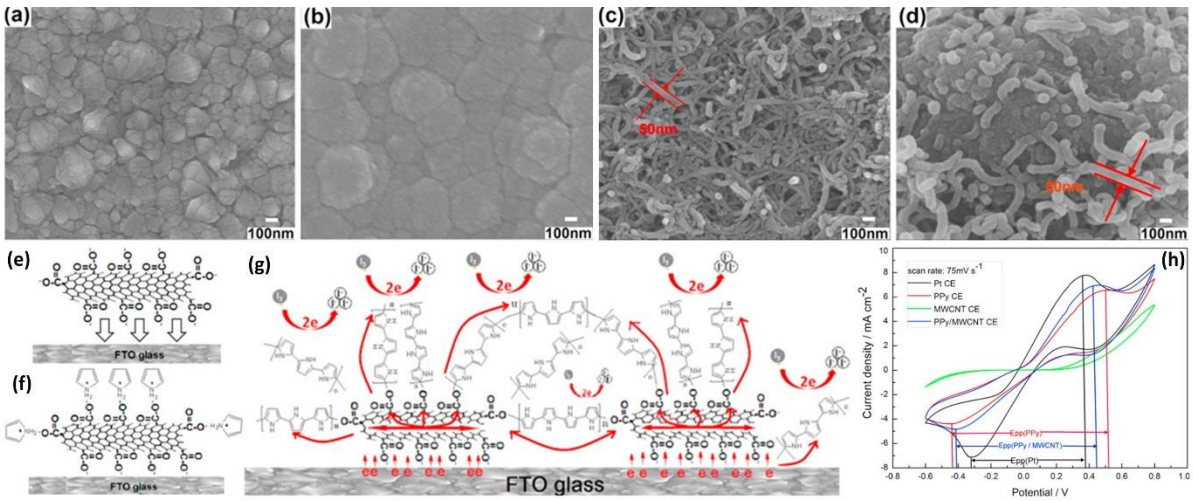

Fig. 11. SEM images of the bare FTO (a), PPy (b), MWCNTs (c), and PPy/MWCNT (d) based CEs. Schematic diagrams of the MWCNTs preparing on the FTO substrate (e), Pyrrole monomer absorbing on the surface of the MWCNTs (f), catalytic mechanism of PPy onto the MWCNTs (g), cyclic voltammetry at 75 mV s^{-1} scan rate (h). (Reproduced with the permission from Ref. [176], Copyright 2016 Elsevier).

Recently, Rafique et al. synthesized Cu-PPy acid functionalized MWCNTs by two-step electrochemical deposition method on stainless steel substrate and utilized them as CE in DSSCs. An efficiency of 7.1% was obtained, which was greater than that shown by Pt CE (6.48%). This was attributed to the presence of Cu in the structure, which led to higher current density and low charge transfer resistance as indicated by Tafel and EIS results [177].

MWCNTs were also applied as filler or matrix with different polymers including PEDOT, PEDOT:PSS, PANI etc. PEDOT:PSS can be used to improve the dispersion of MWCNTs in the solvent as well as their electronic conductivity. Fan et al. fabricated CEs by using MWCNTs dispersion prepared with the help of PEDOT:PSS or polystyrene sulfonate acid (PSSA) as dispersing agent [178]. The solution was coated over FTO utilizing spin coating technique and the DSSC efficiencies obtained with the two different dispersants were 6.5 and 3.6%, respectively. The difference between the PCEs of the two dispersants containing composites is linked with the different nature of the interactions involved. The π-π interactions present in the PEDOT:PSS containing composite are responsible for the increase in the electron transport, while PSSA containing composite is featured by hydrophobic interactions which lead to an insulating barrier for electron transport, as PSSA itself is non-conducting. The efficiencies were lower than that showed by the Pt based CE (8.5%) but still promising. Shin et al. developed CNT/PEDOT composite based CE for DSSCs by chemical oxidative polymerization using iron chloride ($FeCl_3$) and dodecyl benzene sulfonic acid (DBSA) as oxidant and surfactant, respectively [179] (see **Fig. 12**). PVDF was employed as a binder and the viscous paste obtained was directly painted over FTO for CE fabrication. An enhanced PCE of about 4.62% was achieved, in comparison to those obtained with pure CNT (3.88%) and PEDOT (4.32%).

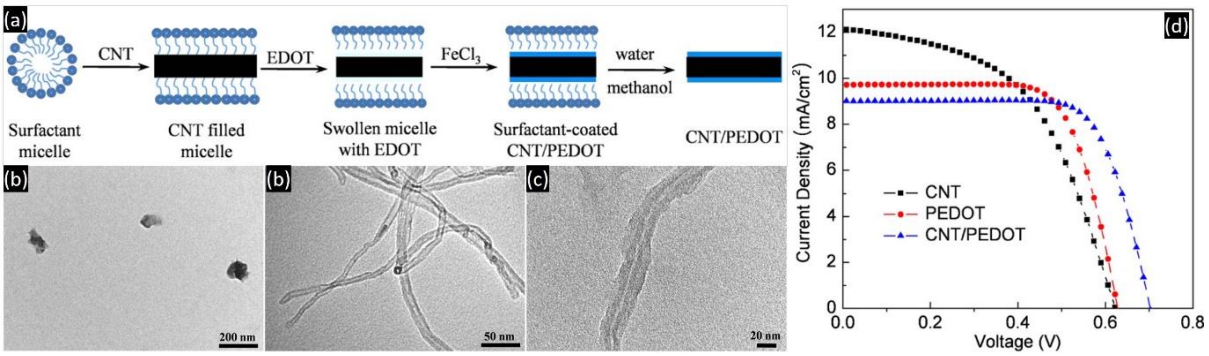

Fig. 12. Schematic illustration for the synthesis of CNT/PEDOT core/shell nanostructures (a). TEM images of PEDOT (b), CNTs (c), and the CNT/PEDOT (d) nanostructures. J-V curves of DSSCs using various CE materials (e). Reproduced with the permission from Ref. [179], Copyright 2011 Elsevier)

Lee et al. also prepared PEDOT and PEDOT/MWCNTs based CEs for application in DSSCs [180]. The efficiency achieved with PEDOT was 7.44% when PEDOT/imidazole was kept equal to 2.0. The efficiency was slightly lower than that exhibited by Pt-sputtered electrode (7.77%) which may be attributed to the increase in the reaction rate of the redox couple regeneration because of the large specific surface area. They further incorporated MWCNTs into PEDOT and spin coated them on different substrates at different spin rates. The highest efficiency of 8.08% was achieved with stainless steel substrate at a spin rate of 370 rpm and MWCNTs concentration of 0.6%. Ali et al. modified a highly aligned MWCNTs fiber using PEDOT:PSS conductive polymer and subsequently fabricated a CE through a simple dip coating method to be applied in DSSC [181]. Modified MWCNTs based CE exhibited a noticeable improvement in catalytic performance in comparison to the pristine MWCNTs fiber electrode and led to an overall conversion efficiency of 5.03%, slightly higher than that obtained in presence of a traditional Pt electrode (4.98%). Good photovoltaic performance even after bending up to 90° was also successfully obtained. Li et al. prepared a honeycomb PEDOT/MWCNTs based CE by using spin coating technique for MWCNTs and polymethyl methacrylate (PMMA) deposition followed by electrodeposition of PEDOT [182] (see **Fig.**

13). The dissolution of PMMA in chloroform gave rise to the honeycomb morphology. The as-prepared film was employed as CE in bifacial DSSCs. High efficiencies equal to 9.07 and 5.62% were achieved for front and rare illumination, respectively, in comparison to 7.51 and 3.49% obtained in presence of the bare PEDOT CE.

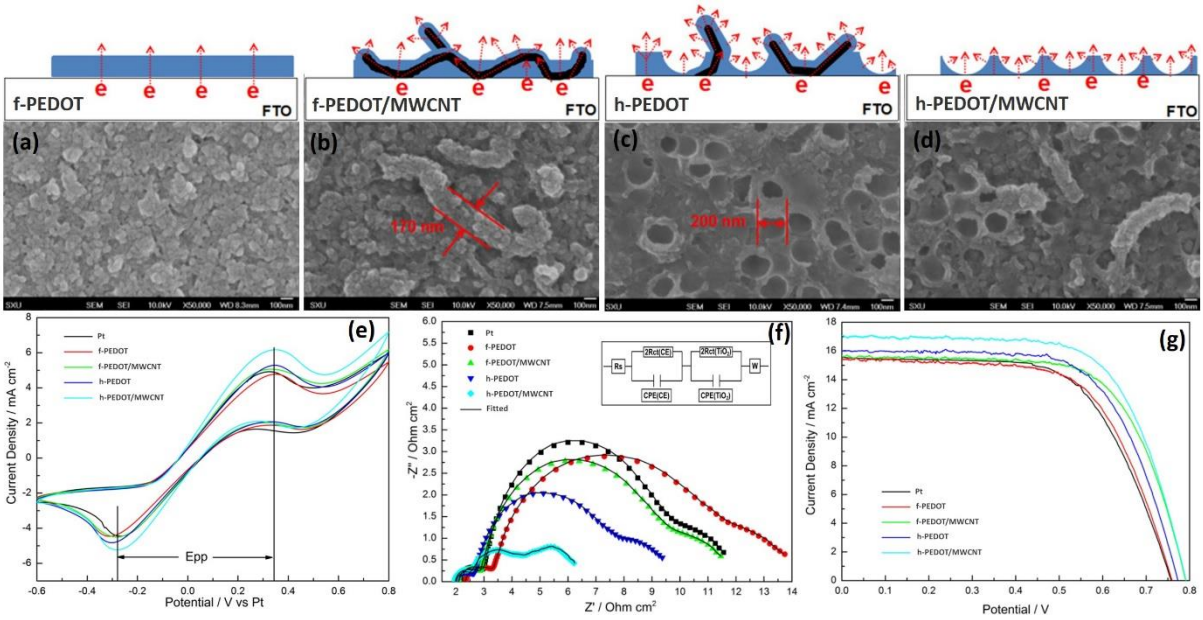

Fig. 13. SEM images and electron transport paths in f-PEDOT (a), f-PEDOT/MWCNT (b), h-PEDOT (c) and h-PEDOT/MWCNT (d) based CEs. Cyclic voltammetry (e), Nyquist plots (f) and J-V characteristics (g) of DSSCs under front illumination. (Reproduced with the permission from Ref. [182], Copyright 2017 Elsevier)

Recently, Samir et al. prepared PANI-SWCNTs electrode through an in-situ electrochemical polymerization obtained an efficiency of 1.55%, that was better than 0.64% of bare PANI [183]. Similarly, Bumika et al. prepared a -COOH functionalized SWCNT-PANI-ZnO composite and employed it as CE in DSSCs. They used functionalized SWCNTs dispersion obtained through the use of sodium dodecyl benzene sulfonate (SDBS) surfactant, which was added into a solution containing ZnO and aniline. This solution was stirred overnight and coated over FTO through electrochemical polymerization. They obtained an efficiency of 3.81% for the ternary composite, which was higher than that shown by the binary SWCNTs-

ZnO composite (3.16%) [184]. The results were supported by the EIS analysis that showed a reduced charge transfer resistance for both the fabricated composite CEs. Wu et. al. [185] prepared a PANI-MWCNTs based CE doped with different cations by coating MWCNTs via an airbrush spraying technique followed by electropolymerziation of aniline monomer containing different cations (see **Fig. 14**). The presence of Ni^{2+} and Co^{2+} ions improved the catalytic activity, while Cu^{2+} showed the opposite effect and Mn^{2+} showed no effect. The highest DSSC efficiency of 6.00% was achieved with Ni^{2+}-doped MWCNTs-PANI CE. These distinct behaviors can be probably attributed to the different doping procedures used for metal ions, which are strongly influenced by the empty d-orbital of the metal. Ni^{2+} and Co^{2+} can form a typical octahedral structure with ammonium cationic ligands favorable for electron transport. Conversely, Mn^{2+} exhibits a tetrahedral structure with ammonium cationic ligands and Cu^{2+} establishes a planar structure with the ligands, which retards the electron transport.

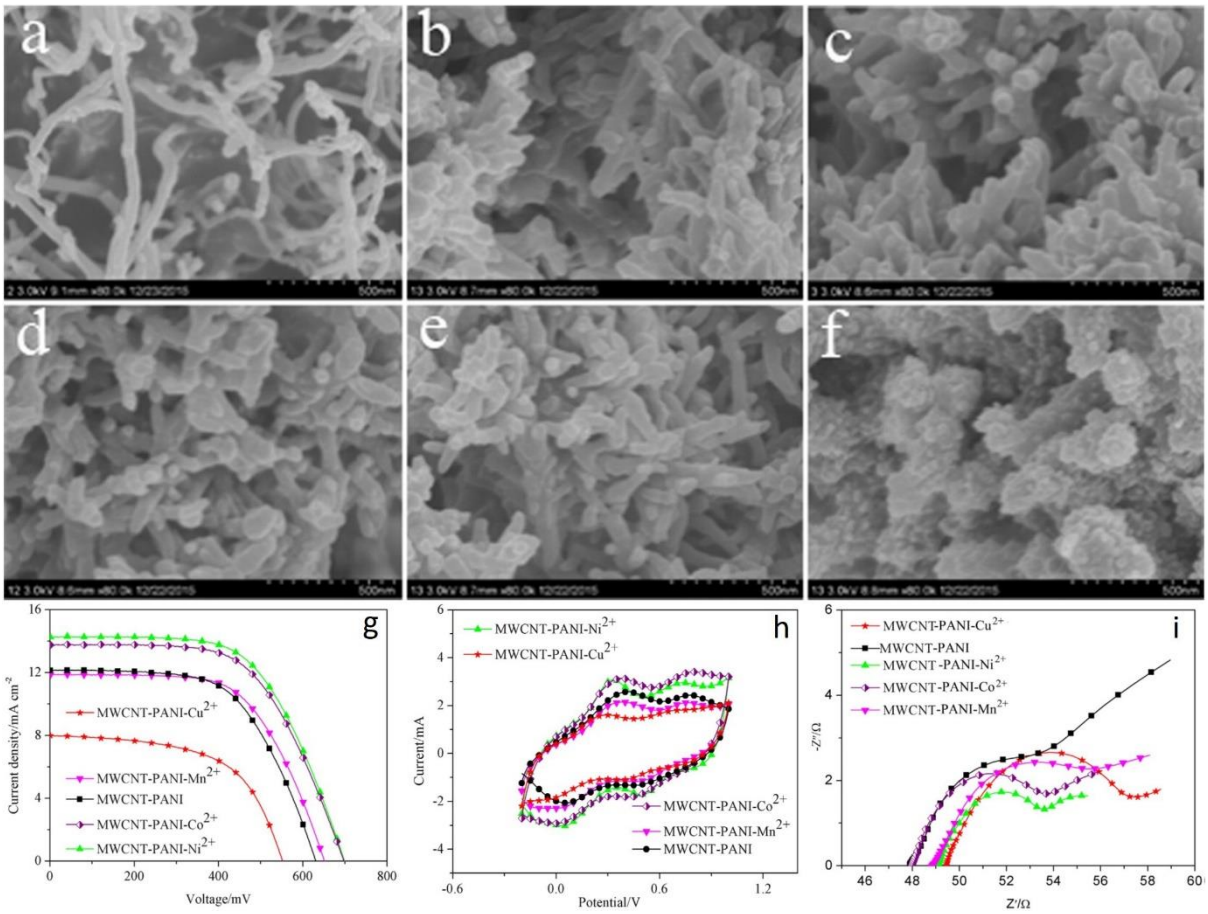

Fig. 14. SEM images of MWCNT (a), MWCNT-PANI (b), MWCNT-PANI-Ni^{2+} (c), MWCNT-PANI-Co^{2+} (d), MWCNT-PANI-Mn^{2+} (e), and MWCNT-PANI-Cu^{2+} (f). J-V characteristic curves of DSSCs (g), CV of symmetrical cells (h), and Nyquist plots (i) of different CEs. (Reproduced with the permission from Ref [185], Copyright 2016 Elsevier)

Other complex polymers are also used for functionalization of MWCNTs. Choi et al. used pyrene functionalized block copolymer poly(maleic acid-co-phydroxystyrene)-block-poly(p-hydroxystyrene) (HSPM) for functionalization of MWCNTs and obtained an efficiency of 5.94%, which was slightly higher than that achieved with a bare CNTs (10 wt%) based CE fabricated by screen printing technique (5.69%) [186]. Chew et al. [187] also prepared gel polymer electrolyte based DSSCs and tested their efficiencies using a CE made up of MWCNTs mixed with polyvinylpyrrolidone-co-vinyl acetate and coated on FTO using two techniques, i.e. spin coating and dropping methods. The electrolyte consisted of sodium iodide salt, polyacrylonitrile polymer, and 1-Hexyl-3-methyl-imidazolium iodide ionic liquid. The obtained efficiencies were 7.07 and 4.25% for spin coating and dropping methods, respectively, which revealed to be higher and then the one achieved with Pt based CE (5.75%).

Recently, Nguyen et al. [188] prepared flexible CE based on CNT mixed with polydiallyldimethylammonium chloride (PDDA), which was deposited over a flexible stainless steel mesh substrate through electrophoresis deposition. The fabricated CE was used in quasi-solid DSSCs made of TiO_2 photo anode, organic MK-2 dye, and PMMA iodide/triiodide redox couple. The resulted device showed an efficiency of 2.5%.

Tab. 2 details the main characteristics and the photovoltaic performance of DSSCs assembled with CNTs-polymer composites based CEs.

Tab. 2. Main features and photovoltaic performance of DSSCs fabricated with CNTs-polymer composites based CEs

No.	CE material	Deposition method	Photoanode	Sensitizer	Redox couple	PCE (%)	PCE vs Pt (%)	Ref.
1	SWCNTs SWCNTs-PVP (1%)	Simple casting	TiO_2	N719	I_3^-/I^-	2.4 4.5	n.a.	[171]
2	PPy PPy-SWCNTs (2%)	In-situ polymerization over FTO	TiO_2	N719	I_3^-/I^-	6.03 8.30	n.a.	[173]
3	flat-PPy MWCNTs-f-PPy honeycomb-PPy MWCNTs-h-PPy	Spin coating and electrodeposition	TiO_2	N719	I_3^-/I^-	5.78 6.18 6.32 7.07	n.a.	[174]
4	PPy-SDS-DSSCs PPy-fMWCNTs-SDS-DSSCs PPy-SDS-ssDSSCs PPy-fMWCNTs-SDS-ssDSSCs	Electro polymerization	TiO_2	N719	I_3^-/I^-	5.84 6.15 1.64 1.79	6.36 2.5 	[175]
5	PPy MWCNT PPy-MWCNTs	Spin coating and electrodeposition	TiO_2	N719	I_3^-/I^-	5.72 1.72 7.15	7.76	[176]
6	PPy PPy-FMWCNTs Cu- PPy-FMWCNTs	Two step electrodeposition on Stainless steel	TiO_2	N719	I_3^-/I^-	3.04 5.49 7.1	6.48	[177]
7	PSSA-MWCNTs PEDOT:PSS-MWCNTs	Spin coating	TiO_2	N719	I_3^-/I^-	3.6 6.5	8.5	[178]
8	MWCNTs PEDOT MWCNTs-PEDOT	Simple casting	TiO_2	N719	I_3^-/I^-	3.88 4.32 4.62	n.a.	[179]
9	PEDOT	Spin coating	TiO_2	N3	I_3^-/I^-	7.44	8.08	[180]

	PEDOT-MWCNTs (0.6%)					7.77		
10	AMWCNTs fiber PEDOT:PSS modified MWCNTs fibers	Dip coating	TiO_2	N719	I_3^-/I^-	2.79 5.03	4.98	[181]
11	PEDOT PEDOT-MWCNTs	Spin coating and electrodeposition	TiO_2	N719	I_3^-/I^-	7.51 9.07	7.71	[182]
12	fSWCNT-PANI fSWCNT-PANI-ZnO	One pot electrochemical polymerization	TiO2	N719	I_3^-/I^-	3.16 3.81	n.a	[184]
13	MWCNT-PANI MWCNT-PANI-Ni^{2+} MWCNT-PANI-Co^{2+} MWCNT-PANI-Mn^{2+} MWCNT-PANI-Cu^{2+}	Coating over FTO with air brush followed by electropolymerization	TiO_2	N719	I_3^-/I^-	4.58 6.00 5.75 4.77 2.57	n.a.	[185]
14	MWCNT-10% MWCNT-HSPM (10/5%)	Screen printing	TiO_2	N719	I_3^-/I^-	5.69 5.94	7.15	[186]
15	MWCNTs	Spin coating Dropping method	TiO_2	N719	I_3^-/I^-	4.25 7.07	5.75	[187]
16	MWCNTs PPy-DBSNa PPy-MWCNTs-DBSNa	Doctor blading and electropolymerization	TiO_2	N719	I_3^-/I^-	2.50 2.75 2.89	4.92	[189]
17	PEDOT:PSS-MWCNTs	Spin coating	TiO_2	N719	I_3^-/I^-	6.1	n.a.	[190]
18	ACNTs ACNTs-PEDOT:PSS ACNTs-Triton-X100 ACNTs-Both	Doctor blading	TiO_2	N719	I_3^-/I^-	2.96 3.85 3.22 3.58	n.a.	[191]
19	MWCNTs PDDA-MWCNTs	Spin coating	TiO_2	N719	I_3^-/I^-	4.48 5.66	6.73	[192]

3.3 CNTs-Transition metal compounds composites based CEs

Transition metal compounds commonly show high catalytic activity but suffer from low conductivity. To overcome this drawback, they are employed in combination with other conductive materials for the fabrication of CEs. Due to their high conductivity, CNTs are a promising material to be incorporated in metal compounds to enhance the cell performance. A number of metal compounds are used for the CE application. The most common oxides include nickel oxide (NiO) [193], tungsten oxide (WO_2) [194], lanthanum oxide (La_2O_3), and sulfides include nickel sulfide (NiS) [195], cobalt sulfide (CoS) [196], tungsten sulfide (WS_2) [197], molybdenum sulfide (MoS2) [198], vanadium sulfide (VS_2) [199] and bismuth sulfide (Bi_2S_3) [200]. Some reports on nitrides[201] and selenides [202]are also present.

Wu et al. [197] fabricated a CE based on glucose aided WS_2-MWCNTs hybrid by hydrothermal process and gained an efficiency of 7.36%. The as-prepared CE exhibited higher surface area and decreased charge transport resistance, which were responsible for an improved catalytic activity comparable to that showed by the Pt based CE. Because of promising results shown by WS_2, other group members combined with CNTs were also studied as CE materials for DSSCs. Tai et al. fabricated MWCNTs-MoS_2 NCs and used it as CE in DSSCs [203]. The synthesis of the catalyst was carried out via simple blending of MoS_2 and MWCNTs into an acidic solution followed by the transformation of the compact intermediate into MWCNT-MoS_2 NCs at an elevated temperature of 650°C in hydrogen flow. The prepared CE revealed an enhanced efficiency of 6.45%, analogous to the 6.41% shown by Pt CE. Recently, Theerthagiri et al. [204] developed flower-like MoS_2 microspheres by using hydrothermal technique that was subsequently mixed with different carbon based materials in order to increase their conductivity. An efficiency as high as 3.17% was reached with the carbon nanofibers based CE, followed by the one based on MWCNTs (3.08%). Theerthagiri et al. [205] also suggested NiS-MWCNTs composite could also be used as cost-effective CE for the fabrication of Pt-free DSSCs.

Recently, Maiaugree et al. decorated Ni_3S_2 over MWCNTs and coated over FTO by hydrothermal procedure. The CE delivered an efficiency of 7.48%, which was even higher than Pt based CE. This was attributed to the increase in active surface area for triiodide reduction and decrease in charge transfer resistance [206]. Lu et al. [207] prepared various DSSCs CE materials, namely Pt, Ni_3S_2, MWCNTs Ni_3S_2/MWCNTs composite, through hydrothermal method and subsequently analyzed their performance (see **Fig. 15**). The highest PCE of 6.87% was achieved with the Ni_3S_2/MWCNTs composite. This value resulted to be higher than the ones obtained with MWCNTs and Ni_3S_2 electrodes taken individually and almost equivalent to the one attained with Pt based CE.

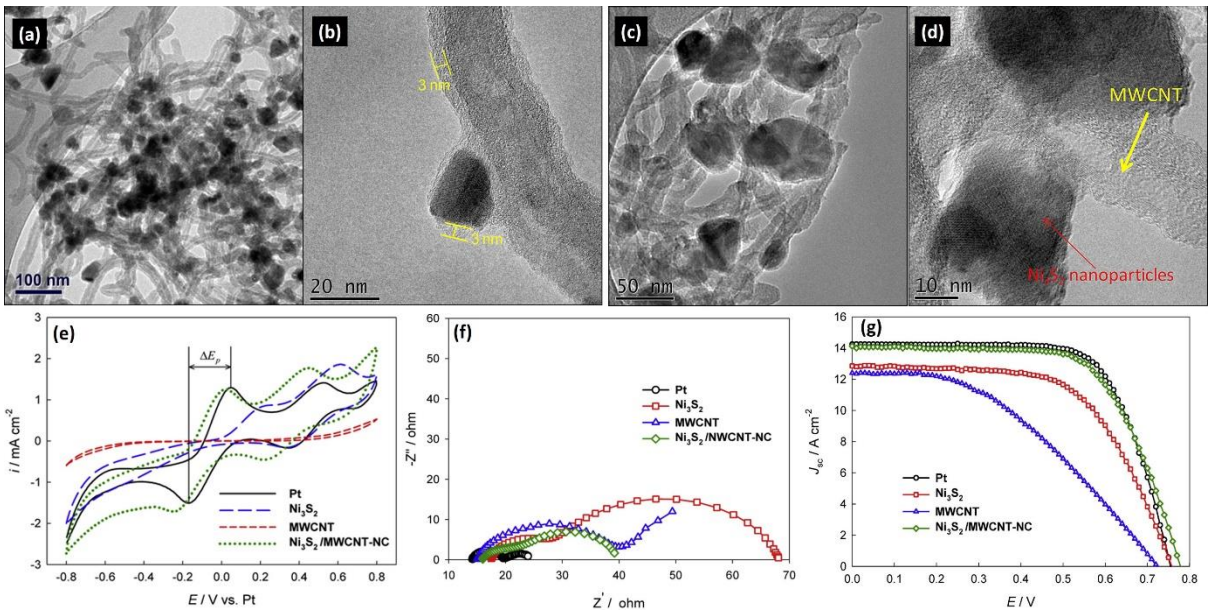

Fig. 15. HR-TEM images of un-annealed (a and b), and annealed (c and d) Ni_3S_2/MWCNT-NCs, CV curves of I_2/I_3^- system (e), Nyquist plots (f), J-V curves (g) of the symmetrical DSSCs assembled with the various CEs. (Reproduced with the permission from Ref. [207], Copyright 2014 Elsevier)

VS_2/CNTs NCs were employed as CE for DSSCs by Yue et al. [199]. An in situ hydrothermal technique was used for the fabrication of the composite material and doctor blading technique for coating the material over FTO. A promising PCE of 8.02%, far higher than that obtained by using a Pt based CE (6.49%), was achieved because of high catalytic activity at the electrode-electrolyte interface. Tai et al. [208] synthesized NCs constituted of carbon

nanotubes and cobalt sulfide in two different forms, i.e. CNT@Co_9S_8 and CNT@$CoS_{1.097}$. Both of the forms were prepared on a conducting glass substrate with the help of simple and straightforward spray coating technique and then annealed in nitrogen atmosphere at 400°C and 600°C, respectively. Despite its comparatively lower surface area, the CNT@Co_9S_8 CE displayed improved electrocatalytic performance as compared to CNT@$CoS_{1.097}$ based CE. As a result, CNT@Co_9S_8 CE based DSSCs exhibited a noticeable efficiency of 7.78%, which was greater than that obtained with CNT@$CoS_{1.097}$ NC CE based (7.29%) and Pt based CE (7.46%).

Memon et al. [200] also prepared a Bi_2S_3-MWCNTs composite based CEs by tape casting over FTO substrate and employed it in quasi-solid state DSSCs. The heteromaterials were mixed in different ratios and a highest PCE of 8.24%, comparable to that achieved with Pt CE (8.47%), was obtained when MWCNTs were kept at 0.8 wt%. Peter et al. [209] synthesized Sb_2S_3 nanorods-MWCNTs composite materials by using microwave irradiation method. They were utilized as CE in DSSCs and a remarkable efficiency of 5.02% was achieved when the composite contained 30 mg MWCNTs. The efficiency was comparable to that of Pt based CE, which was due to the faster reaction kinetics and stronger electro catalytic behavior as revealed by Tafel and EIS analysis. Furthermore, CuS-MWCNTs composite in different ratios were prepared by Zhang et al. and deposited over FTO to be used as CEs in quasi-solid state DSSCs. A maximum PCE of 5.254% higher than that achieved with Pt (PCE~2.680%) was observed when CuS content was kept at 100 wt%. The better PCE of the above mentioned electrode with respect to the standard Pt based one was attributed to its greater catalytic activity and lower charge transfer resistance [210]. Similarly, Lin et al. [211] prepared a CoS-MWCNTs composite based CE for application in DSSCs. MWCNTs were oxidized and deposited over FTO through electrophoresis followed by cathodic deposition of CoS (see **Fig. 16**). The DSSC made with such CE delivered an efficiency of 6.96%, which was higher than the one achieved in presence of a Pt-sputtered CE (5.99%).

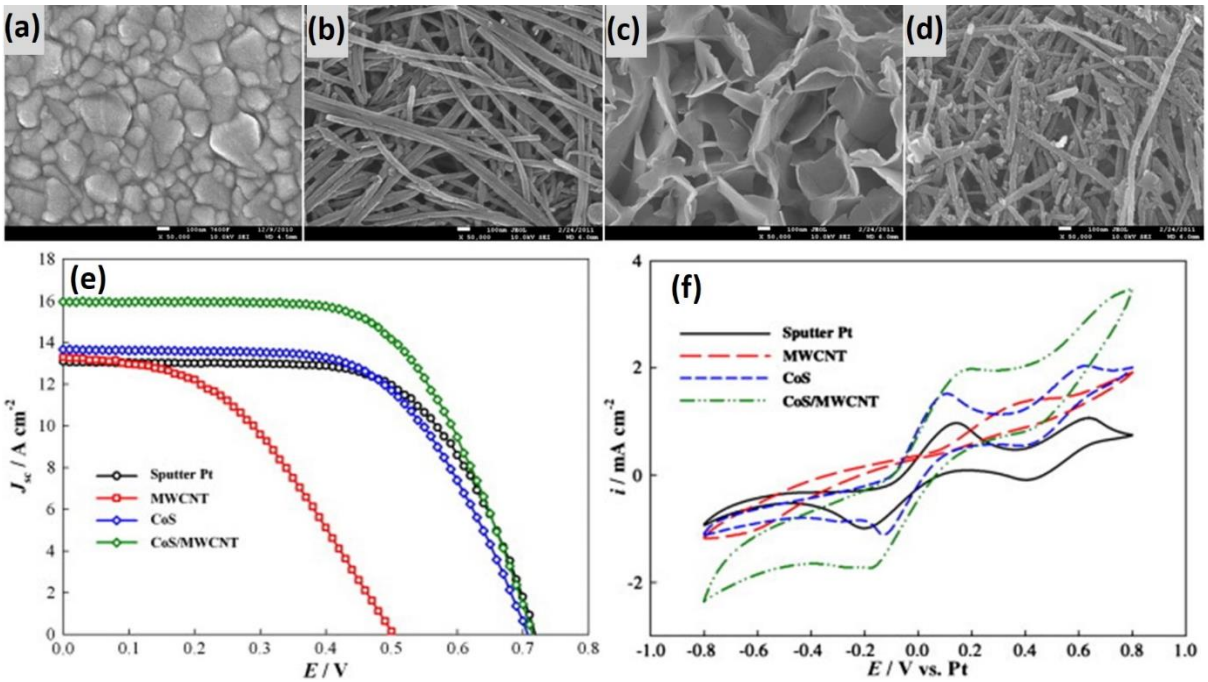

Fig. 16. SEM images of various thin film materials a) Sputtered Pt, b) MWCNTs, c) CoS, and d) CoS/MWCNT, e) J-V characteristics, and f) CV at a scan rate of 10 mVs^{-1}. (Reproduced with the permission from Ref. [211] Copyright 2011 Elsevier)

Beside sulfides, transition metal oxides are also used as CEs. Mehmood et al. synthesized MWCNTs-TiO_2 NC in which TiO_2 acted as binder while MWCNTs provided catalytic activity. They obtained an efficiency of 8.81 % when the concentration of MWCNTs in the composite was increased to 4%. The results were found comparable to Pt (9.40%) [212]. Recently, compounds that were rarely investigated such as La_2O_3 were employed as CE layer for DSSCs in combination with MWCNTs. Wu et al. prepared various La_2O_3-MWCNTs based NCs and employed them in DSSCs as CE. La_2O_3 was synthesized through solid phase reaction followed by mixing with MWCNTs in different ratios, i.e. 5:1, 3:1 and 1:1, by ball milling. The as-obtained composite was finally spray coated over FTO substrate and a maximum PCE of 5.20% was achieved when the La_2O_3-MWCNTs ratio was kept at 5:1. The PCE of all the prepared composites was higher than the one showed by the Pt based electrode (4.54%) [213]. The synthesis of a CE based on the composite of MWCNTs and NiO using a hydrothermal method

was performed by Al-bahrani et al. [214] (see **Fig. 17**). The NiO nano filament (NF) coated on the MWCNTs was verified through various structural and morphological techniques. The NiO-NF/MWCNTs composite showed high catalytic activity because of high surface area and low charge transfer resistance at the interface between the CE and the electrolyte. A PCE of 7.63% was achieved, which is higher than showed by the Pt (6.72%) when employed as CE in DSSCs.

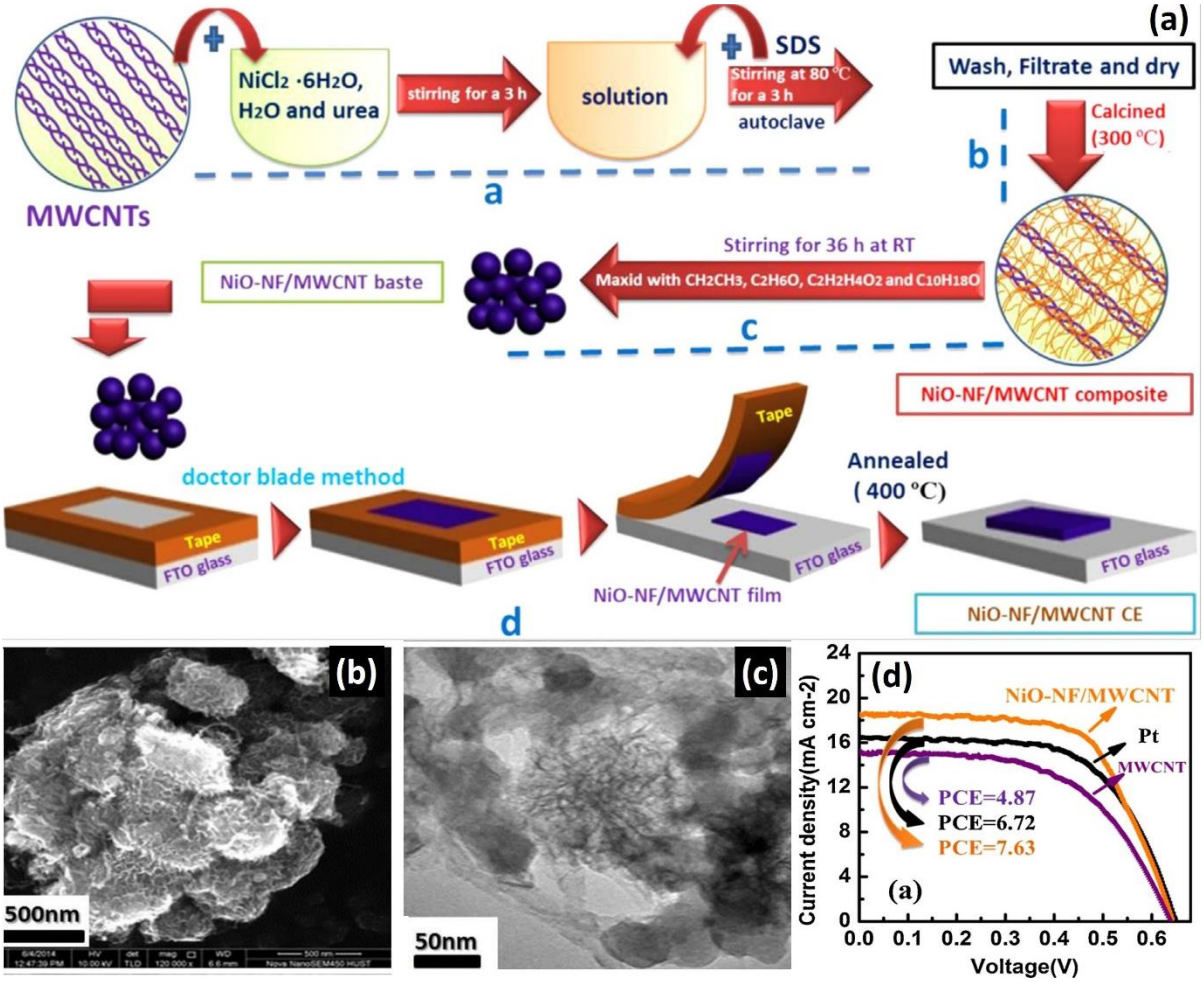

Fig. 17. Schematic illustration of the preparation of NiO-NF/MWCNT CE (a), SEM (b) and TEM (c) Images of NiO-NF/MWCNT composite, J-V characteristics of the various CEs (d). (Reproduced with the permission from Ref [214], Copyright 2015 Elsevier)

Singh et al. prepared Ni^{2+} enriched NiO and Ni_2S_3-MWCNTs NCs using hydrothermal technique and utilized them as CE in DSSCs. They obtained better efficiency for NiO based composite having an efficiency of 3.80% among all other electrodes, which was found comparable to Pt. This was attributed

to the presence of higher content of Ni^{2+} ions as well as greater surface area of 286.10 m^2/g which provided more active sites to the reduction of electrolyte and thus improved efficiency [215].

Metal sulfides and oxide possess low inherent electrical conductivity and two-fixed chemical composition. To overcome these problems researchers tried to synthesize multinary transition metal chalcogenides by adjusting component elements, engineering morphology, and structure designing. Therefore, Saravanakumar et al. prepared thiospinal like nickel tin sulfide (NixSn2xS4x) composited with MWCNTs by hydrothermal as well as co-precipitation method to form CEs for DSSCs. An efficiency of 4.76% was achieved for hydrothermally synthesized MWCNTs containing 20 wt. % MWCNTs. The efficiency was comparable to that of Pt, which was attributed to the rapid charge transfer at the electrode/electrolyte interface due to the presence of MWCNTs in the composite sample [216]. Similarly, Yue et al. prepared hedgehog ball structure $MoIn_2S_4$-MWCNTs composites using hydrothermal technique and utilized them as CE in DSSCs. A high efficiency of 8.38% was achieved for the composite containing 20 mg MWCNTs. The efficiency was higher than Pt based CE, which was attributed to high specific surface area of the composite sample and low charge transfer resistance that enhanced the electrocatalytic activity [217]. Likewise, in another work Di et al. synthesized NiCoP-MWCNTs composite using hydrothermal method followed by phosphorization. Different mass dosages of Ni^{2+} and Co^{2+} were used but their ratio was kept to 1:1. The best efficiency of 7.24% was achieved when the mass dosage used was 15 mM. The efficiency was higher than Pt electrode, which was attributed to the synergistic effects of both components. [218]

Polyoxometalates (POMs) covers a class of molecular clusters of transition metal oxides of V. Mo, W, Co etc. they possess well defined structures and can undergo multi-electron reduction with little modification in structure, therefore are regraded as remarkable active materials in catalysis. Wang et al. have thus prepared a number of structurally and functionally robust POMs/CNTs composites including PMo12-CNTs, P2Mo18-CNTs. PW12-CNTs, P2W18-

CNTs and Co4PW9-CNTs. They were achieved by Nano patterning various POMs on the surface of CNTs through a simple ultrasonic driving mechanism. They achieved remarkable efficiency of 7.60% for Co4PW9-CNTs, which was higher than Pt electrode. This was attributed to the synergistic effect of CNTs conductivity and POMs electrocatalytic ability. The CEs show remarkable cycling stability with almost no decay after 34 days.[219]

Similarly, carbon nanotube aerogel (CAN) and CoS_2 nanoparticle based hybrid CE was prepared by Liu et al. This novel CAN-CoS_2 CE showed a high PCE 8.92% than the conventional Pt based CE 7.32% because of the fast ion diffusion and electron transport [220]. In a very interesting work, Lee et al. synthesized MWCNTs and SWCNTs based CEs for DSSCs starting from a powder of CNTs mixed with $PtCl_4$ solution and an electrolyte [221]. To increase the total conversion efficiency, CNTs were incorporated into the treated $PtCl_4$ electrode and into the electrolyte. The highest efficiency value of 4.36% was attained with the MWCNTs electrode. The SWCNTs and MWCNTs based films were prepared through arc discharge and chemical vapor deposition methods, respectively.

Tab. 3 reports the main characteristics and the photovoltaic performance of DSSCs fabricated with CNTs-transition metal compounds composites based CEs.

Tab. 3. Main features and photovoltaic performance of DSSCs assembled with Transition metal compound-CNTs based CEs.

No.	CE Material	Deposition method	Photoanode	Sensitizer	Redox couple	PCE (%)	PCE vs Pt (%)	Ref.
1	WS_2 MWCNTs (G-A)WS_2-MWCNTs	Doctor blading	TiO_2	N719	I_3^-/I^-	5.32 4.34 7.36	7.54	[197]
2	VS_2 VS_2-CNTs	Doctor blading	TiO_2	N719	I_3^-/I^-	6.49 8.02	6.49	[199]
3	Bi_2S_3 MWCNTs Bi_2S_3-MWCNTs (0.8)	Tape casting method	TiO_2	N719	I_3^-/I^-	4.51 6.82 8.24	8.47	[200]
4	MoS_2 MWCNTs MWCNTs-MoS_2	Drop casting	TiO_2	N719	I_3^-/I^-	4.99 3.53 6.45	6.41	[203]
5	Ni_3S_2 FMWCNTs Ni_3S_2-MWCNTs	-	TiO_2	N719	I_3^-/I^-	6.21 1.66 7.48	7.24	[206]
6	Ni_2S_3 MWCNTs Ni_2S_3-MWCNTs	Doctor blading	TiO_2	N719	I_3^-/I^-	5.77 3.76 6.87	7.24	[207]
7	MWCNTs-$CoS_{1.097}$ MWCNTs-Co_9S_8	Spray coating	TiO_2	N719	I_3^-/I^-	7.29 7.78	7.46	[208]
8	CoS MWCNTs CoS-MWCNTs	Electrophoresis and electrodeposition	TiO_2	N719	I_3^-/I^-	6.96 2.91 5.86	5.99	[211]
9	TiO2 TiO2-MWCNTs-2%	-	TiO_2	N3	I_3^-/I^-	0.10 7.53	9.39	[212]

	TiO2-MWCNTs-4% TiO2-MWCNTs-6%					8.81 6.56		
10	La_2O_3 MWCNTs La_2O_3-MWCNTs (5:1)	Spray coating	TiO_2	N719	I_3^-/I^-	0.77 3.94 5.20	4.54	[213]
11	MWCNTs Ni3S2 Ni3S2-MWCNTs NiO NiO-MWCNTs	Doctor blade technique	TiO_2	N719	I_3^-/I^-	2.80 0.46 3.74 0.75 3.80	3.90	[215]
13	MWCNTs NiO-NF-MWCNTs	Doctor blading	TiO_2	N719	I_3^-/I^-	4.87 7.63	6.72	[214]
15	MWCNTs $MoIn_2S_4$ $MoIn_2S_4$-MWCNTs-10 $MoIn_2S_4$-MWCNTs-20 $MoIn_2S_4$-MWCNTs-30	Hydrothermally grown over FTO	TiO_2	N719	I_3^-/I^-	3.62 7.44 8.16 8.38 8.31	8.01	[217]
16	NiCoP NiCoP-MWCNTs-5 NiCoP-MWCNTs-10 NiCoP-MWCNTs-15 NiCoP-MWCNTs-20	Doctor blade technique	TiO_2	N719	I_3^-/I^-	4.71 6.64 6.94 7.24 7.09	7.12	[218]
17	CNTs PW_{12}-CNTs PMo_{12}-CNTs P_2W_{18}-CNTs P_2Mo_{18}-CNTs Co_4PW_9-CNTs.	Drop casting technique	TiO_2	N719	I_3^-/I^-	5.74 6.57 6.93 6.37 6.49 7.60	6.59	[219]
19	CAN-CoS_2 CAN	Hydrothermal & direct pasting	TiO_2	N719	I_3^-/I^-	8.92 8.28	7.32	[220]

3.4 Doped and metal coated CNTs based CEs

CNTs are one of the most important and easily available dopable material for the manufacturing of CEs for DSSCs, and different heteroatoms can be used for their doping. Heteroatom doping results in lattice distortion and charge redistribution in the conjugated carbon matrix, as they possess different electronegativity and atomic sizes. They do not only enhance intrinsic activity of CNTs but also increases the number of active sites. The most common doped heteroatom in CNTs is nitrogen (N) followed by boron (B). N-doped CNTs are extensively investigated as CE in DSSCs while some literature on B- as well as O-doping is also present. The incorporation of N heteroatoms in CNTs results in the production of more active sites for the catalysis of redox couple due to the presence of lone pair over N atoms, which is incorporated in the large π-conjugated system. Because of electronegativity difference, polarization is induced in CNTs structure, which results in increased electrical conductivity. Lee et al. [222] prepared arrays of vertically aligned N-doped MWCNTs, which were readily transferred to glass substrates. The efficiency obtained from above CE based DSSC was 7.04%, slightly lower to the PCE by the Pt based CE (7.34%). This outstanding performance was attributed to the vertical alignment, which provides large surface area and straight path for electron transfer and ion diffusion, and to the electron rich N-doping that increases the active sites as well as the conductivity.

N-doped CNTs are also used to form complex hybrids with other metals as well as carbon materials. The efficiency achieved with such materials is sufficiently large due to synergistic effect, large surface area, and unique structures. Zheng et al. prepared Pod-like N-doped CNTs with encapsulated FeNi alloy NPs through direct pyrolysis of $Ni_2Fe(CN)_6$ in inert atmosphere. CEs attained by this process are environmental friendly, non-toxic, in-expensive and extremely competent [223]. The Pod(N)-FeNi catalyst demonstrated excellent electrocatalytic activity, low peak separation among the anodic and cathodic peaks, low charge diffusion resistance, higher exchange current density, and enhanced electrochemical stability under extended

cycling with respect to that of sputtered Pt electrode. The DSSCs employing the Pod(N)-FeNi as the CE showed an overall PCE of 8.82%, higher than that of the sputtered Pt CE (8.01%) (See **Fig. 18**). The incapsulated FeNi NPs themselves did not show good catalytic activity, therefore, other metals that are able to interact differently with CNTs have been explored. They further incorporated Ni and Co NPs into N-doped MWCNTs, which revealed good electrocatalytic performance and made possible to achieve efficiencies in DSSC up to 8.39 and 7.75%, respectively which were higher than Pt sputtered electrode [224].

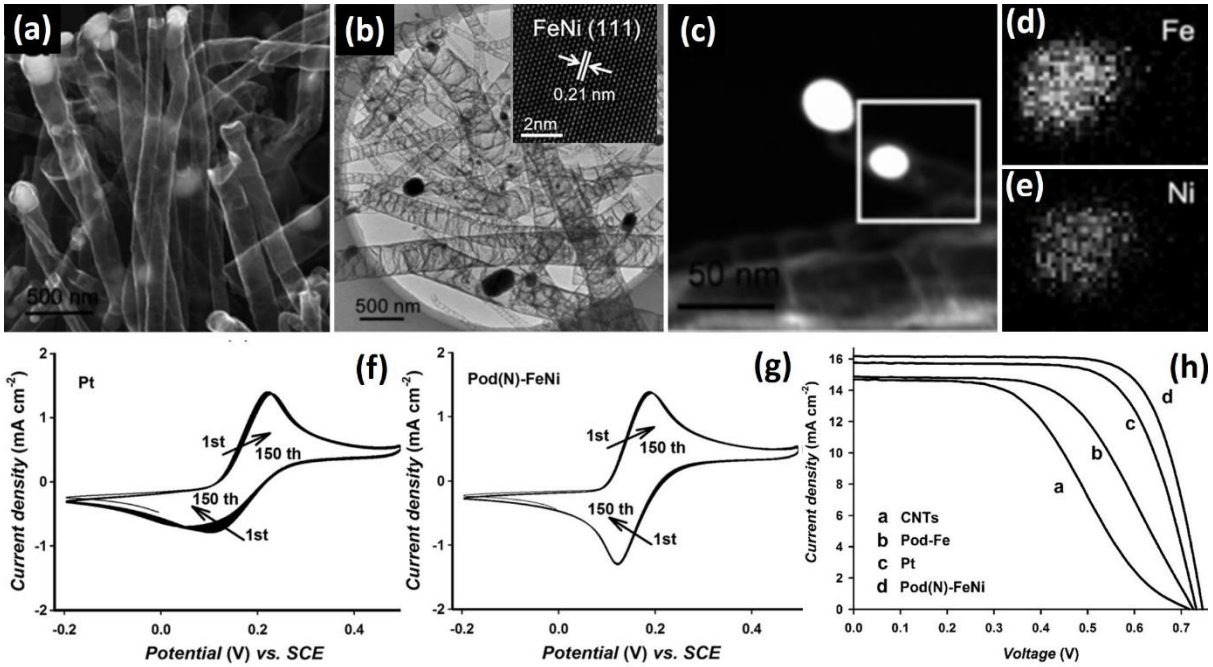

Fig. 18. SEM image (a), TEM image (b) of the Pod (N)-FeNi (inset: HRTEM image of the FeNi alloy nanoparticle), TEM images (c) and elemental mapping of Fe (d) and Ni (e) elements in the metal NPs in boxed area of (c), Sequential cyclic voltammograms for Pod(N)-FeNi (f) and d sputtered Pt CEs (g), J-V curves of the DSSCs assembled with different CEs. (Reproduced with the permission from Ref. [223], Copyright 2014 Wiley-VCH)

Arbab et al. [225] synthesized organic N-doped MWCNTs using an organic compound cationic Bovine Serum Albumin (cBSA) protein complex, which upon cationization releases huge number of activated nitrogen acting as a dopant source. The prepared material, when used as

CE in DSSCs, gave a promising PCE of 9.55%, comparable to the one exhibited by the Pt based CE (9.89%). This performance was attributed to the charge polarization due to the electronegativity difference and to the structural strain caused by the presence of the organic compound. Wang et al. [226] prepared multi metal (Co-Fe-Ni-Mo) incorporated N-doped MWCNTs by using polyoxometalates (POM)-intercalated layered double hydroxide pyrolysis method. They first synthesized CoFe-$NiMo_6$ intercalated material that was subsequently mixed with dicyandiamide (DCA) acting as both carbon and nitrogen source for producing N-doped MWCNTs. They varied the DCA/CoFe-$NiMo_6$ mass ratio and annealed the mixture at various temperatures and for different times. When DCA and CoFe-$NiMo_6$ precursors were pyrolyzed at 800 °C for 5 h at a mass ratio of 6 or 7, hierarchical architectures were observed, in which 2D carbon layer and 1D CNTs sufficiently interconnected. At a higher mass ratio of 8, the hybrid consisted of nanotubes entirely, increasing active surface area. With further enhancing the mass ratio to 9 or 10, completely covered nanotubes gradually disappeared. The CEs for DSSCs were prepared by screen printing technique. A PCE of 6.46%, higher than that shown by Pt based electrode (6.05%), was obtained when using the film annealed to 800 °C for 5 h with a DCA/CoFe-$NiMo_6$ mass ratio of 8.

Ou et al. [227] embedded Co NPs in N-doped MWCNTs by using one-step pyrolysis of ZIF-67 metal organic framework (MOF) under hydrogen atmosphere (see **Fig. 19**). The composite was then spin coated over FTO and the as-obtained film was applied as a CE in a DSSC studying the effect of annealing temperature over its PCE. An efficiency of 8.18%, which was higher than that exhibited by a standard Pt based CE (7.54%), was attained when the film was annealed at 800 °C. This was attributed to the presence of a large number of Co NPs and N-doped atoms in the MWCNTs structure that provide greater active sites for catalytic activity. The efficiency decreased as the temperature was increased to 900 °C because of the aggregation of MWCNTs and loss of N-doped atoms.

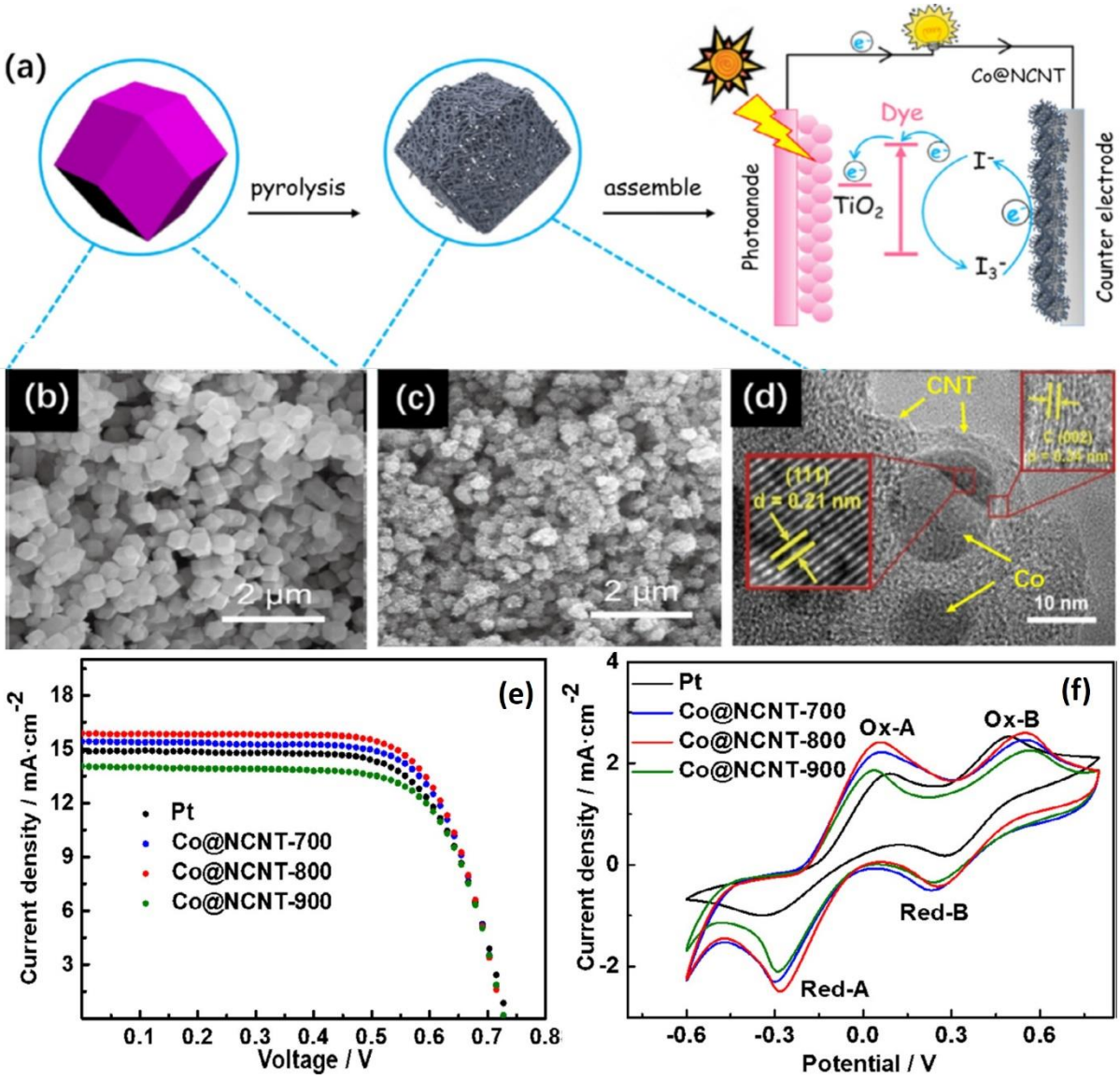

Fig. 19. Schematic diagram of fabrication process of Co@NCNT CE materials for DSSCs (a), SEM image of ZIF-67 (b), SEM and (c) TEM (d) images of Co@ NCNT-800, J-V curves of DSSCs assembled with Co@NCNT and Pt CEs (e) CV curves at a scan rate of 50 mV s^{-1} (Reproduced with the permission from the Ref. [227], Copyright 2018 Elsevier)

Imbrogno et al. [228] used KrF-laser deposition technique for the preparation of MWCNTs decorated with Co-Ni NPs to be used as CEs for DSSC. The efficiency of the developed CEs varied with varying the number of laser ablation pulses (N_{LP}) (500-60000) due to the different structure, surface roughness and coverage of Co-Ni NPs formed over MWCNTs. An optimum PCE of 6.68%, that was better than both pristine MWCNTs and Pt based DSSCs, was achieved

at 40000 N_{LP}. The Co-Ni NPs were found to partially cover the MWCNTs when N_{LP} was lower than 20000, while enhancing the N_{LP} the coverage was complete and the surface roughness was also increased. The Co-Ni NPs layer exhibited a cauliflower-like highly porous structure over MWCNTs showing large surface area, which was lowered at a higher N_{LP} of 600000 due to the coalescence of large aggregates. In addition, the work function of the electrode was found to decrease from 4.8 eV of pristine MWCNTs to 3.9 eV, which was an additional factor that influenced the catalytic activity of the CE.

A complex hybrid constituted by ordered mesoporous carbon (OMC) showing a 3D ordered carbon network for fast electron transport to the embedded NPs and 3D interconnected channel for fast ion diffusion has been reported by Chen et al. [229]. The hybrid consisted of Ni-encapsulated and N-doped MWCNTs pinned on N-doped ordered mesoporous carbon (NOMC) by using a two-step strategy. They utilized these composite materials as CE for DSSCs and obtained a maximum PCE of 8.39%. This noticeable photovoltaic performance was attributed to the reduced particle size and shortened channel length of the NOMC that facilitate ion diffusion along with highly interconnected 3D conductive network of Ni-N-doped MWCNTs that accelerate electron transport. In another work, Mehmood et al. [230] prepared a Ni impregnated MWCNTs composite using tape casting technique and TiO_2 as binder to be utilized as CE for DSSCs. A PCE of 9.72%, higher than that exhibited by Pt based CE (8.85%), was achieved when impregnating MWCNTs with 3% Ni. This was attributed to the highest surface area of 180.85 m^2/g and greater number of active sites shown by the 3% Ni composite that led to a lower charge transfer resistance as evidenced by EIS analysis. The morphology of highly interconnected MWCNTs with little or no damage to the tubes after impregnation and the uniform distribution of Ni over MWCNTs also played an important role in the higher efficiency. Chen et al. [231] synthesized Ni encapsulated N-doped MWCNTs by facile thermal decomposition method and evaluated them as CE material in DSSCs (see **Fig.** 20). An

efficiency of 8.94%, which was higher than the one delivered by Pt based CE (7.53%), was obtained and attributed to the homogeneously distributed Ni-C interfaces, porous structure with various defects, good electrical conductivity as well as corrosion resistance.

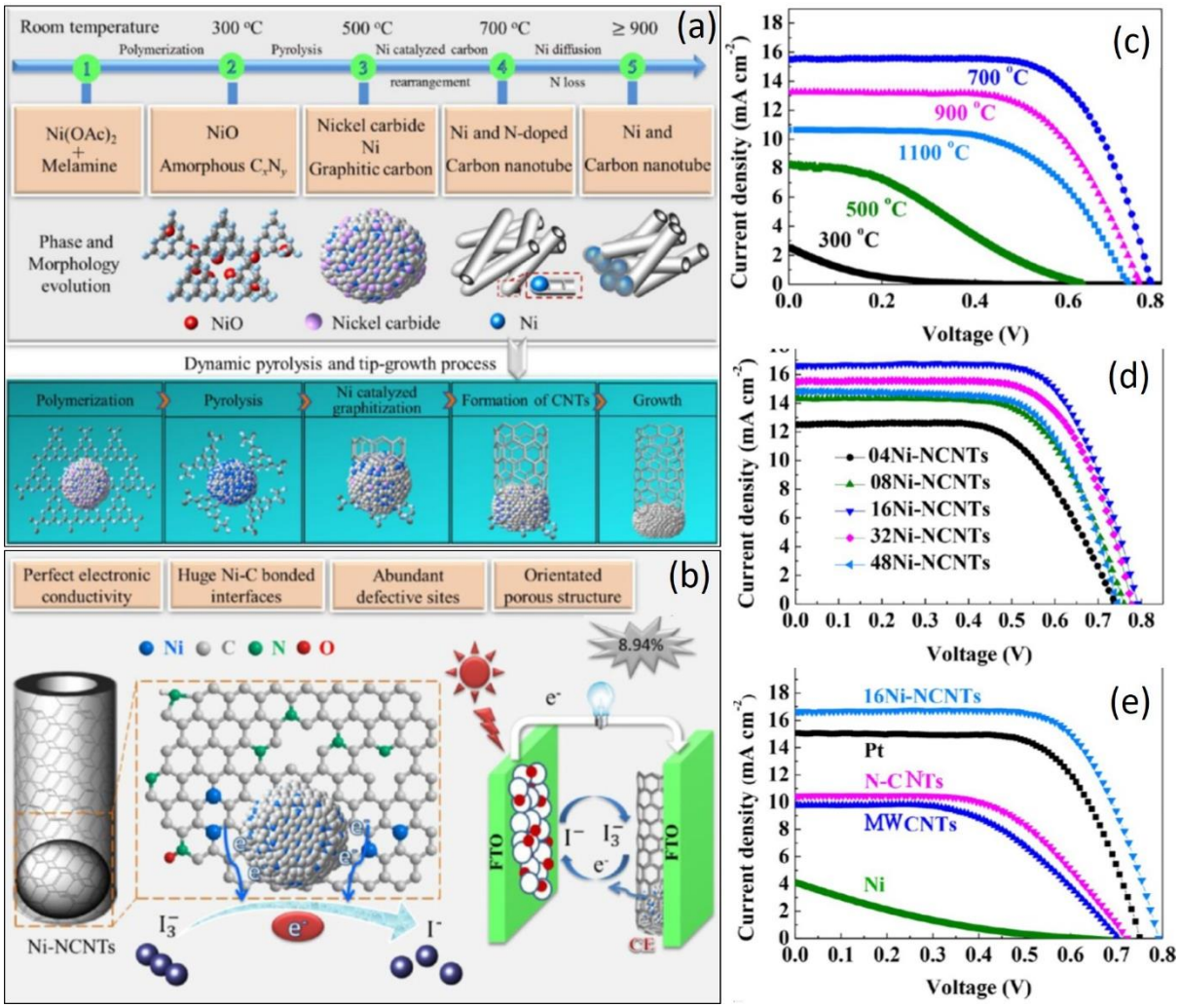

Fig. 20. Schematic illustration of mechanism of synthesis for preparation of Ni- and N-doped-CNT (a), Schematic layout of electrocatalytic activity of the Ni-NCNT CE(b), J-V curves of NiNC-x (c), yNi-NCNTs (d) and reference-CE-based DSSCs (d). (Reproduced with the permission from Ref. [231], Copyright 2017 American Chemical Society).

In addition to metal incorporated N-doped MWCNTs, some researchers have made their hybrids with porous carbon materials as well. Usually they use metal organic framework (MOF) to form these complexes; this strategy allows preparing materials that show

homogenous distribution, a strong interaction between carbon skeleton and metal NPs, and a large number of available active sites. MOFs possess a strong covalent bond between the central metal ion and the organic ligand and an open crystalline framework with high porosity and surface area. After mixing with MOFs precursors, the material is usually pyrolyzed at high temperature in inert atmosphere to form a carbon skeleton with high conductivity and a porous structure with vast surface area for catalytic activity. The use of direct carbonization method for the formation of MOFs based hybrid composites mostly causes agglomeration of either NPs or carbon material which decreases active surface area and hence the efficiency. In addition, the NPs do not form an effective network, which hinder the charge transport process. The formation of 1D nanomaterials using MOFs template is difficult to achieve mainly due to the preference to form polyhedron but is desirable due to shorter diffusion length and easily accessible surface area.

Template assisted strategy to form 1D nanomaterial by using MOFs template is reported by Li et al. they prepared nitrogen doped porous carbon which are coated over hollow CoSe NPs pinned over N-doped MWCNT by using polypyrrole assisted ZIF-67 template. The efficiency achieved with the material used as CE was reported to be 7.58% that was higher than Pt based CE (7.27%). This was attributed to the large number of active sites available for triiodide reduction in the form of CoSe N-doped porous carbon NPs. In addition, the metal nitrogen bond facilitate electron transfer from carbon to the active sites that benefits electrocatalytic activity [232]. Recently, Huang et al. [233] used ZIF-67 as template to form $CoTe_2$ NPs encapsulated in N-doped CNTs-grafted polyhedron (see **Fig. 21**). When utilized as CE in DSSC, the material delivered an efficiency of 9.02%, which was higher than that exhibited by Pt based CE (8.03%). This was attributed to the synergistic effect between $CoTe_2$ NPs and N-doped CNTs in addition to the unique polyhedron structure with high surface area.

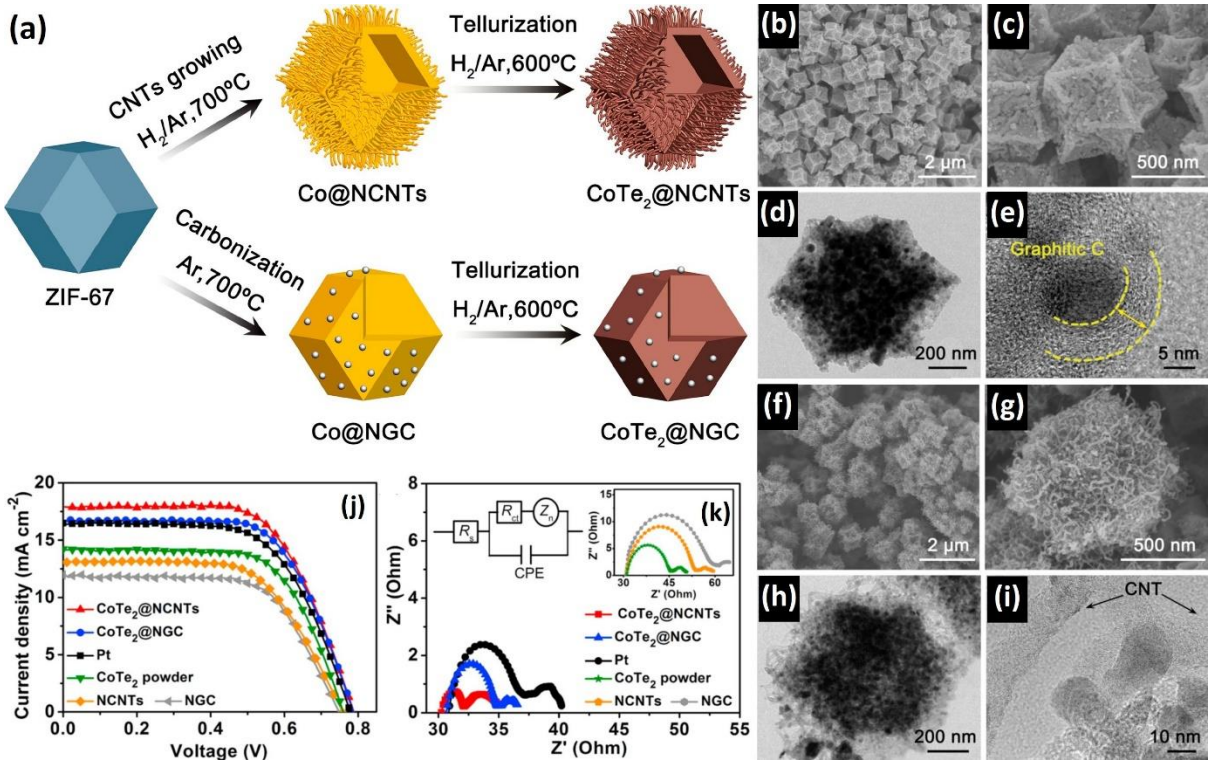

Fig. 21. Schematic of synthesis protocol of the $CoTe_2$@NCNTs and $CoTe_2$@NGC (a), SEM images (b, c) and TEM images (d, e) of $CoTe_2$@NGC, SEM images (f, g) and TEM images (h, i) of $CoTe_2$@NCNTs, J-V Characteristics Curves (j), and Nyquist plots for the symmetrical cells fabricated with different CEs (k). (Reproduced with permission form Ref. [233], Copyright 2019 Elsevier).

Beside nitrogen, other heteroatoms are commonly used to dope CNTs. Among them, Boron with deficiency of an electron is prominent, as it enables to modify the chemically inert sp^2 carbon structure, thus resulting in a large number of free-flowing π electrons. Leu et al. synthesized B-doped MWCNTs and drop casted them on FTO slices to prepare CEs for the fabrication of DSSCs. They annealed the prepared CEs at different temperatures and the highest PCE of 7.91% was achieved at 500°C. The achieved efficiency, is comparable to the one delivered by the counterpart Pt based electrode (8.03%) [234]. Similarly, Yeh et al. prepared B-doped MWCNTs based electrodes using various concentrations of Borons and used them as CE for DSSCs. The highest PCE of 7.17%, comparable to that showed by the Pt based electrode

(7.98%) was obtained when the doping concentration was 0.04% and attributed to the higher catalytic activity and conductivity [235].

In addition to B- and N-doped MWCNTs, oxygen (O)-doped CNTs have also been recently investigated. The research is limited because O-doping may lower the electrical conductivity of CNTs that is unfavorable for the electrochemical process. However, O-doping displays other advantages, such as increasing defects in the structure, enhancing polarity and producing a redistributed electronic structure. Recently Hong et al. investigated the effect of O-doped MWCNTs as CE in DSSCs both experimentally and theoretically [236]. The O-doped MWCNTs were prepared by simple oxygen plasma treatment. Argon (A) plasma treated CNTs were also synthesized for comparison and delivered a lower efficiency. The DSSC, which was assembled using CE made of O-doped MWCNTs, achieved PCE of 8.35%, better than that exhibited by Pt based CE (8.04%). This was attributed to the increased number of edge sites, open ends due to plasma treatment, and activated sidewalls due to introduced O species.

The doping of CNTs with different heteroatoms and the formation of complexes with metal NPs and other porous carbon structures have proved to be effective strategies for the development of DSSC CEs alternative to Pt. Various hybrids materials were prepared incorporating metal NPs in doped CNTs, and such materials have exhibited higher efficiencies than Pt. Beside this, the combination of metal NPs incorporated N-doped CNTs and organic porous carbon structures to form complex hybrids also provided higher efficiencies due to lower charge transfer resistance (R_{ct}) and diffusion resistance (Z_N). O-doped MWCNTs have shown exceptional performance, however, limited work has been done on such dopant materials. **Tab.** 4 summarizes the main characteristics and the photovoltaic performance of DSSCs fabricated with doped CNTs based CEs.

Tab. 4. Main characteristics and photovoltaic performance of DSSCs fabricated with doped CEs

No.	CE Material	Deposition method	Photoanode	Sensitizer	Redox couple	PCE (%)	PCE vs Pt (%)	Ref.
1	NMWCNTs Pod-Fe NMWCNTs-FeNi	Spray coating	TiO_2	N719	I_3^-/I^-	4.87 6.12 8.82	8.01	[223]
2	NMWCNT-Co NMWCNT-Ni	Spray coating	TiO_2	N719	I_3^-/I^-	7.75 8.39	7.67	[224]
3	CoFeNiMo@NCNT-800−6-5 CoFeNiMo@NCNT-800−7-5 CoFeNiMo@NCNT-800−8-5 CoFeNiMo@NCNT-800−9-5 CoFeNiMo@NCNT-800−10-5	Screen printing	TiO_2	N719	I_3^-/I^-	5.76 6.30 6.46 6.12 5.59	6.05	[226]
4	NMWCNT-Co-700 NMWCNT-Co-800 NMWCNT-Co-900	Spin coating	TiO_2	N719	I_3^-/I^-	7.92 8.18 7.22	7.54	[227]
5	NOMC Ni-N-doped MWCNTs NOMC-Ni-N-doped MWCNTs-2 NOMC-Ni-N-doped MWCNTs-4 NOMC-Ni-N-doped MWCNTs-8 NOMC-Ni-N-doped MWCNTs-12	Doctor blading	TiO_2	N719	I_3^-/I^-	6.59 6.20 7.31 7.94 8,39 7.71	7.60	[229]
6	MWCNTs Ni-MWCNTs (1%) Ni-MWCNTs (3%) Ni-MWCNTs (5%) Ni-MWCNTs (7%)	Tape casting	TiO_2	N3	I_3^-/I^-	7.31 9.04 9.72 8.84 8.06	8.85	[230]
7	NMWCNTs	Direct coating	TiO_2	N719	I_3^-/I^-	4.24	7.53	[231]

	NMWCNTs-Ni					8.94		
8	CoSe-N-Porous-C-NMWCNT (small NPs) CoSe-N-Porous-C-NMWCNT (large NPs) CoSe-N-Porous C NMWCNT	Doctor blading	TiO_2	N719	I_3^-/I^-	7.58 6.60 5.88 3.96	7.27	[232]
9	$CoTe_2$ NMWCNT $CoTe_2$-NMWCNT	Spin coating	TiO_2	N719	I_3^-/I^-	7.19 6.18 9.02	8.03	[233]
10	MWCNTs (400°C) BMWCNTs(300°C) BMWCNTs(400°C) BMWCNTs(450°C) BMWCNTs(500°C)	Drop casting	TiO_2	N719	I_3^-/I^-	6.02 5.91 6.53 7.21 7.91	8.03	[234]
11	MWCNTs BMWCNTs (0.40 %) BMWCNTs (2.09 %) BMWCNTs (3.38 %) BMWCNTs (3.92 %)	Drop coating	TiO_2	N719	I_3^-/I^-	5.98 7.17 6.86 6.78 6.37	7.98	[235]
12	MWCNTs Ar-P-MWCNTs O-P-MWCNTs	Doctor blading	TiO_2	N719	I_3^-/I^-	7.29 7.59 8.35	8.04	[236]
13	MWCNTs ACMWCNTs-0.4% ACMWCNTs-0.8% ACMWCNTs-1.6% ACMWCNTs-3.2%	Tape casting	TiO_2	D719	I_3^-/I^-	7.16 8.82 10.05 9.52 7.81	9.30	[237]

3.5 CEs based on hybrid materials

CNTs can be used in pristine as well as in combination with other materials to form hybrid CEs. The composite of CNTs with organic and inorganic materials is a useful strategy, as each component material possesses both weaknesses and strengths. In combination, the individual properties may combine and thus structures can be achieved showing synergistic properties leading to remarkable efficiencies. Beside this, the combination of CNTs with various carbon nanomaterials particularly graphene related materials have also been an interesting option for CEs. CNTs possess the advantage of fast electron transfer due to the ballistic and diffusive transport as their tubular structure make the electron easily available for iodide reduction and can reduce electrolyte diffusion resistance. While graphene show a flat surface that favor electrode-electrolyte contact, thus promote faster diffusion of ions (see **Fig. 22**).

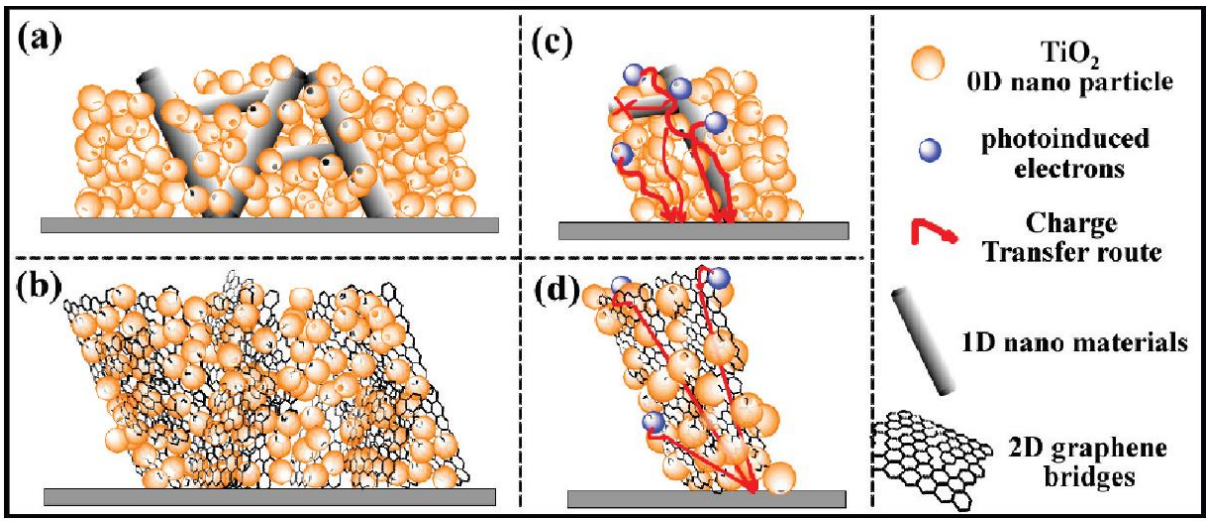

Fig. 22. Schematic representation of charge transfer mechanism in hybrid CE materials based on 1D and 2D matrix materials. (Reproduced with permission from Ref. [238], Copyright 2010 American Chemical Society).

CNTs and Graphene combination would lead to the formation of a highly interconnected structure. Both of them contribute to faster electron and ion transfer in addition to better electrode-electrolyte contact because of lower values for both R_{ct} and Z_N. In addition, graphene

usually suffers from the problem of restacking due to strong π-π interactions that are prevented by incorporating CNTs in their structure in addition to the use of surfactant [97, 238].

Hybrid electrodes show a number of benefits compared to the CEs made of graphene or Pt because of lower internal resistance and higher charge transport rate. A 3D graphene-SWCNTs aerogels CE was developed and a remarkably high PCE~10.56% was achieved which reached a maxima of 10.69% in the stability test when a mirror was placed under the cell. In the absence of mirror, the device delivered PCE~ 9.24%. This attributes to the 3D structure with huge number of active sites, better conductivity, faster electron, and ion diffusion. In addition, the incorporation of SWCNTs decreases agglomeration of rGO and therefore the specific surface area of rGO increases from 271.27 m^2g^{-1} to 325.81 m^2g^{-1} [239]. Similarly, a hybrid material consisting of MWCNTs and graphene was prepared through solution based method and employed as a CE, leading to an overall device PCE of 4.66% [240]. Furthermore in another work reported by Kumar et al. [241] a CE was prepared for DSSCs based on graphene nanosheets infused with MWCNTs paste and coated them on glass micro slides using 3-Aminopropyl triethoxysilane (APTES). The CE delivered an efficiency of 3.08 % while pristine graphene-CNT delivered an efficiency of 4.66% that was comparable to Pt. This was attributed to the better conductivity of CNTs along graphene flakes and the unique morphology.

It is already mentioned that N-doping can enhance the catalytic activity of graphene as well by addition of extra electrons and induction of polarization. A 3D N-doped graphene/reduced hydroxylated CNTs composite aerogel (NG/CNT-OH) was developed through a two-steps hydrothermal reaction using hydroxylated CNTs (CNTs-OH) and graphene oxide (GO) as reactants [242]. NG/CNT-OH composite aerogel exhibited good electrocatalytic performances for I^-/I_3^- redox couple, mainly attributed to its hierarchical porosity structure with large numbers of exposed active edge sites, which provide the efficient pathways of electrons and ions transport. The as prepared NG/CNT-OH composite aerogel was then compressed to form

carbon paper and was used as flexible TCO-free CEs. The fabricated CEs showed excellent carrier transport ability, high electrocatalytic activity, and exceptional mechanical flexibility. The DSSCs assembled with the optimized NG/CNT-OH CE achieved a noticeable PCE~6.36%, higher than that obtained by Pt based CE in similar conditions (PCE~5.74%).

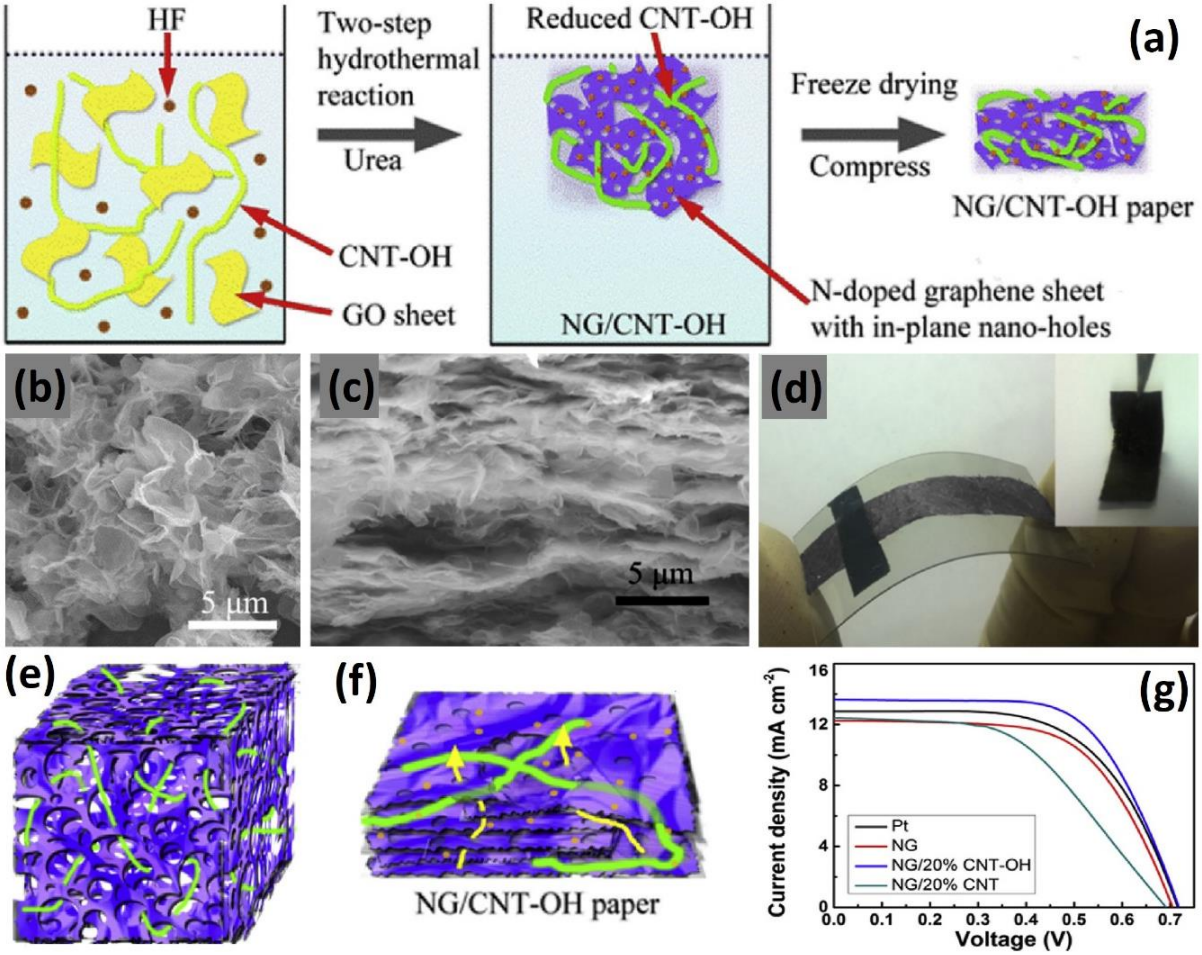

Fig. 23. Preparation protocol of NG/CNT-OH and NG/CNT-OH paper (a), SEM images of NG/CNT-OH composite aerogel (b) and cross sectional image of NG/CNT-OH paper (c), Digital images of NG/CNT-OH paper CE (d), Schematic illustration of inner structures of NG/CNT-OH aerogel (e) and paper (f), J-V Characteristics curves (g). (Reproduced with the permission from Ref. [242], Copyrights 2016 Elsevier).

Metal-based compounds possess great ability for reducing electrolyte but possess the limitation of lower electrical conductivity. When these metal compounds are distributed over the

graphene-CNT matrix than it will mitigate the lower intrinsic catalytic activity problem of CNTs that will act as effective conductive network for transport of electrons and ions. Khan et al. [243] decorated SnS_2 nanoflakes over functionalized MWCNTs and single crystal rGO. The synthesized electrode delivered an efficiency of 8.7%, better than reference Pt CE. In another work, Khan et al. [244] also prepared Co_3O_4 decorated functionalized MWCNTs entangled with N-doped rGO, which delivered an efficiency of 8.42% that was higher than Pt based CE. Recently, Zhang et al. synthesized sunflower like the one $SrCo_2S_4$ nanoflakes decorated over functionalized MWCNTs and nitrogen reduced GO. The material delivered an efficiency of 8.06% that was even better than Pt CE [245].

Such type of work was also conducted by Lin et al. who synthesized through a facile electrophoretic deposition technique of a novel hybrid material by combining molybdenum disulfide (MoS_2) and reduced graphene oxide NCs with CNTs (MoS_2/rGO-CNTs) and its exploitation as a low cost CE [246]. The incorporation of CNTs conductive grids provided extra pathways for electronic transportation, thus resulting in the increase of the charge transfer rate at the CE/electrolyte interface and in a markedly enhanced electrocatalytic activity in the hybrid electrode compared with that of MoS_2/rGO alone. The DSSC assembled with the MoS_2/rGO-CNTs CE revealed a highest PCE of 7.46%, exceeding the PCE values measured with DSSCs based on MoS_2/rGO CE (6.82%) and on Pt CE (7.23%).

Because of the presence of conjugated double bonds, conducting polymers with 3D structures possess higher electrocatalytic activity for the reduction of triiodide ions. Consequently, there combination with CNTs-Graphene or metal compounds/CNTs will result in remarkable efficiencies due to synergistic effects. Al-bahrani et al. [247] prepared a graphene nanosheets-MWCNTs and polyaniline (GNS/MWCNT/PANI) rough and porous NCs via an in-situ polymerization method and successfully applied as a low cost and highly efficient CE for DSSCs using a spin coating (see **Fig. 24**). The combination of the greater intrinsic catalytic

performance of PANI and excellent electrical conductivity of GNS/MWCNT led to a reduced charge transfer resistance at the electrolyte/CE interface, along with the consequent increase of both the catalytic activity as well as photovoltaic performance of the hybrid composite CE. When incorporated in the DSSC, the GNS/MWCNT/PANI CE showed a noticeable PCE of 7.52% greater than that obtained with the Pt CE (6.69%) in similar conditions.

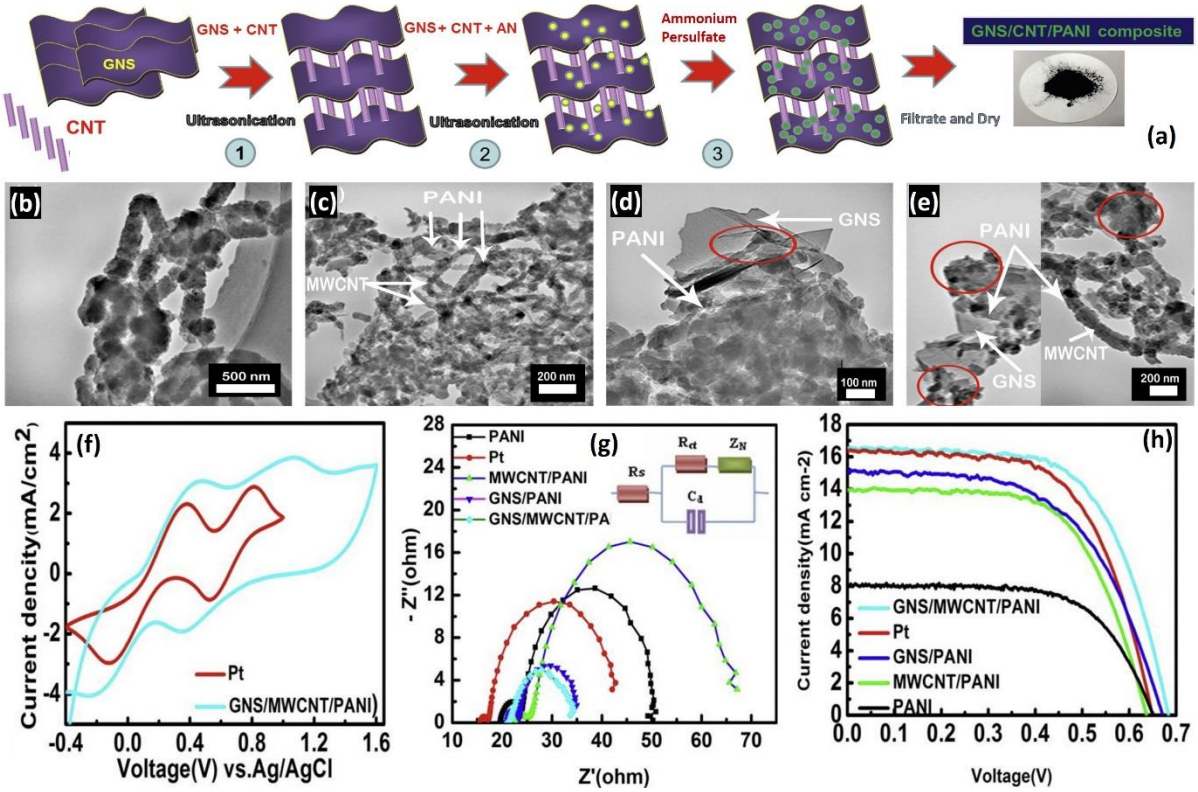

Fig. 24. Synthesis protocols for graphene nanosheets GNS/CNT/PANI composite (a), TEM images of PANI (b), CNT/PANI (c), GNS/PANI (d), and GNS/CNT/PANI (e), CV comparison for Pt and GNS/CNT/PANI electrodes (f), EIS analysis of various CEs and equivalent circuit (g). J-V curves of various CEs based devices (h). (Reproduced with the permission from Ref. [247], Copyright 2014 Elsevier).

Likewise, in another work, Liu et al. prepared fiber shaped graphene/MWCNTs hollow tube, which was further functionalized with PANI. The composite when utilized as CE in DSSCs delivered an efficiency of 4.20%, higher than bare Pt wire. This was attributed to the fast charge

transport due to the covalently linked graphene-MWCNTs fiber and to the synergistic effect of the composite and PANI. The tube also showed good mechanical stability when bent at various angles. This work may be further modified by using other polymers or active materials decoration over the fiber [248]. Yue et al. prepared glucose and PEDOT: PSS assisted SWCNTs-MoS_2 composite based CEs using an in-situ hydrothermal method. A promising PCE of about 8.14%, analogous to that shown by the Pt CE (7.78%), was achieved [249].

The film thickness noticeably affects the overall performance of the cell. In particular, an increase in the film thickness leads to the rise of the overall device efficiency, due to the simultaneous increase of fill factor, voltage, and current density. Al-bahrani et al. synthesized rGO-MWCNTs-NiO NC CE that delivered an efficiency of 8.13%, higher than all other electrodes. The efficiency increased with increasing film thickness and maxima was achieved at 12.32 µm thick film [250]. The remarkable performance of these materials were attributed to the presence of metal based nanomaterials over graphene-CNTs, which provide greater number of active sites and better electrical conductivity and electrode electrolyte contact, which reduce charge transfer and ion diffusion resistance. This increases the electrocatalytic activity of these materials towards triiodide.

Metal oxide particles, in combination with MWCNTs and polymer composite are also used as CE materials for DSSCs. Xiao et al. carried out the synthesis of a MWCNT and PANI/cobalt sulfide (PANI/MWCNT@$CoS_{1.097}$) NC via drop casting technique followed by in situ electropolymerization on FTO glass substrate (see **Fig. 25**). The prepared electrode displayed an enhanced electrocatalytic activity compared to PANI and MWCNT@$CoS_{1.097}$, when employed as a metal free CE for DSSCs [251]. This can probably be attributed to the high intrinsic electrocatalytic activity of MWCNT@$CoS_{1.097}$ and to its increased adhesion to the FTO glass substrate guaranteed by the conducting PANI. Furthermore, the DSSC based on the PANI/MWCNT@$CoS_{1.097}$ CE achieved an enhanced efficiency of 7.02% with great chemical

and electrochemical stability, which is close to that of the DSSC with Pt CE (7.16%) and higher than those of the DSSCs using PANI (6.06%) and MWCNT@$CoS_{1.097}$ CEs (5.54%).

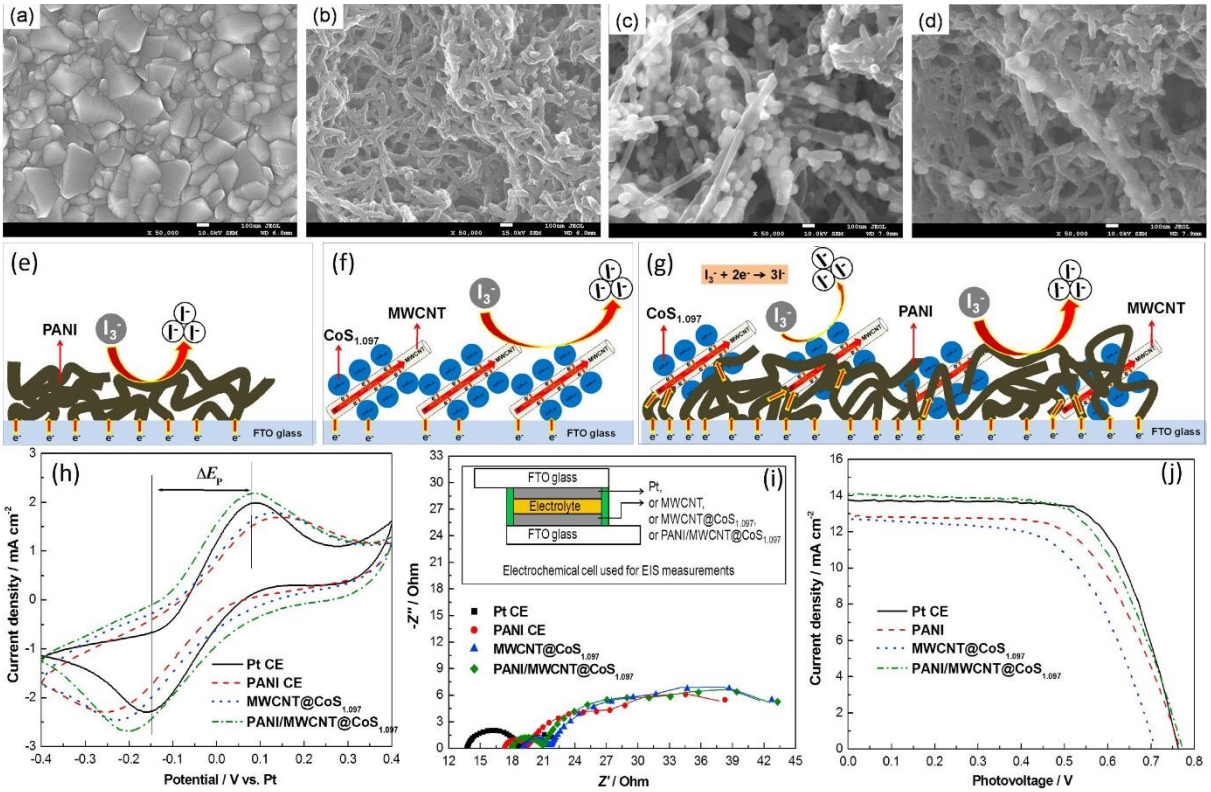

Fig. 25. SEM images of the FTO substrate (a), PANI (b), MWCNT@$CoS_{1.097}$ (c), and PANI/MWCNT@$CoS_{1.097}$ (d). Schematic illustration for electrocatalytic mechanisms in PANI (e), MWCNT@$CoS_{1.097}$ (f), and PANI/MWCNT@$CoS_{1.097}$ (g). Cyclic voltammetry (h), Nyquist plots (i), and J-V characteristics of DSSCs (j) based on various CEs. (Reproduced with the permission from Ref. [251], Copyright 2014 Elsevier).

Instead of using combination of graphene and CNTs, a layer-by-layer formation is also employed as CE in DSSCs. Ma et al. synthesized a bilayer rGO-ACNT CEs with the assistance of different surfactants. The first layer deposited was consisted of ACNT while the second layer was of rGO. The aggregation of rGO was inhibited by the use of different surfactants namely Triton X-100, SDBS and cetylpyridinium chloride (CPC), out of which CPC functionalized rGO showed better performance (PCE~3.9%). This was attributed to the uniform coating of

rGO achieved over ACNT with the help of CPC which lead to decrease in R_{ct} and Z_N [252]. Similarly, Wahyuono et al. also prepared bilayer CE consisting of MWCNT layer deposited over graphene layer using a simple double self-assembly procedure. The film was then annealed under N_2 atmosphere that enhanced conductivity as well as catalytic activity of the electrode. The graphene-MWCNT annealed CE provided PCE of 4.1 % that was much better than Pt based CE as well as CEs in which graphene and MWCNTs are only used. The annealing results in surface roughness of both graphene and MWCNTs and increases the surface area that results in great catalytic activity of the composite. These CEs are also mechanically stable which allows recycling without loss of performance [253].

In addition to the above discussed hybrid materials, MWCNTs are also combined with other carbon related compounds, such as graphite, carbon black, and mesoporous carbon. Zhang et al. prepared CE using different carbon materials including MWCNTs, graphite, carbon black and graphene. A PCE of 6.29% for the optimum mixture containing the above mentioned carbon materials in the ratio 30:12:03:05. This was due to the fine morphology of the film and high conductivity. When the hybrid formed was employed as flexible CE in DSSCs than still a PCE of 4.32% was achieved [254].

Based on efficiency, stability, and cost aspects, this hybrid electrode can be regarded as a suitable alternative material to Pt for the CE of DSSCs because of the synergistic effects of the various components of such materials, which provide low charge transfer and ion diffusion resistance and high electrocatalytic activity. Furthermore, conducting polymers when used in combination with CNTs, graphene and metal compounds as CE for DSSCs, lead to higher efficiencies than Pt. **Tab. 5** summarizes the main characteristics and the photovoltaic performance of DSSCs fabricated with hybrid CEs.

Tab. 5. Main characteristics and photovoltaic performance of DSSCs fabricated with CNTs based hybrid CEs

No.	CE Material	Deposition method	Photoanode	Sensitizer	Redox couple	PCE (%)	PCE vs Pt (%)	Ref.
1	rGO rGO-SWCNT rGO-SWCNT (mirror)	Drop coating	TiO_2	N719	I_3^-/I^-	7.25 9.24 10.56	7.64	[239]
2	CNT Graphene CNT-APTES CNT-Graphene CNT-Graphene-APTES	Doctor blading	TiO_2	N719	I_3^-/I^-	3.39 0.0009 0.915 4.66 3.08	5.66	[241]
3	SnS_2 FMWCNTs rGO SnS_2-rGO SnS_2-FMWCNTs SnS_2-FMWCNTs-rGO	Doctor blading	TiO_2	N719	I_3^-/I^-	5.4 5.2 6.3 6.1 6.5 8.7	7.9	[243]
4	Co_3O_4 Co_3O_4-FMWCNTs Co_3O_4-N doped rGO Co_3O_4-FMWCNTs-rGO	Doctor blading	TiO_2	N719	I_3^-/I^-	0.71 6.88 7.25 8.42	7.81	[244]
5	$SrCo_2S_4$ $SrCo_2S_4$-FMWCNTs $SrCo_2S_4$-FMWCNTs-N doped rGO	Tape casting	TiO_2	N719	I_3^-/I^-	5.37 7.21 8.06	7.51	[245]
6	NiO rGO NiO-rGO NiO-rGO-MWCNTs	Doctor blading	TiO_2	N719	I_3^-/I^-	2,71 6.77 7.63 8.13	N.A	[250]

7	PANI GNS/PANI MWCNT/PANI GNS/MWCNT/PANI	Spin coating	TiO_2	N719	I_3^-/I^-	3.1 6.14 5.35 7.52	6.69	[247]
8	Graphene Graphene-MWCNTs Graphene-MWCNTs-PANI	Fiber	TiO_2	N719	I_3^-/I^-	1.29 2.54 4.20	3.41	[248]
9	MWCNTs-MoS_2 (G-A)MWCNTs-MoS_2 (G-P-A)MWCNTs-MoS_2	Doctor blading	TiO_2	N719	I_3^-/I^-	7.33 7.63 8.14	7.78	[249]
10	PANI MWCNTs-$CoS_{1.097}$ PANI-MWCNTs-$CoS_{1.097}$	Drop casting & electropolymerization	TiO_2	N719	I_3^-/I^-	6.06 5.54 7.02	7.16	[251]
11	ACNT ACNT-rGO ACNT-rGO-CPC ACNT-rGO-Triton X-100 ACNT-rGO-SDBS	Spray coating	TiO_2	N719	I_3^-/I^-	3.14 3.14 3.90 3.56 3.33	N.A	[252]
12	Graphite-carbon black Graphite-carbon black-MWCNTs Graphite-carbon black-Graphene Graphite-carbon black-Graphene-MWCNTs	Doctor blading	TiO_2	N719	I_3^-/I^-	5.32 5.61 4.94 6.9	N.A	[254]
13	MWCNTs Graphene MWCNTs-Graphene	Spray coating	CdS	N719	I_3^-/I^-	0.044 0.037 0.056	N.A	[255]
14	Graphitic-C_3N_4 MWCNTs Graphitic-C_3N_4-MWCNTs	Doctor blading	TiO_2	N719	I_3^-/I^-	1.95 4.27 6.34	6.84	[256]

4 Concluding Remarks

In recent decades, CNTs have attracted broad interests in the energy community due to their gifted advantages of high conductivity, superior chemical stability, excellent catalytic activity, mechanical flexibility, and long-term stability. Their high performances made them good candidates to be used as CE materials in substitution of the conventional Pt electrode. In this perspective, this review systematically summarized the significant progress in preparing various types of CNTs based CEs for DSSCs, and the pivotal factors in determining PCE of such electrodes were highlighted in detail. The authors have reviewed more than few viewpoints of using CNTs based materials as alternative to Pt. Astoundingly, in most cases, the PCE of CNTs based CEs revealed to be comparable to that of Pt electrodes, or even superior.

CNTs can be used as CE in pristine forms as well as in combination with other verity of materials. Their tubular structure also facilitates rapid iodide reduction and reduces electrolyte diffusion resistance because of fast electron transfer. While using CNTs and their composite materials as CEs, they have shown diverse performance in term of efficiency and stability because of varied synthesis and manufacturing strategies. All kind of CNTs are thoroughly investigated, however, most of the research is conducted on MWCNTs based CEs because of their low cost and easy manufacturing. Comparative study under same condition indicated that DWCNTs are better candidate due to their larger surface area, however, they are highly expensive. SWCNTs represent a good choice but they also possess the disadvantage of weak structure stability and high cost. In contrast, MWCNTs exhibit relatively low specific surface area and inhomogeneous conductivity. However, their structure can be easily tuned using various reagents while keeping the strength of the inner walls intact, though their electrocatalytic performance is still controversial and cannot be clearly associates neither to structural defects nor metallic impurities generated during the synthesis process. The aligned

and self-standing CNT have performed even better than Pt as they are well crystalline and highly interconnected.

Doping is another way of tuning CNTs to act as good catalyst as it does not only enhance the intrinsic activity of CNTs but also increases the number of active sites. N-doped CNTs are extensively investigated as the incorporation of N-heteroatoms in CNTs results in the production of more active sites for the catalysis of redox couple due to the presence of lone pair over N-atoms. Polymers composites have shown inconsistent performance as CE materials, because of their complex structural features and degree of polymerization. Multinary transition metal compound can also be synthesized by adjusting component elements, engineering morphology, and structure designing, as transition metal compounds possess low inherent electrical conductivity. Based on efficiency, stability, and cost, the hybrid CEs can be regarded as a suitable alternative material to Pt as the combination of two or three materials to form CE is a useful strategy. Each component of a hybrid material possesses both strengths and weaknesses, thus, in combination, the lone properties may combine, and the structures can be achieved showing synergistic properties leading to remarkable efficiencies. Beside the type of material, the film thickness noticeably affects the overall performance of the device. In particular, an increase in the film thickness leads to the rise of the overall device efficiency, due to the simultaneous increase of fill factor, voltage, and current density.

Nevertheless, in view of the definitive commercialization of the DSSCs, an intense research effort has yet to be performed in order to find new effective strategies to further enhance the solar cell PCE and long-term stability and at the same time to reduce its costs.

Bibliography

[1] Kay Andreas GM. Low cost photovoltaic modules based on dye sensitized nanocrystalline titanium dioxide and carbon powder. Solar Energy Materials and Solar Cells. 1996;44:99-117.

[2] Zervos A. Renewables 2018 - Global Status Report. 2018.

[3] Bolhan A, Ludin NA. Incorporation of Graphene into Counter Electrode to Enhance the Performance of Dye-Sensitized Solar Cells. Malaysian Journal of Analytical Science. 2017;21:1120-6.

[4] Badawy WA. A review on solar cells from Si-single crystals to porous materials and quantum dots. J Adv Res. 2015;6:123-32.

[5] Yang D, Hartman MR, Derrien TL, Hamada S, An D, Yancey KG, et al. DNA materials: bridging nanotechnology and biotechnology. Acc Chem Res. 2014;47:1902-11.

[6] Qi W, Shapter JG, Wu Q, Yin T, Gao G, Cui D. Nanostructured anode materials for lithium-ion batteries: principle, recent progress and future perspectives. Journal of Materials Chemistry A. 2017;5:19521-40.

[7] Chaudhary LS, Ghatmale PR, Chavan SS. Review On: Application of Nanotechnology in Computer Science. International Journal of Science and Research (IJSR) 2016;5:1542 - 5.

[8] Chen S, Zhang Q, Hou Y, Zhang J, Liang X-J. Nanomaterials in medicine and pharmaceuticals: nanoscale materials developed with less toxicity and more efficacy. European Journal of Nanomedicine. 2013;5.

[9] Sawin JL, Seyboth K, Sverrisson F. RENEWABLES 2017 - GLOBAL STATUS REPORT. In: Sawin JL, editor. Rebewable Energy Policy Network-21. Paris: REN21 Secretariat, Paris, France; 2017.

[10] Zervos A. Renewables 2019, Global Status Report- REN21. 2019.

[11] Togonal AS, Foldyna M, Chen W, Wang JX, Neplokh V, Tchernycheva M, et al. Core–Shell Heterojunction Solar Cells Based on Disordered Silicon Nanowire Arrays. The Journal of Physical Chemistry C. 2016;120:2962-72.

[12] Khadka DB, Kim S, Kim J. Effects of Ge Alloying on Device Characteristics of Kesterite-Based CZTSSe Thin Film Solar Cells. The Journal of Physical Chemistry C. 2016;120:4251-8.

[13] Best Research Cell Efficiences. Golden, Colorado (CO) National Renewable Energy Labortary, US Department of ENERGY, USA; 2021.

[14] Kyaw AKK, Tantang H, Wu T, Ke L, Wei J, Demir HV, et al. Dye-sensitized solar cell with a pair of carbon-based electrodes. Journal of Physics D: Applied Physics. 2012;45:165103.

[15] Kakiage K, Aoyama Y, Yano T, Oya K, Fujisawa J, Hanaya M. Highly-efficient dye-sensitized solar cells with collaborative sensitization by silyl-anchor and carboxy-anchor dyes. Chemical communications. 2015;51:15894-7.

[16] Ahmed U, Alizadeh M, Rahim NA, Shahabuddin S, Ahmed MS, Pandey AK. A comprehensive review on counter electrodes for dye sensitized solar cells: A special focus on Pt-TCO free counter electrodes. Solar Energy. 2018;174:1097-125.

[17] Choi J, Song S, Horantner MT, Snaith HJ, Park T. Well-Defined Nanostructured, Single-Crystalline TiO2 Electron Transport Layer for Efficient Planar Perovskite Solar Cells. ACS nano. 2016;10:6029-36.

[18] Pazos-Outon LM, Xiao TP, Yablonovitch E. Fundamental Efficiency Limit of Lead Iodide Perovskite Solar Cells. The journal of physical chemistry letters. 2018;9:1703-11.

[19] Jayawardena KD, Rozanski LJ, Mills CA, Beliatis MJ, Nismy NA, Silva SR. 'Inorganics-in-organics': recent developments and outlook for 4G polymer solar cells. Nanoscale. 2013;5:8411-27.

[20] Azpiroz JM, Infante I, De Angelis F. First-Principles Modeling of Core/Shell Quantum Dot Sensitized Solar Cells. The Journal of Physical Chemistry C. 2015;119:12739-48.

[21] Sanehira EM, Marshall AR, Christians JA, Harvey SP, Ciesielski PN, Wheeler LM, et al. Enhanced mobility CsPbI3 quantum dot arrays for record-efficiency, high-voltage photovoltaic cells. Sci Adv. 2017;3:eaao4204.

[22] Jin J, Zhang X, He T. Self-Assembled CoS2 Nanocrystal Film as an Efficient Counter Electrode for Dye-Sensitized Solar Cells. The Journal of Physical Chemistry C. 2014;118:24877-83.

[23] O'Regan BG, Michael. A low-cost, high-efficiency solar cell based on dye-sensitized colloidal TiO2 films. Nature. 1991;353:737-40.

[24] Chen Y, Zhang H, Chen Y, Lin J. Study on Carbon Nanocomposite Counterelectrode for Dye-Sensitized Solar Cells. Journal of Nanomaterials. 2012;2012:1-6.

[25] Xue Y, Liu J, Chen H, Wang R, Li D, Qu J, et al. Nitrogen-doped graphene foams as metal-free counter electrodes in high-performance dye-sensitized solar cells. Angewandte Chemie. 2012;51:12124-7.

[26] Kroto HW, Heath JR, O'Brien SC, Curl RF, Smalley RE. C60: Buckminsterfullerene. Nature. 1985;318:162-3.

[27] Sumio I. Helical Microtubules of graphitic carbon. Nature. 1991;354:56-8.

[28] Geim AK, Novoselov KS. The rise of graphene. Nat Mater. 2007;6:183-91.

[29] Koprinarov N, Stefanov R, Pchelarov G, Konstantinova M, Stambolova I. Carbon electrodes for solar cells and other semiconductor devices. Synthetic Metals. 1996;77:47-9.

[30] sedghi Am, nourmohammadi hoda. Effect of Multi Walled Carbon Nanotubes as Counter Electrode on Dye Sensitized Solar Cells. International Journal of ELECTROCHEMICAL SCIENCE. 2014;9:2029-37.

[31] Jha N, Ramesh P, Bekyarova E, Tian X, Wang F, Itkis ME, et al. Functionalized single-walled carbon nanotube-based fuel cell benchmarked against US DOE 2017 technical targets. Scientific reports. 2013;3:2257.

[32] Dai L, Chang DW, Baek JB, Lu W. Carbon nanomaterials for advanced energy conversion and storage. Small. 2012;8:1130-66.

[33] Rangom Y, Tang XS, Nazar LF. Carbon Nanotube-Based Supercapacitors with Excellent ac Line Filtering and Rate Capability via Improved Interfacial Impedance. ACS nano. 2015;9:7248-55.

[34] Landi BJ, Ganter MJ, Cress CD, DiLeo RA, Raffaelle RP. Carbon nanotubes for lithium ion batteries. Energy & Environmental Science. 2009;2:638-54.

[35] Hwang S, Batmunkh M, Nine MJ, Chung H, Jeong H. Dye-sensitized solar cell counter electrodes based on carbon nanotubes. Chemphyschem : a European journal of chemical physics and physical chemistry. 2015;16:53-65.

[36] Ahmad MS, Pandey AK, Rahim NA, Shahabuddin S, Tyagi SK. Chemical sintering of TiO2 based photoanode for efficient dye sensitized solar cells using Zn nanoparticles. Ceramics International. 2018;44:18444-9.

[37] Saltan GM, Dinçalp H, Kıran M, Zafer C, Erbaş SÇ. Novel organic dyes based on phenyl-substituted benzimidazole for dye sensitized solar cells. Materials Chemistry and Physics. 2015;163:387-93.

[38] Cicero G, Musso G, Lamberti A, Camino B, Bianco S, Pugliese D, et al. Combined experimental and theoretical investigation of the hemi-squaraine/TiO2 interface for dye sensitized solar cells. Physical chemistry chemical physics : PCCP. 2013;15:7198-203.

[39] Gong J, Liang J, Sumathy K. Review on dye-sensitized solar cells (DSSCs): Fundamental concepts and novel materials. Renewable and Sustainable Energy Reviews. 2012;16:5848-60.

[40] Andualem A, Demiss S. Review on Dye-Sensitized Solar Cells (DSSCs). Edelweiss Applied Science and Technology. 2018;2:6.

[41] Polo AS, Itokazu MK, Murakami Iha NY. Metal complex sensitizers in dye-sensitized solar cells. Coordination Chemistry Reviews. 2004;248:1343-61.

[42] Zhang Y, Ren P, Li Y, Su R, Zhao M. Optical Absorption and Electron Injection of 4-(Cyanomethyl)benzoic Acid Based Dyes: A DFT Study. Journal of Chemistry. 2015;2015:1-9.

[43] Shahzad N, Risplendi F, Pugliese D, Bianco S, Sacco A, Lamberti A, et al. Comparison of Hemi-Squaraine Sensitized TiO2 and ZnO Photoanodes for DSSC Applications. The Journal of Physical Chemistry C. 2013;117:22778-83.

[44] Calogero G, Di Marco G, Cazzanti S, Caramori S, Argazzi R, Di Carlo A, et al. Efficient dye-sensitized solar cells using red turnip and purple wild sicilian prickly pear fruits. International journal of molecular sciences. 2010;11:254-67.

[45] Qin Y, Peng Q. Ruthenium Sensitizers and Their Applications in Dye-Sensitized Solar Cells. International Journal of Photoenergy. 2012;2012:1-21.

[46] Suriati SMS, Mukhzeer Alahmed Z.A , Chyský,J Reshak,A. H Materials for Enhanced Dye-sensitized Solar Cell Performance Electrochemical Application. International Journal of ELECTROCHEMICAL SCIENCE. 2015;10:2859-71.

[47] Moehl T, Im JH, Lee YH, Domanski K, Giordano F, Zakeeruddin SM, et al. Strong Photocurrent Amplification in Perovskite Solar Cells with a Porous TiO2 Blocking Layer under Reverse Bias. The journal of physical chemistry letters. 2014;5:3931-6.

[48] Yu Q, Wang Y, Yi Z, Zu N, Zhang J, Zhang M, et al. High-efficiency dye-sensitized solar cells: the influence of lithium ions on exciton dissociation, charge recombination, and surface states. ACS nano. 2010;4:6032-8.

[49] Wei L, Na Y, Yang Y, Fan R, Wang P, Li L. Efficiency of ruthenium dye sensitized solar cells enhanced by 2,6-bis[1-(phenylimino)ethyl]pyridine as a co-sensitizer containing methyl substituents on its phenyl rings. Physical chemistry chemical physics : PCCP. 2015;17:1273-80.

[50] Lee C-P, Lin RY-Y, Lin L-Y, Li C-T, Chu T-C, Sun S-S, et al. Recent progress in organic sensitizers for dye-sensitized solar cells. RSC Advances. 2015;5:23810-25.

[51] Yella A, Lee HW, Tsao HN, Yi C, Chandiran AK, Nazeeruddin MK, et al. Porphyrin-sensitized solar cells with cobalt (II/III)-based redox electrolyte exceed 12 percent efficiency. Science. 2011;334:629-34.

[52] Mathew S, Yella A, Gao P, Humphry-Baker R, Curchod BF, Ashari-Astani N, et al. Dye-sensitized solar cells with 13% efficiency achieved through the molecular engineering of porphyrin sensitizers. Nature chemistry. 2014;6:242-7.

[53] Kenji Kakiage aYA, a Toru Yano,*a Keiji Oya,a Jun-ichi Fujisawab and Minoru Hanaya*. Highly-efficient dye-sensitized solar cells with collaborative sensitization by silyl-anchor and carboxy-anchor dyes†. J Name. 2013.

[54] Nagarajan B, Kushwaha S, Elumalai R, Mandal S, Ramanujam K, Raghavachari D. Novel ethynyl-pyrene substituted phenothiazine based metal free organic dyes in DSSC with 12% conversion efficiency. Journal of Materials Chemistry A. 2017;5:10289-300.

[55] Wang J, Wu H, Jin L, Zhang J, Yuan Y, Wang P. A Perylene-Based Polycyclic Aromatic Hydrocarbon Electron Donor for a Highly Efficient Solar Cell Dye. ChemSusChem. 2017;10:2962-7.

[56] Jamalullail N, Mohamad IS, Norizan MN, Baharum NA. Short Review: Natural Pigments Photosensitizer for Dye-Sensitized Solar Cell (DSSC). 15th Student Conference on Research and Development (SCOReD). Perlis, Malaysia.: IEEE; 2017.

[57] Hyo JLK, Dae-Young Yoo, JungSuk Bang, Jiwon Kim,Sungjee Park,Su Moon Anchoring Cadmium Chalcogenide Quantum Dots (QDs) onto Stable Oxide Semiconductors for QD Sensitized Solar Cells. Bulletin Korean Chemical Society. 2007;28 953-8.

[58] Pan Z, Rao H, Mora-Sero I, Bisquert J, Zhong X. Quantum dot-sensitized solar cells. Chemical Society reviews. 2018;47:7659-702.

[59] Kojima A, Teshima K, Shirai Y, Miyasaka T. Organometal halide perovskites as visible-light sensitizers for photovoltaic cells. Journal of the American Chemical Society. 2009;131:6050-1.

[60] Shi Z, Jayatissa AH. Perovskites-Based Solar Cells: A Review of Recent Progress, Materials and Processing Methods. Materials (Basel). 2018;11.

[61] Liu X, Fang J, Liu Y, Lin T. Progress in nanostructured photoanodes for dye-sensitized solar cells. Frontiers of Materials Science. 2016;10:225-37.

[62] Fan K, Yu J, Ho W. Improving photoanodes to obtain highly efficient dye-sensitized solar cells: a brief review. Materials Horizons. 2017;4:319-44.

[63] Cao Y, Dong Y-J, Feng H-L, Chen H-Y, Kuang D-B. Electrospun TiO 2 nanofiber based hierarchical photoanode for efficient dye-sensitized solar cells. Electrochimica Acta. 2016;189:259-64.

[64] Pugliese D, Shahzad N, Sacco A, Musso G, Lamberti A, Caputo G, et al. Fast TiO2Sensitization Using the Semisquaric Acid as Anchoring Group. International Journal of Photoenergy. 2013;2013:1-8.

[65] Lai FI, Yang JF, Kuo SY. Efficiency Enhancement of Dye-Sensitized Solar Cells' Performance with ZnO Nanorods Grown by Low-Temperature Hydrothermal Reaction. Materials (Basel). 2015;8:8860-7.

[66] Shahzad N, Pugliese D, Lamberti A, Sacco A, Virga A, Gazia R, et al. Monitoring the dye impregnation time of nanostructured photoanodes for dye sensitized solar cells. Journal of Physics: Conference Series. 2013;439.

[67] Mehmood U, Rahman S-u, Harrabi K, Hussein IA, Reddy BVS. Recent Advances in Dye Sensitized Solar Cells. Advances in Materials Science and Engineering. 2014;2014:1-12.

[68] Cho T-Y, Ko K-W, Yoon S-G, Sekhon SS, Kang MG, Hong Y-S, et al. Efficiency enhancement of flexible dye-sensitized solar cell with sol–gel formed Nb2O5 blocking layer. Current Applied Physics. 2013;13:1391-6.

[69] Lin HCS, Chaochin Li, Wen Ren The effect of ZnO coatings on the performance of WO3 dye-sensit. 2013:1063-9.

[70] Jiang Q, Gao J, Yi L, Hu G, Zhang J. Enhanced performance of dye-sensitized solar cells based on P25/Ta2O5 composite films. Applied Physics A. 2016;122:442-8.

[71] Lee H, Wang M, Chen P, Gamelin DR, Zakeeruddin SM, Gratzel M, et al. Efficient CdSe quantum dot-sensitized solar cells prepared by an improved successive ionic layer adsorption and reaction process. Nano letters. 2009;9:4221-7.

[72] Kim SF, Brent Eisler,Hans Jurgen Bawendi, Moungi Type-II Quantum Dots: CdTe/CdSe(Core/Shell) and CdSe/ZnTe(Core/Shell) Heterostructures. journal of american chemical society. 2003;125:11466-7.

[73] Lee HJ, Lee Y, Altantuya U. Quantum Dot (QD) Sensitizer on the Surface of TiO2Film: Effect of Metal Salt Anions Dissolved in Chemical Bath on the Distribution Density of SILAR-Grown PbS QDs. Journal of the Korean Chemical Society. 2015;59:97-102.

[74] Dubey RS, Jadkar SR, Bhorde AB. Synthesis and Characterization of Various Doped TiO2 Nanocrystals for Dye-Sensitized Solar Cells. ACS Omega. 2021;6:3470-82.

[75] Gunawan B, Musyaro'ah, Huda I, Indayani W, S SR, Endarko. The influence of various concentrations of N-doped TiO2 as photoanode to increase the efficiency of dye-sensitized solar cell. 2017.

[76] Krishnapriya R, Nizamudeen C, Saini B, Mozumder MS, Sharma RK, Mourad AI. MOF-derived Co(2+)-doped TiO2 nanoparticles as photoanodes for dye-sensitized solar cells. Scientific reports. 2021;11:16265.

[77] Xu B, Chen Z, Li S. Aluminum-Doped SnO2Hollow Microspheres as Photoanode Materials for Dye-Sensitized Solar Cells. International Journal of Photoenergy. 2016;2016:1-5.

[78] Ringleb A, Ruess R, Hofeditz N, Heimbrodt W, Yoshida T, Schlettwein D. Influence of Mg-doping on the characteristics of ZnO photoanodes in dye-sensitized solar cells. Physical chemistry chemical physics : PCCP. 2021;23:8393-402.

[79] Ye M, Wen X, Wang M, Iocozzia J, Zhang N, Lin C, et al. Recent advances in dye-sensitized solar cells: from photoanodes, sensitizers and electrolytes to counter electrodes. Materials Today. 2015;18:155-62.

[80] Sulaeman U, Zuhairi Abdullah A. The way forward for the modification of dye-sensitized solar cell towards better power conversion efficiency. Renewable and Sustainable Energy Reviews. 2017;74:438-52.

[81] Kouhestanian E, Mozaffari SA, Ranjbar M, SalarAmoli H, Armanmehr MH. Electrodeposited ZnO thin film as an efficient alternative blocking layer for TiCl 4 pre-treatment in TiO 2 -based dye sensitized solar cells. Superlattices and Microstructures. 2016;96:82-94.

[82] Duong T-T, Choi H-J, He Q-J, Le A-T, Yoon S-G. Enhancing the efficiency of dye sensitized solar cells with an SnO2 blocking layer grown by nanocluster deposition. Journal of Alloys and Compounds. 2013;561:206-10.

[83] Kim DH, Woodroof M, Lee K, Parsons GN. Atomic layer deposition of high performance ultrathin TiO(2) blocking layers for dye-sensitized solar cells. ChemSusChem. 2013;6:1014-20.

[84] Guai GH, Song QL, Lu ZS, Ng CM, Li CM. Tailor and functionalize TiO2 compact layer by acid treatment for high performance dye-sensitized solar cell and its enhancement mechanism. Renewable Energy. 2013;51:29-35.

[85] Noh SI, Bae K-N, Ahn H-J, Seong T-Y. Improved efficiency of dye-sensitized solar cells through fluorine-doped TiO2 blocking layer. Ceramics International. 2013;39:8097-101.

[86] Xu J, Wang G, Fan J, Liu B, Cao S, Yu J. g-C3N4 modified TiO2 nanosheets with enhanced photoelectric conversion efficiency in dye-sensitized solar cells. Journal of Power Sources. 2015;274:77-84.

[87] Suresh S, Deepak TG, Ni C, Sreekala CNO, Satyanarayana M, Nair AS, et al. The role of crystallinity of the Nb2O5 blocking layer on the performance of dye-sensitized solar cells. New Journal of Chemistry. 2016;40:6228-37.

[88] Parthiban S, Anuratha KS, Arunprabaharan S, Abinesh S, Lakshminarasimhan N. Enhanced dye-sensitized solar cell performance using TiO2:Nb blocking layer deposited by soft chemical method. Ceramics International. 2015;41:205-9.

[89] Wang C, Yu Z, Bu C, Liu P, Bai S, Liu C, et al. Multifunctional alumina/titania hybrid blocking layer modified nanocrystalline titania films as efficient photoanodes in dye sensitized solar cells. Journal of Power Sources. 2015;282:596-601.

[90] Costenaro D, Bisio C, Carniato F, Gatti G, Oswald F, Meyer TB, et al. Size effect of synthetic saponite-clay in quasi-solid electrolyte for dye-sensititized solar cells. Solar Energy Materials and Solar Cells. 2013;117:9-14.

[91] Hassan HC, Abidin ZHZ, Chowdhury FI, Arof AK. A High Efficiency Chlorophyll Sensitized Solar Cell with Quasi Solid PVA Based Electrolyte. International Journal of Photoenergy. 2016;2016:1-9.

[92] Sacco A, Lamberti A, Gerosa M, Bisio C, Gatti G, Carniato F, et al. Toward quasi-solid state Dye-sensitized Solar Cells: Effect of γ-Al2 O 3 nanoparticle dispersion into liquid electrolyte. Solar Energy. 2015;111:125-34.

[93] Wu J, Lan Z, Hao S, Li P, Lin J, Huang M, et al. Progress on the electrolytes for dye-sensitized solar cells. Pure and Applied Chemistry. 2008;80:2241-58.

[94] Wu J, Lan Z, Lin J, Huang M, Huang Y, Fan L, et al. Electrolytes in dye-sensitized solar cells. Chemical reviews. 2015;115:2136-73.

[95] Yang Y, Tao J, Ma L. Study on Properties of Quasi Solid Polymer Electrolyte Based on PVdF-PMMA Blend for Dye-Sensitized Solar Cells. Materials Science Forum. 2009;610-613:347-52.

[96] Wu J, Li Y, Tang Q, Yue G, Lin J, Huang M, et al. Bifacial dye-sensitized solar cells: a strategy to enhance overall efficiency based on transparent polyaniline electrode. Scientific reports. 2014;4:4028.

[97] Li GR, Gao XP. Low-Cost Counter-Electrode Materials for Dye-Sensitized and Perovskite Solar Cells. Advanced materials. 2020;32:e1806478.

[98] Tang Z, Wu J, Zheng M, Huo J, Lan Z. A microporous platinum counter electrode used in dye-sensitized solar cells. Nano Energy. 2013;2:622-7.

[99] Chen X, Tang Q, He B, Lin L, Yu L. Platinum-free binary Co-Ni alloy counter electrodes for efficient dye-sensitized solar cells. Angewandte Chemie. 2014;53:10799-803.

[100] Lin X, Wu M, Wang Y, Hagfeldt A, Ma T. Novel counter electrode catalysts of niobium oxides supersede Pt for dye-sensitized solar cells. Chemical communications. 2011;47:11489-91.

[101] Ozel F, Sarilmaz A, Istanbullu B, Aljabour A, Kus M, Sonmezoglu S. Penternary chalcogenides nanocrystals as catalytic materials for efficient counter electrodes in dye-synthesized solar cells. Scientific reports. 2016;6:29207.

[102] Li GR, Song J, Pan GL, Gao XP. Highly Pt-like electrocatalytic activity of transition metal nitrides for dye-sensitized solar cells. Energy & Environmental Science. 2011;4:1680-3.

[103] Zhao W, Zhu X, Bi H, Cui H, Sun S, Huang F. Novel two-step synthesis of NiS nanoplatelet arrays as efficient counter electrodes for dye-sensitized solar cells. Journal of Power Sources. 2013;242:28-32.

[104] Wu M, Lin X, Wang Y, Wang L, Guo W, Qi D, et al. Economical Pt-free catalysts for counter electrodes of dye-sensitized solar cells. Journal of the American Chemical Society. 2012;134:3419-28.

[105] Dou YY, Li GR, Song J, Gao XP. Nickel phosphide-embedded graphene as counter electrode for dye-sensitized solar cells. Physical chemistry chemical physics : PCCP. 2012;14:1339-42.

[106] Al Mamun MZ, Haimin Porun ,Liu Yun Wang, Jun Caoa Zhao, Huijun. Directly hydrothermal growth of ultrathin MoS2 nanostructured films as high performance counter electrodes for dye sensitised solar cells. RSC Advance. 2014;4:21277-83.

[107] Zhou Q, Shi G. Conducting Polymer-Based Catalysts. Journal of the American Chemical Society. 2016;138:2868-76.

[108] Veerappan G, Bojan K, Rhee SW. Sub-micrometer-sized graphite as a conducting and catalytic counter electrode for dye-sensitized solar cells. ACS applied materials & interfaces. 2011;3:857-62.

[109] Yen M-Y, Teng C-C, Hsiao M-C, Liu P-I, Chuang W-P, Ma C-CM, et al. Platinum nanoparticles/graphene composite catalyst as a novel composite counter electrode for high performance dye-sensitized solar cells. Journal of Materials Chemistry. 2011;21:12880.

[110] Widodo S, Wiranto G, Hidayat MN. Fabrication of Dye Sensitized Solar Cells with Spray Coated Carbon Nano Tube (CNT) Based Counter Electrodes. Energy Procedia. 2015;68:37-44.

[111] Trancik JE, Barton SC, Hone J. Transparent and catalytic carbon nanotube films. Nano letters. 2008;8:982-7.

[112] Huang Z, Liu X, Li K, Li D, Luo Y, Li H, et al. Application of carbon materials as counter electrodes of dye-sensitized solar cells. Electrochemistry Communications. 2007;9:596-8.

[113] Kouhnavard M, Ludin NA, Ghaffari BV, Sopian K, Ikeda S. Carbonaceous materials and their advances as a counter electrode in dye-sensitized solar cells: challenges and prospects. ChemSusChem. 2015;8:1510-33.

[114] Cheng Y, Liu J. Carbon Nanomaterials for Flexible Energy Storage. Materials Research Letters. 2013;1:175-92.

[115] Nabae Y, Nagata S, Hayakawa T, Niwa H, Harada Y, Oshima M, et al. Pt-free carbon-based fuel cell catalyst prepared from spherical polyimide for enhanced oxygen diffusion. Scientific reports. 2016;6:23276.

[116] Rasu Ramachandran2 VM, Shen-Ming Chen1,*, George peter Gnana kumar3, Pandi Gajendran2, Natarajan Biruntha Devi4, Rajkumar Devasenathipathy1. Recent Progress in Electrode Fabrication Materials and Various Insights in Solar cells: Review. international Journal of ELECTROCHEMICAL SCIENCE. 2015;10:3301-18.

[117] Candelaria SL, Shao Y, Zhou W, Li X, Xiao J, Zhang J-G, et al. Nanostructured carbon for energy storage and conversion. Nano Energy. 2012;1:195-220.

[118] Chen T, Dai L. Carbon nanomaterials for high-performance supercapacitors. Materials Today. 2013;16:272-80.

[119] Guofa Dong‡ a, b, Ming Fang‡,a,b, Hongtao Wangc, Senpo Yipa,b, Ho-Yuen Cheungd, Fengyun Wange, Chun- Yuen Wongd, Saitak Chu*,a and Johnny C. Ho*. Insight into the Electrochemical Activation of Carbon-Based Cathodes for Hydrogen Evolution Reaction. Journal of Materials Chemistry. 2015:1-9.

[120] López-Naranjo EJ, González-Ortiz LJ, Apátiga LM, Rivera-Muñoz EM, Manzano-Ramírez A. Transparent Electrodes: A Review of the Use of Carbon-Based Nanomaterials. Journal of Nanomaterials. 2016;2016:1-12.

[121] Liu X, Dai L. Carbon-based metal-free catalysts. Nature Reviews Materials. 2016;1:16064.

[122] Xu Y, Kraft M, Xu R. Metal-free carbonaceous electrocatalysts and photocatalysts for water splitting. Chemical Society reviews. 2016;45:3039-52.

[123] Gundiah G, Govindaraj A, Rajalakshmi N, Dhathathreyan KS, Rao CNR. Hydrogen storage in carbon nanotubes and related materials. Journal of Materials Chemistry. 2003;13:209-13.

[124] Ilango V, Gupta A. Carbon Nanotubes A Successful Hydrogen Storage Medium. International Journal of Chemical, Molecular, Nuclear, Materials and Metallurgical Engineering. 2013;7:678-81.

[125] Roy-Mayhew JD, Boschloo G, Hagfeldt A, Aksay IA. Functionalized graphene sheets as a versatile replacement for platinum in dye-sensitized solar cells. ACS applied materials & interfaces. 2012;4:2794-800.

[126] Lee WJ, Ramasamy E, Lee DY, Song JS. Efficient dye-sensitized solar cells with catalytic multiwall carbon nanotube counter electrodes. ACS applied materials & interfaces. 2009;1:1145-9.

[127] Imoto K, Takahashi K, Yamaguchi T, Komura T, Nakamura J-i, Murata K. High-performance carbon counter electrode for dye-sensitized solar cells. Solar Energy Materials and Solar Cells. 2003;79:459-69.

[128] Murakami TN, Ito S, Wang Q, Nazeeruddin MK, Bessho T, Cesar I, et al. Highly Efficient Dye-Sensitized Solar Cells Based on Carbon Black Counter Electrodes. Journal of The Electrochemical Society. 2006;153:A2255.

[129] Chou C-S, Chen C-Y, Lin S-H, Lu W-H, Wu P. Preparation of TiO2/bamboo-charcoal-powder composite particles and their applications in dye-sensitized solar cells. Advanced Powder Technology. 2015;26:711-7.

[130] Gupta R, Kumar R, Sharma A, Verma N. Novel Cu-carbon nanofiber composites for the counter electrodes of dye-sensitized solar cells. International Journal of Energy Research. 2015;39:668-80.

[131] Shahzad N, Alexe-Ionescu AL, Tresso E, Barbero G. Physical description of the impregnation mechanism of dye molecules in contact with porous electrodes. Physics Letters A. 2013;377:915-9.

[132] Saito Y, Nakahira T, Uemura S. Growth Conditions of Double-Walled Carbon Nanotubes in Arc Discharge. The Journal of Physical Chemistry B. 2003;107:931-4.

[133] Li WZ, Wen JG, Sennett M, Ren ZF. Clean double-walled carbon nanotubes synthesized by CVD. Chemical Physics Letters. 2003;368:299-306.

[134] Fujisawa K, Kim H, Go S, Muramatsu H, Hayashi T, Endo M, et al. A Review of Double-Walled and Triple-Walled Carbon Nanotube Synthesis and Applications. Applied Sciences. 2016;6.

[135] Tison Y, Giusca CE, Stolojan V, Hayashi Y, Silva SRP. The Inner Shell Influence on the Electronic Structure of Double-Walled Carbon Nanotubes. Advanced materials. 2008;20:189-94.

[136] Yang S, Huo J, Song H, Chen X. A comparative study of electrochemical properties of two kinds of carbon nanotubes as anode materials for lithium ion batteries. Electrochim Acta. 2008;53:2238-44.

[137] Belin T, Epron F. Characterization methods of carbon nanotubes: a review. Mat Sci Eng B-Solid. 2005;119:105-18.

[138] Peigney A, Laurent C, Flahaut E, Bacsa RR, Rousset A. Specific surface area of carbon nanotubes and bundles of carbon nanotubes. Carbon. 2001;39:507-14.

[139] Sinnott SB, Andrews R. Carbon Nanotubes: Synthesis, Properties, and Applications. Crit Rev Solid State. 2001;26:145-249.

[140] Suzuki K, Yamaguchi M, Kumagai M, Yanagida S. Application of Carbon Nanotubes to Counter Electrodes of Dye-sensitized Solar Cells. Chemistry Letters. 2003;32:28-9.

[141] Zhang DW, Li XD, Chen S, Tao F, Sun Z, Yin XJ, et al. Fabrication of double-walled carbon nanotube counter electrodes for dye-sensitized solar sells. Journal of Solid State Electrochemistry. 2009;14:1541-6.

[142] Siuzdak K, Klein M, Sawczak M, Wróblewski G, Słoma M, Jakubowska M, et al. Spray-deposited carbon-nanotube counter-electrodes for dye-sensitized solar cells. physica status solidi (a). 2016;213:1157-64.

[143] Chen J-Z, Wang C, Hsu C-C, Cheng IC. Ultrafast synthesis of carbon-nanotube counter electrodes for dye-sensitized solar cells using an atmospheric-pressure plasma jet. Carbon. 2016;98:34-40.

[144] Dumlich H, Gegg M, Hennrich F, Reich S. Bundle and chirality influences on properties of carbon nanotubes studied with van der Waals density functional theory. physica status solidi (b). 2011;248:2589-92.

[145] Ibrahim I, Zhang Y, Popov A, Dunsch L, Buchner B, Cuniberti G, et al. Growth of all-carbon horizontally aligned single-walled carbon nanotubes nucleated from fullerene-based structures. Nanoscale Res Lett. 2013;8:265.

[146] Dong P, Pint CL, Hainey M, Mirri F, Zhan Y, Zhang J, et al. Vertically aligned single-walled carbon nanotubes as low-cost and high electrocatalytic counter electrode for dye-sensitized solar cells. ACS applied materials & interfaces. 2011;3:3157-61.

[147] Shahzad MI, Rajan K, Shahzad N, Arshad M, Perrone D, Giorcelli M, et al. Extensive growth of MWCNTs on copper substrates using various diffusion barrier layers. Diamond and Related Materials. 2018;82:124-31.

[148] Nam JG, Park YJ, Kim BS, Lee JS. Enhancement of the efficiency of dye-sensitized solar cell by utilizing carbon nanotube counter electrode. Scripta Materialia. 2010;62:148-50.

[149] Seo SH, Kim SY, Koo BK, Cha SI, Lee DY. Influence of electrolyte composition on the photovoltaic performance and stability of dye-sensitized solar cells with multiwalled carbon nanotube catalysts. Langmuir. 2010;26:10341-6.

[150] Kim JH, Hong SK, Yoo S-J, Woo CY, Choi JW, Lee D, et al. Pt-free, cost-effective and efficient counter electrode with carbon nanotube yarn for solid-state fiber dye-sensitized solar cells. Dyes and Pigments. 2021;185.

[151] Zhang D, Li X, Chen S, Sun Z, Jiang Yin X, Huang S. Performance of dye-sensitized solar cells with various carbon nanotube counter electrodes. Microchimica Acta. 2011;174:73-9.

[152] Niyogi S, Hamon MA, Hu H, Zhao B, Bhowmik P, Sen R, et al. Chemistry of single-walled carbon nanotubes. Acc Chem Res. 2002;35:1105-13.

[153] Marshall MW, Popa-Nita S, Shapter JG. Measurement of functionalised carbon nanotube carboxylic acid groups using a simple chemical process. Carbon. 2006;44:1137-41.

[154] Chou C-S, Huang C-I, Yang R-Y, Wang C-P. The effect of SWCNT with the functional group deposited on the counter electrode on the dye-sensitized solar cell. Advanced Powder Technology. 2010;21:542-50.

[155] Kim S, Dovjuu O, Choi S-H, Jeong H, Park J-T. Photovoltaic Characteristics of Multiwalled Carbon Nanotube Counter-Electrode Materials for Dye-Sensitized Solar Cells Produced by Chemical Treatment and Addition of Dispersant. Coatings. 2019;9.

[156] Arbab AA, Sun KC, Sahito IA, Qadir MB, Jeong SH. Fabrication of highly electro catalytic active layer of multi walled carbon nanotube/enzyme for Pt-free dye sensitized solar cells. Applied Surface Science. 2015;349:174-83.

[157] Martínez-Muíño A, Rana M, Vilatela JJ, Costa RD. Origin of the electrocatalytic activity in carbon nanotube fiber counter-electrodes for solar-energy conversion. Nanoscale Advances. 2020;2:4400-9.

[158] Siwach B, Mohan D, Barala M. Fabrication and characterization of MWCNTs and Pt/MWCNTs counter electrodes for dye sensitized solar cells. Advances in Basic Science (Icabs 2019)2019.

[159] Mithari PA, Mendhe AC, Sankapal BR, Patrikar SR. Process optimization of dip-coated MWCNTs thin-films: Counter electrode in dye sensitized solar cells. Journal of the Indian Chemical Society. 2021;98.

[160] Ahn JY, Kim JH, Kim JM, Lee D, Kim SH. Multiwalled carbon nanotube thin films prepared by aerosol deposition process for use as highly efficient Pt-free counter electrodes of dye-sensitized solar cells. Solar Energy. 2014;107:660-7.

[161] Ramasamy E, Lee WJ, Lee DY, Song JS. Spray coated multi-wall carbon nanotube counter electrode for tri-iodide (I3-) reduction in dye-sensitized solar cells. Electrochemistry Communications. 2008;10:1087-9.

[162] Sun KC, Arbab AA, Sahito IA, Qadir MB, Choi BJ, Kwon SC, et al. A PVdF-based electrolyte membrane for a carbon counter electrode in dye-sensitized solar cells. RSC Advances. 2017;7:20908-18.

[163] Arbab AA, Peerzada MH, Sahito IA, Jeong SH. A complete carbon counter electrode for high performance quasi solid state dye sensitized solar cell. Journal of Power Sources. 2017;343:412-23.

[164] Younas M, Gondal MA, Dastageer MA, Baig U. Fabrication of cost effective and efficient dye sensitized solar cells with WO3-TiO2 nanocomposites as photoanode and MWCNT as Pt-free counter electrode. Ceramics International. 2019;45:936-47.

[165] Siwach B, Mohan D, Singh KK, Kumar A, Barala M. Effect of carbonaceous counter electrodes on the performance of ZnO-graphene nanocomposites based dye sensitized solar cells. Ceramics International. 2018;44:21120-6.

[166] Monreal-Bernal A, Vilatela JJ, Costa RD. CNT fibres as dual counter-electrode/current-collector in highly efficient and stable dye-sensitized solar cells. Carbon. 2019;141:488-96.

[167] Chen T, Qiu L, Cai Z, Gong F, Yang Z, Wang Z, et al. Intertwined aligned carbon nanotube fiber based dye-sensitized solar cells. Nano letters. 2012;12:2568-72.

[168] Pan S, Yang Z, Li H, Qiu L, Sun H, Peng H. Efficient dye-sensitized photovoltaic wires based on an organic redox electrolyte. Journal of the American Chemical Society. 2013;135:10622-5.

[169] Anothumakkool B, Agrawal I, Bhange SN, Soni R, Game O, Ogale SB, et al. Pt- and TCO-Free Flexible Cathode for DSSC from Highly Conducting and Flexible PEDOT Paper Prepared via in Situ Interfacial Polymerization. ACS applied materials & interfaces. 2016;8:553-62.

[170] Tai Q, Chen B, Guo F, Xu S, Hu H, Sebo B, et al. In situ prepared transparent polyaniline electrode and its application in bifacial dye-sensitized solar cells. ACS nano. 2011;5:3795-9.

[171] Park J-G, Akhtar MS, Li ZY, Cho D-S, Lee W, Yang OB. Application of single walled carbon nanotubes as counter electrode for dye sensitized solar cells. Electrochimica Acta. 2012;85:600-4.

[172] Holubowitch NE, Landon J, Lippert CA, Craddock JD, Weisenberger MC, Liu K. Spray-Coated Multiwalled Carbon Nanotube Composite Electrodes for Thermal Energy Scavenging Electrochemical Cells. ACS applied materials & interfaces. 2016;8:22159-67.

[173] He B, Tang Q, Luo J, Li Q, Chen X, Cai H. Rapid charge-transfer in polypyrrole–single wall carbon nanotube complex counter electrodes: Improved photovoltaic performances of dye-sensitized solar cells. Journal of Power Sources. 2014;256:170-7.

[174] Li H, Xiao Y, Han G, Li M. Honeycomb-like polypyrrole/multi-wall carbon nanotube films as an effective counter electrode in bifacial dye-sensitized solar cells. Journal of Materials Science. 2017;52:8421-31.

[175] Lee JH, Jang YJ, Kim DW, Cheruku R, Thogiti S, Ahn K-S, et al. Application of polypyrrole/sodium dodecyl sulfate/carbon nanotube counter electrode for solid-state dye-sensitized solar cells and dye-sensitized solar cells. Chemical Papers. 2019;73:2749-55.

[176] Hou W, Xiao Y, Han G, Zhou H. Electro-polymerization of polypyrrole/multi-wall carbon nanotube counter electrodes for use in platinum-free dye-sensitized solar cells. Electrochimica Acta. 2016;190:720-8.

[177] Rafique S, Rashid I, Sharif R. Cost effective dye sensitized solar cell based on novel Cu polypyrrole multiwall carbon nanotubes nanocomposites counter electrode. Scientific reports. 2021;11:14830.

[178] Fan B, Mei X, Sun K, Ouyang J. Conducting polymer/carbon nanotube composite as counter electrode of dye-sensitized solar cells. Applied Physics Letters. 2008;93.

[179] Shin H-J, Jeon SS, Im SS. CNT/PEDOT core/shell nanostructures as a counter electrode for dye-sensitized solar cells. Synthetic Metals. 2011;161:1284-8.

[180] Lee K-M, Chiu W-H, Wei H-Y, Hu C-W, Suryanarayanan V, Hsieh W-F, et al. Effects of mesoscopic poly(3,4-ethylenedioxythiophene) films as counter electrodes for dye-sensitized solar cells. Thin Solid Films. 2010;518:1716-21.

[181] Ali A, Shah SM, Bozar S, Kazici M, Keskin B, Kaleli M, et al. Metal-free polymer/MWCNT composite fiber as an efficient counter electrode in fiber shape dye-sensitized solar cells. Nanotechnology. 2016;27:384003.

[182] Li H, Xiao Y, Han G, Zhang Y. A transparent honeycomb-like poly(3,4-ethylenedioxythiophene)/multi-wall carbon nanotube counter electrode for bifacial dye-sensitized solar cells. Organic Electronics. 2017;50:161-9.

[183] Samir M.AbdulAlmohsin a b, *, Alaa Ayad Khedhair a, Sadq K.Ajee. Facile Synthesis of Polyaniline-Single Wall Carbon Nanotube Nanocomposite as Hole Transport Material and Zinc Oxide Nanorodes as Metal Oxide to Integration Solid-State Dye-sensitized Solar Cells. University of Thi-Qar Journal. 2019.

[184] Bumika M, Kumar Mallick M, Mohanty S, Nayak SK, Palai AK. One-pot electrodeposition of polyaniline/SWCNT/ZnO film and its positive influence on photovoltaic performance as counter electrode material. Materials Letters. 2020;279.

[185] Wu K, Chen L, Duan C, Gao J, Wu M. Effect of ion doping on catalytic activity of MWCNT-polyaniline counter electrodes in dye-sensitized solar cells. Materials & Design. 2016;104:298-302.

[186] Choi HJ, Shin JE, Lee G-W, Park N-G, Kim K, Hong SC. Effect of surface modification of multi-walled carbon nanotubes on the fabrication and performance of carbon nanotube based counter electrodes for dye-sensitized solar cells. Current Applied Physics. 2010;10:S165-S7.

[187] Chew JW, Khanmirzaei MH, Numan A, Omar FS, Ramesh K, Ramesh S. Performance studies of ZnO and multi walled carbon nanotubes-based counter electrodes with gel polymer electrolyte for dye-sensitized solar cell. Materials Science in Semiconductor Processing. 2018;83:144-9.

[188] Nguyen D-T, Iwai T, Taguchi K. Dye-sensitized solar cells based on MK2 dye, PMMA-based quasi-solid electrolyte, and flexible CNT counter electrode. Energy Reports. 2020;6:872-6.

[189] Kuliček J, Gemeiner P, Omastová M, Mičušík M. Preparation of polypyrrole/multi-walled carbon nanotube hybrids by electropolymerization combined with a coating method for counter electrodes in dye-sensitized solar cells. Chemical Papers. 2018;72:1651-67.

[190] Yun D-J, Jeong YJ, Ra H, Kim J-M, An TK, Rhee S-W, et al. Systematic optimization of MWCNT-PEDOT:PSS composite electrodes for organic transistors and dye-sensitized solar cells: Effects of MWCNT diameter and purity. Organic Electronics. 2018;52:7-16.

[191] Ma J, Yang H, Ren W, Yang Y. Functionalization of aligned carbon nanotubes used as counter electrode for dye-sensitized solar cells. Materials Research Express. 2019;6.

[192] Mao X, Zhang S, Ma Q, Wan L, Niu H, Qin S, et al. Non-covalent construction of non-Pt counter electrodes for high performance dye-sensitized solar cells. Journal of Sol-Gel Science and Technology. 2015;74:240-8.

[193] Okumura T, Sugiyo T, Inoue T, Ikegami M, Miyasaka T. Nickel Oxide Hybridized Carbon Film as an Efficient Mesoscopic Cathode for Dye-Sensitized Solar Cells. Journal of The Electrochemical Society. 2013;160:H155-H9.

[194] Wu M, Lin X, Hagfeldt A, Ma T. A novel catalyst of WO2 nanorod for the counter electrode of dye-sensitized solar cells. Chemical communications. 2011;47:4535-7.

[195] Sun H, Qin D, Huang S, Guo X, Li D, Luo Y, et al. Dye-sensitized solar cells with NiS counter electrodes electrodeposited by a potential reversal technique. Energy & Environmental Science. 2011;4:2630.

[196] Kung CW, Chen HW, Lin CY, Huang KC, Vittal R, Ho KC. CoS acicular nanorod arrays for the counter electrode of an efficient dye-sensitized solar cell. ACS nano. 2012;6:7016-25.

[197] Wu J, Yue G, Xiao Y, Huang M, Lin J, Fan L, et al. Glucose aided preparation of tungsten sulfide/multi-wall carbon nanotube hybrid and use as counter electrode in dye-sensitized solar cells. ACS applied materials & interfaces. 2012;4:6530-6.

[198] Wu M, Wang Y, Lin X, Yu N, Wang L, Wang L, et al. Economical and effective sulfide catalysts for dye-sensitized solar cells as counter electrodes. Physical chemistry chemical physics : PCCP. 2011;13:19298-301.

[199] Yue G, Liu X, Mao Y, Zheng H, Zhang W. A promising hybrid counter electrode of vanadium sulfide decorated with carbon nanotubes for efficient dye-sensitized solar cells. Mater Today Energy. 2017;4:58-65.

[200] Memon AA, Patil SA, Sun KC, Mengal N, Arbab AA, Sahito IA, et al. Carbonous metallic framework of multi-walled carbon Nanotubes/Bi2S3 nanorods as heterostructure composite films for efficient quasi-solid state DSSCs. Electrochimica Acta. 2018;283:997-1005.

[201] Prasad S, Durai G, Devaraj D, AlSalhi MS, Theerthagiri J, Arunachalam P, et al. 3D nanorhombus nickel nitride as stable and cost-effective counter electrodes for dye-sensitized solar cells and supercapacitor applications. RSC Advances. 2018;8:8828-35.

[202] Guo J, Liang S, Shi Y, Hao C, Wang X, Ma T. Transition metal selenides as efficient counter-electrode materials for dye-sensitized solar cells. Physical Chemistry Chemical Physics. 2015;17:28985-92.

[203] Tai S-Y, Liu C-J, Chou S-W, Chien FS-S, Lin J-Y, Lin T-W. Few-layer MoS2 nanosheets coated onto multi-walled carbon nanotubes as a low-cost and highly electrocatalytic counter electrode for dye-sensitized solar cells. Journal of Materials Chemistry. 2012;22:24753-9.

[204] Theerthagiri J, Senthil RA, Arunachalam P, Madhavan J, Buraidah MH, Santhanam A, et al. Synthesis of various carbon incorporated flower-like MoS2 microspheres as counter electrode for dye-sensitized solar cells. Journal of Solid State Electrochemistry. 2016;21:581-90.

[205] Theerthagiri J, Senthil RA, Arunachalam P, Bhabu KA, Selvi A, Madhavan J, et al. Electrochemical deposition of carbon materials incorporated nickel sulfide composite as counter electrode for dye-sensitized solar cells. Ionics. 2016;23:1017-25.

[206] Maiaugree W, Tansoonton T, Amornkitbamrung V, Swatsitang E. Ni3S2@MWCNTs films for effective counter electrodes of dye-sensitized solar cells. Current Applied Physics. 2019;19:1355-61.

[207] Lu M-N, Dai C-S, Tai S-Y, Lin T-W, Lin J-Y. Hierarchical nickel sulfide/carbon nanotube nanocomposite as a catalytic material toward triiodine reduction in dye-sensitized solar cells. Journal of Power Sources. 2014;270:499-505.

[208] Tai S-Y, Lu M-N, Ho H-P, Xiao Y, Lin J-Y. Investigation of carbon nanotubes decorated with cobalt sulfides of different phases as nanocomposite catalysts in dye-sensitized solar cells. Electrochimica Acta. 2014;143:216-21.

[209] Peter IJ, Vijaya S, Anandan S, Nithiananthi P. Sb2S3 entrenched MWCNT composite as a low-cost Pt-free counter electrode for dye-sensitized solar cell and a viewpoint for a photo-powered energy system. Electrochimica Acta. 2021;390.

[210] Zhang Y, Wang D, Wang Q, Zheng W. One-step synthesized CuS and MWCNTs composite as a highly efficient counter electrode for quantum dot sensitized solar cells. Materials & Design. 2018;160:870-5.

[211] Lin J-Y, Liao J-H, Hung T-Y. A composite counter electrode of CoS/MWCNT with high electrocatalytic activity for dye-sensitized solar cells. Electrochemistry Communications. 2011;13:977-80.

[212] Mehmood U, Ishfaq A, Sufyan M. Nanocomposites of Multi-walled Carbon Nanotubes and Titanium dioxide (MWCNTs/TiO2) as affective counter electrode materials for Platinum-free Dye-Sensitized Solar Cells (DSSCs). Solar Energy. 2021;220:949-52.

[213] Wu K, Zhao J, Xiong Y, Ruan B, Wu M. Synthesis and performance of La2O3@MWCNT composite materials as Pt-free counter electrodes for dye-sensitized solar cells. Ionics. 2018;24:4055-61.

[214] Raissan Al-bahrani M, Liu L, Ahmad W, Tao J, Tu F, Cheng Z, et al. NiO-NF/MWCNT nanocomposite catalyst as a counter electrode for high performance dye-sensitized solar cells. Applied Surface Science. 2015;331:333-8.

[215] Singh R, Kaur N, Navjyoti, Mahajan A. Ni2+ enriched carbon nanotubes nanohybrids based non-platinum counter electrodes for dye sensitized solar cells. Solar Energy. 2021;226:31-9.

[216] Saravanakumar T, Selvaraju T, Bhojanaa KB, Ramesh M, Pandikumar A, Akilan R, et al. Exploring the synergistic effect of NixSn2xS4x thiospinel with MWCNTs for enhanced performance in dye-sensitized solar cells, the hydrogen evolution reaction, and supercapacitors. Dalton transactions. 2020;49:5336-51.

[217] Yue G, Cheng R, Gao X, Fan L, Mao Y, Gao Y, et al. Synthesis of MoIn2S4@CNTs Composite Counter Electrode for Dye-Sensitized Solar Cells. Nanoscale Res Lett. 2020;15:179.

[218] Di Y, Xiao Z, Zhao Z, Ru G, Chen B, Feng J. Bimetallic NiCoP nanoparticles incorporating with carbon nanotubes as efficient and durable electrode materials for dye sensitized solar cells. Journal of Alloys and Compounds. 2019;788:198-205.

[219] Wang T, Xu M, Li X, Wang C, Chen W. Highly dispersed redox-active polyoxometalates' periodic deposition on multi-walled carbon nanotubes for boosting electrocatalytic triiodide reduction in dye-sensitized solar cells. Inorganic Chemistry Frontiers. 2020;7:1676-84.

[220] Liu T, Mai X, Chen H, Ren J, Liu Z, Li Y, et al. Carbon nanotube aerogel-CoS2 hybrid catalytic counter electrodes for enhanced photovoltaic performance dye-sensitized solar cells. Nanoscale. 2018;10:4194-201.

[221] Uk Lee S, Seok Choi W, Hong B. A comparative study of dye-sensitized solar cells added carbon nanotubes to electrolyte and counter electrodes. Solar Energy Materials and Solar Cells. 2010;94:680-5.

[222] Lee KS, Lee WJ, Park NG, Kim SO, Park JH. Transferred vertically aligned N-doped carbon nanotube arrays: use in dye-sensitized solar cells as counter electrodes. Chemical communications. 2011;47:4264-6.

[223] Zheng X, Deng J, Wang N, Deng D, Zhang WH, Bao X, et al. Podlike N-doped carbon nanotubes encapsulating FeNi alloy nanoparticles: high-performance counter electrode materials for dye-sensitized solar cells. Angewandte Chemie. 2014;53:7023-7.

[224] Xing Y, Zheng X, Wu Y, Li M, Zhang WH, Li C. Nitrogen-doped carbon nanotubes with metal nanoparticles as counter electrode materials for dye-sensitized solar cells. Chemical communications. 2015;51:8146-9.

[225] Arbab AA, Memon AA, Sahito IA, Mengal N, Sun KC, Ali M, et al. An evidence for an organic N-doped multiwall carbon nanotube heterostructure and its superior electrocatalytic properties for promising dye-sensitized solar cells. Journal of Materials Chemistry A. 2018;6:8307-22.

[226] Wang T, Xu M, Li F, Li Y, Chen W. Multimetal-based nitrogen doped carbon nanotubes bifunctional electrocatalysts for triiodide reduction and water-splitting synthesized from polyoxometalate- intercalated layered double hydroxide pyrolysis strategy. Applied Catalysis B: Environmental. 2021;280.

[227] Ou J, Gong C, Xiang J, Liu J. Noble metal-free Co@N-doped carbon nanotubes as efficient counter electrode in dye-sensitized solar cells. Solar Energy. 2018;174:225-30.

[228] Imbrogno A, Pandiyan R, Barberio M, Macario A, Bonanno A, El khakani MA. Pulsed-laser-ablation based nanodecoration of multi-wall-carbon nanotubes by Co–Ni nanoparticles for dye-sensitized solar cell counter electrode applications. Materials for Renewable and Sustainable Energy. 2017;6.

[229] Chen M, Shao L-L, Lv X-W, Wang G-C, Yang W-Q, Yuan Z-Y, et al. In situ growth of Ni-encapsulated and N-doped carbon nanotubes on N-doped ordered mesoporous carbon for high-efficiency triiodide reduction in dye-sensitized solar cells. Chemical Engineering Journal. 2020;390.

[230] Mehmood U, Ahmad W, Ahmed S. Nickel impregnated multi-walled carbon nanotubes (Ni/MWCNT) as active catalyst materials for efficient and platinum-free dye-sensitized solar cells (DSSCs). Sustainable Energy & Fuels. 2019;3:3473-80.

[231] Chen M, Zhao G, Shao L-L, Yuan Z-Y, Jing Q-S, Huang K-J, et al. Controlled Synthesis of Nickel Encapsulated into Nitrogen-Doped Carbon Nanotubes with Covalent Bonded Interfaces: The Structural and Electronic Modulation Strategy for an Efficient Electrocatalyst in Dye-Sensitized Solar Cells. Chemistry of Materials. 2017;29:9680-94.

[232] Li Y, Liu X, Li H, Shi D, Jiao Q, Zhao Y, et al. Rational design of metal organic framework derived hierarchical structural nitrogen doped porous carbon coated CoSe/nitrogen doped carbon nanotubes composites as a robust Pt-free electrocatalyst for dye-sensitized solar cells. Journal of Power Sources. 2019;422:122-30.

[233] Huang S, Li S, He Q, An H, Xiao L, Hou L. Formation of CoTe2 embedded in nitrogen-doped carbon nanotubes-grafted polyhedrons with boosted electrocatalytic properties in dye-sensitized solar cells. Applied Surface Science. 2019;476:769-77.

[234] Leu Y-A, Yeh M-H, Lin L-Y, Li T-J, Chang L-Y, Shen S-Y, et al. Thermally Stable Boron-Doped Multiwalled Carbon Nanotubes as a Pt-free Counter Electrode for Dye-Sensitized Solar Cells. ACS Sustainable Chemistry & Engineering. 2016;5:537-46.

[235] Yeh M-H, Leu Y-A, Chiang W-H, Li Y-S, Chen G-L, Li T-J, et al. Boron-doped carbon nanotubes as metal-free electrocatalyst for dye-sensitized solar cells: Heteroatom doping level effect on tri-iodide reduction reaction. Journal of Power Sources. 2018;375:29-36.

[236] Hong J, Yu C, Song X, Meng X, Huang H, Zhao C, et al. Theoretical and Experimental Insights into the Effects of Oxygen-Containing Species within CNTs toward Triiodide Reduction. ACS Sustainable Chemistry & Engineering. 2019;7:7527-34.

[237] Arbab AA, Sun KC, Sahito IA, Qadir MB, Choi YS, Jeong SH. A Novel Activated-Charcoal-Doped Multiwalled Carbon Nanotube Hybrid for Quasi-Solid-State Dye-Sensitized Solar Cell Outperforming Pt Electrode. ACS applied materials & interfaces. 2016;8:7471-82.

[238] Yang N, Zhai J, Wang D, Chen Y, Jiang L. Two-dimensional graphene bridges enhanced photoinduced charge transport in dye-sensitized solar cells. ACS nano. 2010;4:887-94.

[239] Yu F, Shi Y, Yao W, Han S, Ma J. A new breakthrough for graphene/carbon nanotubes as counter electrodes of dye-sensitized solar cells with up to a 10.69% power conversion efficiency. Journal of Power Sources. 2019;412:366-73.

[240] Chang L-H, Hsieh C-K, Hsiao M-C, Chiang J-C, Liu P-I, Ho K-K, et al. A graphene-multi-walled carbon nanotube hybrid supported on fluorinated tin oxide as a counter electrode of dye-sensitized solar cells. Journal of Power Sources. 2013;222:518-25.

[241] Ratul Kumar B, Nemala SS, Mallick S. Platinum and Transparent Conducting Oxide Free Graphene-CNT Composite Based Counter-Electrodes for Dye-Sensitized Solar Cells. Surface Engineering and Applied Electrochemistry. 2019;55:472-80.

[242] Zhang J, Yu M, Li S, Meng Y, Wu X, Liu J. Transparent conducting oxide-free nitrogen-doped graphene/reduced hydroxylated carbon nanotube composite paper as flexible counter electrodes for dye-sensitized solar cells. Journal of Power Sources. 2016;334:44-51.

[243] Khan MW, Zuo X, Yang Q, Tang H, Ur Rehman KM, Wu M, et al. Functionalized multi-walled carbon nanotubes embedded with nanoflakes boost the short-circuit current of Ru (II) based dye-sensitized solar cells. Dyes and Pigments. 2020;181.

[244] Khan MW, Yao J, Zhang K, Zuo X, Yang Q, Tang H, et al. Engineering N-reduced graphene oxide wrapped Co3O4@f-MWCNT hybrid for enhance performance dye-sensitized solar cells. Journal of Electroanalytical Chemistry. 2019;844:142-54.

[245] Zhang W, Wasim Khan M, Zuo X, Yang Q, Tang H, Jin S, et al. Sunflower-Like SrCo2S4@f-MWCNTs Hybrid Wrapped by Engineering N-Reduced Graphene Oxide for High Performance Dye-Sensitized Solar Cells. Journal of Renewable Materials. 2020;8:431-46.

[246] Lin J-Y, Su A-L, Chang C-Y, Hung K-C, Lin T-W. Molybdenum Disulfide/Reduced Graphene Oxide-Carbon Nanotube Hybrids as Efficient Catalytic Materials in Dye-Sensitized Solar Cells. ChemElectroChem. 2015;2:720-5.

[247] Al-bahrani MR, Xu X, Ahmad W, Ren X, Su J, Cheng Z, et al. Highly efficient dye-sensitized solar cell with GNS/MWCNT/PANI as a counter electrode. Materials Research Bulletin. 2014;59:272-7.

[248] Liu K, Chen Z, Lv T, Yao Y, Li N, Li H, et al. A Self-supported Graphene/Carbon Nanotube Hollow Fiber for Integrated Energy Conversion and Storage. Nanomicro Lett. 2020;12:64.

[249] Yue G, Ma X, Jiang Q, Tan F, Wu J, Chen C, et al. PEDOT:PSS and glucose assisted preparation of molybdenum disulfide/single-wall carbon nanotubes counter electrode and served in dye-sensitized solar cells. Electrochimica Acta. 2014;142:68-75.

[250] Al-Bahrani MR, Ahmad W, Mehnane HF, Chen Y, Cheng Z, Gao Y. Enhanced Electrocatalytic Activity by RGO/MWCNTs/NiO Counter Electrode for Dye-sensitized Solar Cells. Nanomicro Lett. 2015;7:298-306.

[251] Xiao Y, Wang W-Y, Chou S-W, Lin T-W, Lin J-Y. In situ electropolymerization of polyaniline/cobalt sulfide decorated carbon nanotube composite catalyst toward triiodide reduction in dye-sensitized solar cells. Journal of Power Sources. 2014;266:448-55.

[252] Ma J, Yang HL, Ren WH. Functionalized Reduced Graphene Oxide Loaded Aligned Carbon Nanotube Layer Used as Counter Electrode for Dye-Sensitized Solar Cells. J Nanosci Nanotechnol. 2020;20:1749-55.

[253] Wahyuono RA, Jia G, Plentz J, Dellith A, Dellith J, Herrmann-Westendorf F, et al. Self-Assembled Graphene/MWCNT Bilayers as Platinum-Free Counter Electrode in Dye-Sensitized Solar Cells. Chemphyschem : a European journal of chemical physics and physical chemistry. 2019;20:3336-45.

[254] Zhang S, Jin J, Li D, Fu Z, Gao S, Cheng S, et al. Increased power conversion efficiency of dye-sensitized solar cells with counter electrodes based on carbon materials. RSC Advances. 2019;9:22092-100.

[255] Alkuam E. Preparation of Multi-Wall Carbon Nanotubes/Graphene Composites with Cadmium Sulfide in Dye-Sensitized Solar Cells (DSSCs). Advances in Materials Physics and Chemistry. 2021;11:111-9.

[256] Wang G, Kuang S, Zhang J, Hou S, Nian S. Graphitic carbon nitride/multiwalled carbon nanotubes composite as Pt-free counter electrode for high-efficiency dye-sensitized solar cells. Electrochimica Acta. 2016;187:243-8.